Ludwig-Maximilians-Universität
München

Dissertation

Gluons and the spin of the proton

Author: Oleksandr Kubelskyi

November 12, 2010

Erstgutachter: Prof. Dr. Harald Fritzsch
Zweitgutachter: Prof. Dr. Dieter Lüst
Tag der mündlichen Prüfung: 23.12.2010

Gluons and the spin of the Proton

Dissertation and der Fakultät für Physik der Ludwig-Maximilians-Universität München

vorgelegt von Oleksandr Kubelskyi aus Kiew

München, den November 12, 2010

Abstract

The structure of the proton and the origin of the proton spin has been a puzzle for many years. The EMC collaboration at CERN provided the first experimental data on the spin structure of the proton. The result was almost zero net contribution from quarks. Over the past 20 years new measurements of polarized parton distributions became available.

The present value of the quark contribution to the proton spin is one third. The remaining 60 percent of the proton spin come from the gluons and orbital angular momentum of quarks and gluons.

We investigate how the spin of the proton originates from the spin of its constituents. We study the proton using the phenomenologically accessible parameters such as distribution functions for quarks and gluons.

The basic understanding of the proton structure (and in particular its spin structure) is important for interpreting the results of the LHC, which in turn can be used to refine the present knowledge.

The proton spin structure gives a detailed information about the dynamical structure of the proton. Based on the present experimental data we suggest that the gluons and quarks play equally important role in the structure of the proton.

Contents

Chapter 1

Introduction

In the years 1922-25 physicists introduced the spin of particles. The spin of the electron, which is a pointlike object , is $\frac{1}{2}\hbar$. The spin of the proton is the sum of the spins of the constituents (quarks and gluons), plus contribution from orbital angular momentum. In this thesis we investigate how the proton spin is formed.

An introductory section is devoted to the brief history of the subject and the role of proton spin puzzle. Today we see the proton as a complex object which consists of three different elements (quarks) interacting in a complex way with each other.

Baryons (protons, neutrons) interact with each other by the strong force. This interaction is described by the theory of Quantum Chromodynamics (QCD). QCD is a generalization of Quantum Electrodynamics (QED).

1.1 The Standard Model of Particle Physics

The elementary particles can be divided into two groups:

- matter particles: quarks and leptons
- particles which mediate interactions between matter particles: the gluons, the weak interaction bosons (W^+,W_-, Z), and the photon.

Today we know 6 leptons and 6 quarks. The interactions between them are mediated by gauge bosons. There are 12 gauge bosons: 8 bosons (gluons) for the strong interaction and 4 for the electroweak interaction (photon, W^+,W^-, Z). The properties of the fundamental particles are summarized in Tables 1.1,1.2 and 1.3

The experiments tell us that quarks are not free particles. They are confined inside hadrons which build up most of the matter in the universe (protons, neutrons). The electron is the most important lepton. Protons, neutrons and electrons form atoms.

The number of different interactions is much smaller then the number of particles (now we know more then hundred particles). To every interaction we associate a charge - a number which describes how strongly the particle interacts. Each interaction has its own parameter of strength - a coupling constant, which depends on the energy of the interaction. At different scales of separation different interactions are important. At cosmological scales the gravitational interaction is the most important one, at macroscopical distances it is the electromagnetic interaction. The strong and weak interaction become dominant at small distances. Table 1.4 gives a comparison of interaction strengths at a given scale.

Particle physics is studied in the framework of the Standard Model. The Standard Model is not believed to be fundamental due to its complexity, but a low energy approximation to a more fundamental theory.

In classical mechanics the Lagrangian depends on dynamical variables which are usually the coordinates and momenta of particles. Field theory is a generalization of this approach for an infinite number of particles.

The Lagrangian of the theory indicates how the particles interact with one another. Each particle corresponds to a field in a Lagrangian.

The most fundamental example of a field theory is electrodynamics. The Lagrangian of this theory is given by:

$$L_{\text{Maxwell}} = -\frac{1}{4} F_{\mu\nu} F^{\mu\nu} + e A_\mu j^\mu \tag{1.1}$$

where $A^\mu = (\phi, \vec{A})$ is the four-vector potential (fields are given by $\vec{E} = -\partial_t \vec{A} - \vec{\nabla}\phi$ and $\vec{B} = \vec{\nabla} \times \vec{A}$, respectively), $F^{\mu\nu} = \partial^\mu A^\nu - \partial^\nu A^\mu$ is the antisymmetric field strength tensor. The first term describes the dynamics of the electromagnetic field, the second term contains a four-dimensional current which describes the spacial distribution and moving of the electric charges.

This simple Lagrangian demonstrates the main ideas and methods used to construct models such us the Standard Model.

The next step is to turn electrodynamics into a quantum theory. We have to take into account the creation and annihilation of particles according to

Table 1.1: Leptons (Spin 1/2)

Lepton	Charge	Mass (MeV)	Lifetime	Principal decays
e	-1	0.511003	∞	stable
ν_e	0	0	∞	stable
μ	-1	105.659	2.197*10^{-6}	e$\nu_\mu\overline{\nu_e}$
ν_μ	0	0	∞	stable
τ	-1	1784	3.3*10^{-13}	$\nu\nu_\tau\overline{\nu_\mu}$, $e\nu_\tau\overline{\nu_e}$, $\rho\nu_\tau$
ν_τ	0	0	∞	stable

Table 1.2: *Quark quantum numbers: charge Q, baryon number B, strangeness S, charm c, "beauty" or bottomness b, and "truth" or topness t.*

name	symbol	Q	B	S	c	b	t
up	u	$\frac{2}{3}$	$\frac{1}{3}$	0	0	0	0
down	d	$-\frac{1}{3}$	$\frac{1}{3}$	0	0	0	0
strange	s	$-\frac{1}{3}$	$\frac{1}{3}$	-1	0	0	0
charm	c	$\frac{2}{3}$	$\frac{1}{3}$	0	1	0	0
bottom	b	$-\frac{1}{3}$	$\frac{1}{3}$	0	0	-1	0
top	t	$-\frac{1}{3}$	$\frac{1}{3}$	0	0	0	1

Table 1.3: Gauge bosons (mediators) (Spin 1)

Mediator	Charge (Electrical)	Mass (MeV)	Lifetime	Force
gluon	0	0	∞	strong
photon (γ)	0	0	∞	electromagnetic
$W^{\pm}$	± 1	81800		(charged) weak
Z^0	0	92600		(neutral) weak

the principle of uncertainty.

The Lagrangian of QED is:

$$L_{\mathrm{QED}} = -\frac{1}{4}F_{\mu\nu}F^{\mu\nu} + \overline{\psi}(i\not{\partial} - m)\psi - e\overline{\psi}\not{A}\psi \,. \tag{1.2}$$

The first term is the kinetic term for the photon field (EM field). The second term describes the quantum nature of the electron field. This term is called Dirac term. The last term in the Lagrangian is the interaction term. It describes how the electron creates the electromagnetic field, and how the field affects the electron. Based on this simple function we can compute the QED observables - such as the electron-positron scattering cross section, the hyperfine structure of the hydrogen atom, the magnetic moments of electron and muon. QED is the most precise theory of physics.

The Lagrangian of QED has the important property of local gauge invariance. Gauge invariance is a freedom to transform the local phase of the electron field without affecting the physics of the theory. Mathematically it means that the Lagrangian will not change if we transform in each point the phase of the electron field.

$$\psi \to \psi' \equiv \exp[i\alpha(x)]\ \psi \,. \tag{1.3}$$

This invariance dictates the form of the interaction term between the electron and photon fields.

Table 1.4: *Relative strength of the four forces for two protons inside a nucleus.*

Type	Relative Strength	Field Particle
Strong	1	gluons
Electromagnetic	10^{-2}	photon
Weak	10^{-6}	$W^{\pm}$ Z^0
Gravitational	10^{-38}	graviton

This is also important for building the Lagrangian of Quantum Chromodynamics - the theory which describes the strong interactions. To construct the Lagrangian of QCD, we need to agree how quarks interact between one another through the gluon field. The form of this interaction is dictated by local gauge invariance. In analogy to QED each quark is represented by a Dirac particle. To account for the complexity of the strong interaction phenomena we need to generalize the group of local gauge transformations. Particle can not only change its phase from point to point, but also other quantum numbers (color) change. The gauge group of QCD is SU(3). The physics of the strong interactions will not change if we transform locally the phases and the colors of the quarks. The color of the quarks are conveniently named blue, green, and red.

To account for the gauge transformations, the gauge field (gluon field) is not just a function of space and time, but a matrix function of space and time. Each field becomes a matrix, each element of which is a function of space-time itself.

The Lagrangian of QCD has the following form:

$$L_{\mathrm{QCD}} = \bar{q}_j(i\gamma^\mu\partial_\mu - m)q_j + g_s(\bar{q}_j\gamma^\mu t_a q_j)G^a_\mu - \frac{1}{4}G^a_{\mu\nu}G^{\mu\nu}_a \ , \qquad (1.4)$$

where q_1, q_2, and q_3 denote the three color fields. Just one quark flavor is presented for simplicity. Gauge invariance requires the 8 gluons to restore the invariance of the Lagrangian. A mass term for the gluon field is not allowed since it will spoil gauge invariance. Hence the gluon is massless by construction of the theory.

From the Lagrangian we can see that QCD is a very simple theory, based solely on symmetry arguments. One of the important features of QCD is the absence of free parameters (except for the quark masses).

The self-interaction of gluons leads to the important result of asymptotic freedom. At very small distances the quarks behave as free particles. Their QCD color charges become almost zero, due to antiscreening of charge provided by the gluon self-interactions.

An important property of QCD is the quark confinement. In experiments one has never observed free quarks. The quarks are confined in hadrons, because the strong force rises with distance (gluons self-interactions play again a crucial role here). One believes that the theory of QCD has this property.

We discussed the two main interactions in the standard model Lagrangian - the electromagnetic and strong interactions. The third interaction is the weak interaction.

According to the principle of uncertainty, the interaction has an infinite range if it has a massless mediator. This is the case for the electromagnetic and strong interactions. If the mediator is massive, the interaction is limited to a certain distance. This is the case for weak interactions. They are mediated by the massive gauge bosons $W^{\pm}$ and Z. The properties of the gauge bosons can be seen in the table.

The weak interaction plays an important role in nuclear physics (e.g. in the neutron decay). There is no particular name for the weak force charge. We shall call it the weak charge. All quarks and leptons carry a weak charge. They can emit or absorb quantas of weak field - the weak gauge bosons.

We can summarize our knowledge about the particle interactions by giving rules what quanta particles can emit and which quanta they can absorb. The laws of particle physics can be presented in a form of Feynman diagrams depicting the most fundamental processes of emission or absorption of mediators by matter. All other processes can be built from this simple ones by a set of specific rules. A numerical value can be attributed to each particular diagram.

The interactions are given by the following Feynmann diagrams:

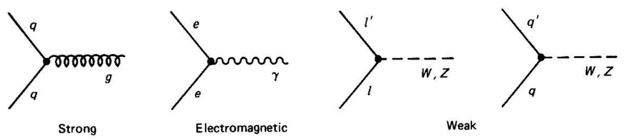

Each diagram represents a process of emitting quanta of force, time proceeds from bottom to top. We see that leptons can emit photons and weak bosons. Quarks participate in all interactions.

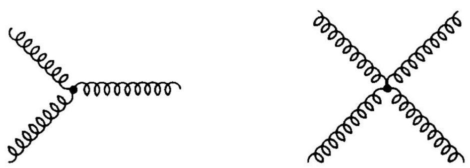

This picture depicts the fact that gluon can emit or absorb another gluon (self interaction).

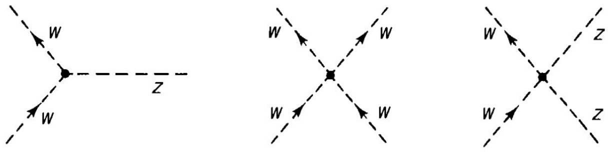

Weak bosons can also interact with one another, as well with the photon (see the pictures above and below).

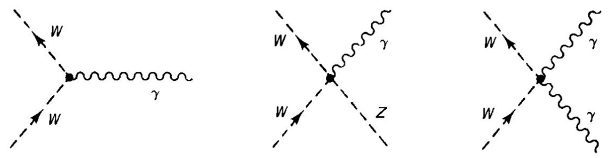

The strength of an interaction depends on the scale (energy of the reaction). It is believed that the strength of the electromagnetic, strong and weak interactions becomes the same at high energy ("Grand Unification"). At the energy of the Grand Unification there is only one interaction, one coupling, and one gauge group. There has been many attempts to build such a theory, based e.g. on the gauge groups SU(5) and SO(10), but thus far it remains unclear, weather such theories are correct.

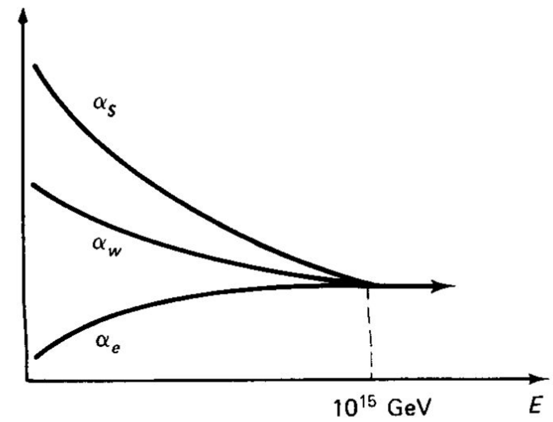

Figure 1.1: Unification of the coupling constants

References

- Introduction to Elementary Particles, by David Griffiths
- Handbook of Particle physics, by M.K. Sundaresan

- The Experimental Foundations of Particle Physics, by Robery Cahn and Gerson Goldhaber

Creation and development of QCD is captivatingly described by Prof. Harald Fritzsch, one of the founders of QCD, in the series of articles:

- The Development of Quantum Chromodynamics, 1984
- QCD - 20 years later, 1992
- QCD and Heart of the Matter, 1994

1.2 The Proton

The proton is the nucleus of the lightest element in the Universe - the hydrogen. It is positively charged and has a mass of 938.27231 ± 0.00028 MeV. The proton is a fermion, and according to the spin-statistics theorem has spin $\frac{1}{2}\hbar$. The proton is one of the hadrons, the particles participating in the strong interactions. If we describe the proton by the Dirac equation, we will find that its magnetic moment is equal $\frac{e}{2M_{proton}}$ (nuclear magneton).The experiments however show considerable deviation from this value. The experimental value is $2.79284739 \pm 0.00000006$ nuclear magnetons. Thus the proton is not a structureless particle like the electron. A theoretical calculation of the proton magnetic moment is not possible. For this we need to know the exact dynamics of the quarks and gluons inside the proton.

Using electron or positron scattering off the proton, we can study its electromagnetic structure, the spacial distribution of its charge. The proton structure is parametrized in terms of form factors and has been measured in a wide range of energies, and wide range of momentum transfer from incident electron to the proton.

Using neutrinos instead of electrons, we can measure the weak form factors of the proton.

Elastic electron-proton scattering

The electron scattering off the proton target in the first approximation can be modeled as an exchange of a single virtual photon between them. The scattering of a relativistic electron ($E >> m_e$) off a known charge distribution can be calculated using methods of quantum mechanics. In case of spinless electron scattered from a static point charge, the cross section would be given by the Rutherford formula:

$$\frac{d\sigma}{d\Omega} = \frac{\alpha^2}{4E^2 \sin^4 \frac{1}{2}\theta} \tag{1.5}$$

where E is the energy of incident electron and θ is its scattering angle in the laboratory frame. If we take into account the electron spin, we have the Mott cross section:

$$\frac{d\sigma}{d\Omega} = \frac{\alpha^2 \cos^2 \frac{1}{2}\theta}{4E^2 \sin^4 \frac{1}{2}\theta} \tag{1.6}$$

The cross section for an electron scattered off a Dirac point particle is:

$$\frac{d\sigma}{d\Omega} = \frac{\alpha^2 \cos^2 \frac{1}{2}\theta}{4E^2 \sin^4 \frac{1}{2}\theta} \frac{E'}{E}[1 - \frac{q^2}{2m^2} \tan^2 \frac{1}{2}\theta] \tag{1.7}$$

where E' is the energy of scattered electron, $q^2 = -4E^2 \sin^2 \frac{1}{2}\theta$ is the four-momentum transfer squared from electron to the Dirac particle, and M is the Dirac particle mass. This cross section reduces to the Mott formula for infinite mass of the scattering source.

In case of a spatially distributed charge the cross

$$F(q^2) = \int d^3r \exp^{i\mathbf{qr}} \rho(r) \tag{1.8}$$

so that the Rutherford or Mott cross sections will be multiplied by the factor $\left|F(q^2)\right|^2$. In case of zero momentum transfer the form factor reduces to unity since $\int d^3r\rho(r) = 1$ (the total charge is equal to 1).

The relativistic scattering amplitude for the electron proton scattering is given by the product of three factors:

$$M = \frac{4\pi\alpha}{q^2} J_{\mu}^{electron}(q) J^{\mu}_{proton}(q) \tag{1.9}$$

where q is the four-momentum exchange between the electron and proton. The factor $\frac{1}{q^2}$ arises from one photon exchange between electron and proton currents.

The electron current has the following form:

$$J_{\mu}^{electron}(q) = \overline{u}(k_f)\gamma_{\mu}u(k_i) \tag{1.10}$$

where k_i and k_f are the initial and final momenta, $\overline{u}$ and u are Dirac spinors describing the electron state. The electromagnetic current for the proton involves two from factors:

$$J_{\mu}^{proton} = \overline{u}(p_f)[F_1(q^2)\gamma_{\mu} + i\frac{q^{\nu}\sigma_{\mu\nu}k}{2M}F_2(q^2)]u(p_i) \tag{1.11}$$

In this equation p_i and p_f are initial and final momenta of the proton and $q = k_i - k_f = p_f - p_i$ is the four-momenta transfer. The term proportional to form factor $F_2(q^2)$ is the anomalous magnetic moment coupling, and $k = 1.79$ is the anomalous magnetic moment of the proton in units of the nuclear magneton, $\frac{e\hbar}{2Mc}$. The form factors $F_1(q^2)$ and $F_2(q^2)$ are analogues of the form factor F mentioned above for the fixed charge distribution. In case of zero momentum transfer $F_1(q^2) = F_2(q^2) = 1$. If the proton were a point-like Dirac particle like the electron we would have $F_1(q^2) = 1$ and $F_2(q^2) = 0$. In case of the neutron the total charge is zero and $F_1(q^2) = 0$. The value of the anomalous magnetic moment for the neutron is $k = -1.91$. It is impossible at the moment to calculate the anomalous magnetic moments of the proton and neutron from basic principles, but it is possible to calculate their ratio based on a simple SU(6) quark model. We can now write the formula for the electromagnetic structure of the proton (Rosenbluth formula):

$$\frac{d\sigma}{d\Omega} = \frac{\alpha^2 \cos^2 \frac{1}{2}\theta}{4E^2 \sin^4 \frac{1}{2}\theta} \frac{E'}{E}[(F_1^2 + \frac{k^2 Q^2)}{4M^2} F_2^2) + \frac{Q^2}{M^2}(F_1 + kF_2)^2 \tan^2 \frac{1}{2}\theta] \quad (1.12)$$

where θ is the scattering angle in the laboratory frame and E is its initial energy. We wrote Q^2 for $-q^2$, so Q^2 is positive.

The Rosenbluth crossection formula follows from the assumption of a single photon exchange between the electron and the proton. The effect of the proton structure is encoded in two unknown form factors, which are functions of momenta. The formula can be experimentally verified by multiplying observed cross section by $\frac{E^3}{E'} \sin^2 \frac{1}{2}\theta \tan^2 \frac{1}{2}\theta$ and plotting the result at fixed momentum transfer Q^2 as a function of $\tan^2 \frac{1}{2}\theta$. The outcome should be a straight line.

The elastic electron-proton scattering was measured in 1956 by McAllister and Hofstadter using 188-MeV electrons at Stanford.

They could extract the root-mean square charge radius of the proton, by measuring the form factors at low momentum transfer. In this region the following expansion is valid:

$$F(q^2) = \int d^3 r \rho(r) \exp i\mathbf{qr} = \int d^3 r \rho(r)[1 + i\mathbf{qr} - \frac{1}{2}(\mathbf{qr})^2 \ldots] = 1 - \frac{\mathbf{q}^2}{6} < r^2 > \ldots \quad (1.13)$$

With assumption that $< r^2 >$ is the same for both form factors, it was found that $\sqrt{< r^2 >} = 0.74 \pm 0.24 fm$

Similar form factors exist for processes like $ep \to e\Delta(1232)$. The form factors should decrease with momentum transfer, reflecting the spread in charge and current distributions of the initial and final particles.

At high energy the electron beam is able to disintegrate the proton. There is no final state proton, but instead we have many different final state particles. Such a scattering is called deep inelastic scattering. Usually only the final state electron is detected, and the rest are fragments of the initial proton in form of different hadrons.

1.3 Deep Inelastic Scattering

The first deep inelastic scattering was carried out at SLAC in the late 1960s with a 18 GeV electron beam. The scattered electrons were measured by a magnetic spectrometer. Typical processes at this energies were $ep- > ep\pi\pi\ldots$ or $ep- > en\pi\pi\ldots$. In case of inelastic scattering the energy and direction of the scattered electron are independent variables (contrary to elastic case, see Rosenbluth formula).The four-momentum transfer can be calculated from the measurement of direction in solid angle $d\Sigma$ and the energy E' of the scattered electron. The differential cross section $\frac{d\Sigma}{d\Omega dE'}$ is determined as a function of E' and Q^2. The outgoing hadrons were generally not detected. The kinematics is shown in the picture (picture).

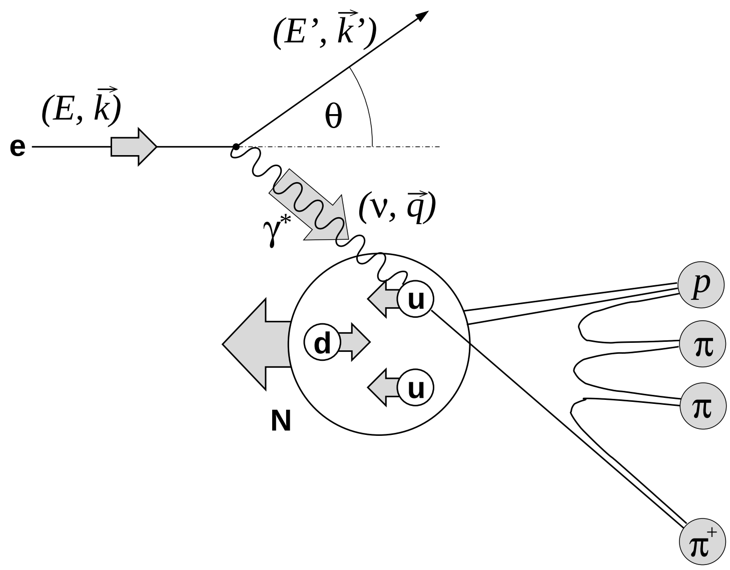

The surprising result of the first DIS experiments was that for the mass of the hadronic system (final debris of the initial proton) W the cross section did not fall with increasing Q^2. Similar to the case of elastic scattering we can write down a general expression for the cross section for electron proton scattering when only the final electron is detected. The inelastic cross section depends on two functions, W_1 and W_2. These structure functions depend on two variables, ν, the energy lost by the electron in the laboratory, and Q^2 - the four-momentum transfer.

$$\frac{d\Sigma}{d\Omega dE'} = \frac{\alpha^2 \cos^2 \frac{1}{2}\theta}{4E^2 \sin^4 \frac{1}{2}\theta}[W_2 + 2W_1 \tan^2 \frac{1}{2}\theta] \tag{1.14}$$

This cross section is analogous to the Rosenbluth formula (elastic case). Again we assume single photon exchange and parametrize the unknown physics in two structure functions. The important difference is that the structure functions became dependent on two variables ν and Q^2, not just one. For elastic scattering these variables are related - $(P+q)^2 = M^2$, so $Q^2 = 2M\nu$. To determine W_1 and W_2 separately, it is needed to measure the cross section at two different values of E' and θ that correspond for the same values of ν and Q^2. This is possible by varying the incident energy E.

The experiment at SLAC revealed that the quantity νW_2 did not fall off with increasing momentum transfer, but approached a value that depended on the single variable $\omega = \frac{2M\nu}{Q^2}$. This behavior was called scaling, and had been anticipated first by Bjorken.

Independently Feynman concluded from the study of DIS data that the proton should be composed of pointlike constituents. He called them partons. Each parton could carry a fraction of the proton momenta x, with a probability, described by a function $f(x)$. It was natural to assume the partons to be quarks. Thus inside of the proton would be not just quarks, but also quark antiquark pairs and gluons. The distributions function for the different quarks are $u(x), \overline{u}(x), d(x), \overline{d}(x)$ etc. The fractions of the momenta of all partons has to add up to 1:

$$\int dxx[u(x) + \overline{u}(x) + d(x) + \overline{d}(x) + \ldots] = 1 \tag{1.15}$$

The quantum numbers of the proton put another constraint:

$$\int dx[u(x) - \overline{u}(x)] = 2 \tag{1.16}$$

$$\int dx[d(x) - \overline{d}(x)] = 1 \tag{1.17}$$

$$\int dx[s(x) - \overline{s}(x)] = 0 \tag{1.18}$$

since the proton has two u quarks and one d quark, and no s quarks.

These considerations give a simple explanation for scaling of structure functions. If quarks-partons are real, then they have to be on-shell ($p^2 = m^2$) before and after being scattered by the virtual photon. In this case $p_f^2 = (p_i + q)^2 = (xP + q)^2 \approx 0$, if the masses of quarks and the proton could be ignored. This seems reasonable for a 18 GeV beam ($M_p \approx 1GeV$). From this follows:

$$Q^2 = 2xPq = 2xM\nu \tag{1.19}$$

The variable ω is simply the reciprocal of fraction x of proton momentum carried by the struck quark. In this picture we have to assume that the scattering of the electron by the proton is the incoherent (independent) sum of scattering processes by individual quarks-partons.

We can also give an interpretation of the structure functions $W_{1,2}$. If we introduce Lorentz invariant variables $2ME = s, x = \frac{Q^2}{2M\nu}, y = \frac{\nu}{E}$, the cross section for incoherent scattering of electrons by a system of Dirac fermions would be:

$$\frac{d\sigma}{dy} = \frac{4\pi\alpha^2 xs}{Q^4}\frac{1}{2}[1+(1-y)^2] - \frac{M}{2E}xy \tag{1.20}$$

If we express the cross section defining $W_{1,2}$ in terms of new variables and compare with the formula above we will get the following expression of the structure functions in the parton model:

$$\begin{aligned} W_1 &= \frac{1}{2M}[\frac{4}{9}u(x) + \frac{1}{9}d(x) + \frac{4}{9}\overline{u}(x) + \frac{1}{9}\overline{d}(x) + \ldots] \\ W_2 &= \frac{x}{\nu}[\frac{4}{9}u(x) + \frac{1}{9}d(x) + \frac{4}{9}\overline{u}(x) + \frac{1}{9}\overline{d}(x) + \ldots] \end{aligned} \tag{1.21}$$

The factors in front of the distribution functions arise from squares of the quark charges. The relation $\nu W_2 = 2xMW_1$ know as the Callan-Gross relation, follows since the quarks are fermions with spin $\frac{1}{2}$. This relation can be verified experimentally.

QCD explains why Feynman's assumption of incoherent scattering of several fermion sources give the correct result. This is due to the asymptotic freedom. At very high energies the strong interaction between quarks becomes very weak. We can treat them as almost free particles and thus justify Feynman assumption. In reality the interaction between quarks is never zero. This will give small correction to the observed behavior of scaling. This correction can be calculated in QCD and compared with experiment. The comparison is shown in the picture. Thus scaling is only an approximate feature of the DIS processes.

The quark-parton model makes analogous predictions for neutrino-proton scattering:

$$\nu_\mu + nucleon \to \mu^- + hadrons \tag{1.22}$$

$$\overline{\nu_\mu} + nucleon \to \mu^+ + hadrons \tag{1.23}$$

Due to the fact that parity is not conserved in weak processes, there are more structure functions for neutrino proton scattering:

$$\frac{d\sigma^\nu}{dxdy} = \frac{G_F^2 ME}{\pi}[(1-y)F_2^\nu + y^2 xF_1^\nu + (y - \frac{y^2}{2})xF_3^\nu] \tag{1.24}$$

$$\frac{d\sigma^{\overline{\nu}}}{dxdy} = \frac{G_F^2 ME}{\pi}[(1-y)F_2^{\overline{\nu}} + y^2 xF_1^{\overline{\nu}} - (y - \frac{y^2}{2})xF_3^{\overline{\nu}}] \tag{1.25}$$

These cross section are general (we have ignored the Cabbibo angle and corrections of order $\frac{M}{E}$), and $F_1^\nu, F_2^\nu, F_3^\nu$ are functions of Q^2 and ν.

The important result of the neutrino experiments is the possibility to measure different relations between distribution functions for the quarks inside the proton:

$$\begin{aligned} F_1^{\nu} &= d(x) + \overline{u}(x) \\ F_2^{\nu} &= 2x[d(x) + \overline{u}(x)] \\ F_3^{\nu} &= 2[d(x) - \overline{u}(x)] \\ F_1^{\overline{\nu}} &= u(x) + \overline{d}(x) \\ F_2^{\overline{\nu}} &= 2x[u(x) + \overline{d}(x)] \\ F_3^{\overline{\nu}} &= 2[u(x) + \overline{d}(x)] \end{aligned}$$

From the quark model we anticipate that most of the momentum of the proton is carried by the quarks. The following prediction can be measured experimentally:

$$\frac{\sigma^{\overline{\nu}}}{\sigma^{\nu}} \approx \frac{1}{3} \tag{1.26}$$

The main assumption of the parton model is that the same quark distribution function can be applied to different processes. For an isoscalar target the electromagnetic structure function is

$$F_2 = \frac{5}{18}x(u + d + \overline{u} + \overline{d}) + \frac{1}{9}x(s + \overline{s}) \tag{1.27}$$

Neglecting the s quark contribution for $x > 0.3$, we see that it is $\frac{5}{18}$ times the corresponding neutrino scattering structure function. The experimental verification is shown in the picture:

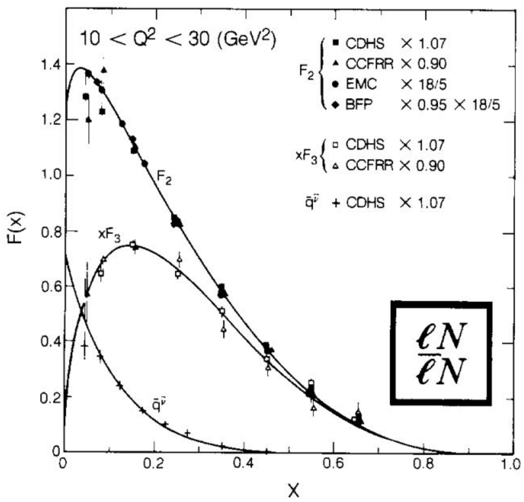

Figure 1.2: Neutrino-moun data, 1986.

Detailed studies of muon, electron and neutrino DIS have confirmed the Q^2 dependence predicted by QCD - the deviation from scaling due to the quark-gluon interactions. At high x, increasing Q^2 reduces the quark distribution due to production of quarks and gluons which share initial quark momentum. At low x, the structure functions increase with Q^2, since the momentum of the high x quark is reduced by the emission processes similar to bremstralung. These features are seen in the plot. Deviations from the parton model scaling provide indirect evidence for the existence of the gluons. Direct evidence can be found in hight energy e^+e^- collisions.

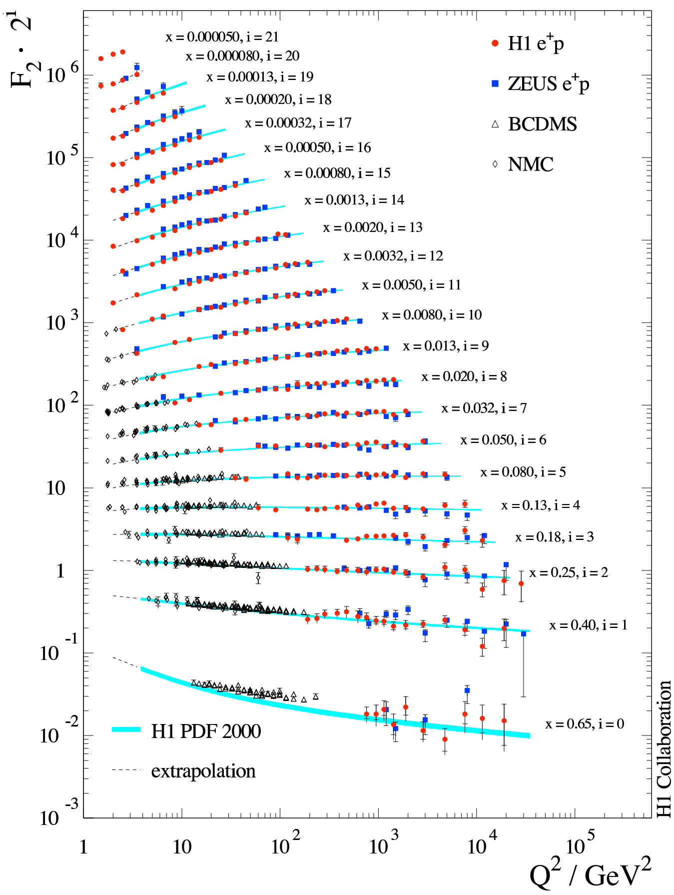

Figure 1.3: QCD fit to the structure function F2.

This gives a short account of modern methods in the studies of the proton structure. Summing up we can say that our picture of proton is formed from the knowledge accumulated at different energy scales (different distances):

- At a very big scale the proton looks like an elementary particle with static properties

- Middle range: elastic scattering, the proton looks like an extended object with inner structure.

- Small distances: inelastic scattering, the proton looks like a collection of interacting particles - quarks and gluons.

1.4 The Mystery of the Proton Spin

From electrodynamics we know that all magnets in nature are dipoles. The force lines of a magnetic field in space are equivalent to the force lines of two imaginary magnetic charges of opposite signs separated from one another. The field produced by every magnet has a preferred direction which is a line connecting two poles of the magnet (analogues of magnetic charges).

If we generalize this to point-like objects, we will have a picture of point-like particle which has a magnetic moment, i.e. the magnetic field of a magnetic dipole.

The electron has an electric charge and is a magnetic dipole. It creates a uniform electric field and a non-uniform magnetic field.

In the quark model the proton is an ensemble of free parallel-moving quarks. The spin of the proton is the sum of the spins of its quarks. The quark picture can be obtained from QCD by setting the QCD coupling constant g to 0. In that case quark fields become free fields, and the proton is a superposition of the free-quarks states. The total spin of the proton is given by:

$$\Delta\Sigma = \int_0^1 \Delta\Sigma(x)dx \tag{1.28}$$

where

$$\Delta\Sigma(x) \equiv \delta u(x) + \delta\overline{u}(x) + \delta d(x) + \delta\overline{d}(x) + \delta s(x) + \delta\overline{s}(x) \tag{1.29}$$

is the sum over quark distribution functions, x is a fraction of the proton momentum carried by the quark.

$\Delta\Sigma$ can be related to the flavor singlet axial charge of the proton:

$$g_A^{(0)} = \Delta\Sigma = 2\left\langle S_z^{quarks}\right\rangle \tag{1.30}$$

The flavor-singlet axial charge can be measured in DIS, using the following relation:

$$\int_0^1 dx\; g_1^p(x,Q^2) \;\; = \;\; \left(\frac{1}{12}g_A^{(3)} + \frac{1}{36}g_A^{(8)}\right) + \frac{1}{9}g_A^{(0)}|_{\rm inv} \tag{1.31}$$

Here $g_A^{(3)}$, $g_A^{(8)}$ and $g_A^{(0)}|_{\rm inv}$ are the isovector, SU(3) octet and scale-invariant flavour-singlet axial-charges. In terms of the nucleon matrix elements one has:

$$2Ms_\mu \Delta q = \langle p, s|\overline{q}\gamma_\mu\gamma_5 q|p, s\rangle \tag{1.32}$$

The isovector, octet and singlet axial-charges are:

$$\begin{aligned} g_A^{(3)} &= \Delta u - \Delta d \\ g_A^{(8)} &= \Delta u + \Delta d - 2\Delta s \\ g_A^{(0)}|_{\rm inv}/E(\alpha_s) \equiv g_A^{(0)} &= \Delta u + \Delta d + \Delta s. \end{aligned}$$

The left hand side of this relation is the proton spin structure function g_1 measured in the DIS experiment. Making assumptions about the behavior of this function in the experimentally inaccessible regions $x \approx 1$ and $x \approx 0$ we can calculate the integral on the left side. The isovector and octet axial charges ($g_A^{(3)}$ and $g_A^{(8)}$) can be extracted from β decays of neutrons and hyperons respectively. The present values are $g_A^{(3)} = 1.270 \pm 0.003$ [1] and $g_A^{(8)} = 0.58 \pm 0.03$ [2]. Using these values and the result of the EMC-experiment [9] one was able to extract the singlet axial charge of the proton. This charge is compatible with zero and led to the 'spin crisis'. It seems that the quarks do not contribute to the proton spin.

The present value is:

$$g_A^{(0)} = 0.33 \pm 0.03(\text{stat.}) \pm 0.05(\text{syst.}) \tag{1.33}$$

This implies that the quarks carry one third of the proton spin. The crisis arises from the discrepancy between theory and experiment. The quark model predicts this number to be 1, relativistic quark models make it smaller (around 0.6), but still much bigger then the experimental value.

There are many proposed solutions for the proton spin crisis. One of them is to include a gluonic contribution to the spin [4, 5, 6, 7]:

$$g_A^{(0)} = \left(\sum_q \Delta q - 3\frac{\alpha_s}{2\pi}\Delta g\right)_{\rm partons} + \mathcal{C}_\infty. \tag{1.34}$$

Here $\Delta g_{partons}$ is the spin carried by gluons in the polarized proton and $\Delta q_{partons}$ is the spin of quarks and antiquarks carrying small transverse momentum compare to gluon virtuality and the mass of the light quark. The gluon term can be associated with events in polarized deep inelastic scattering where the energetic proton strikes a quark or antiquark generated from photon-gluon fusion and carrying $k_t^2 \approx Q^2$

In this thesis we try to study the possible importance of the gluon angular momentum for the complete description of the proton spin structure.

The current status of the experimental and theoretical research on the spin crisis will be described in chapter 3.

Chapter 2

The Spin

2.1 History of the Spin

Otto Stern and Walter Gerlach in 1922 demonstrated that the quantization of the angular momentum is real. In their experiment a collimated beam of silver atoms passed through an inhomogeneous magnetic field onto a glass slide where the deposits formed a pattern. Classical physics predicted continuous spot of silver on the screen, but the experiment showed a clear separation of several discrete parts corresponding to different values of the angular momentum of the atoms. A historical postcard documents the result. The observed behavior is a manifestation of the spin of the unpaired electron in the atomic structure of silver.

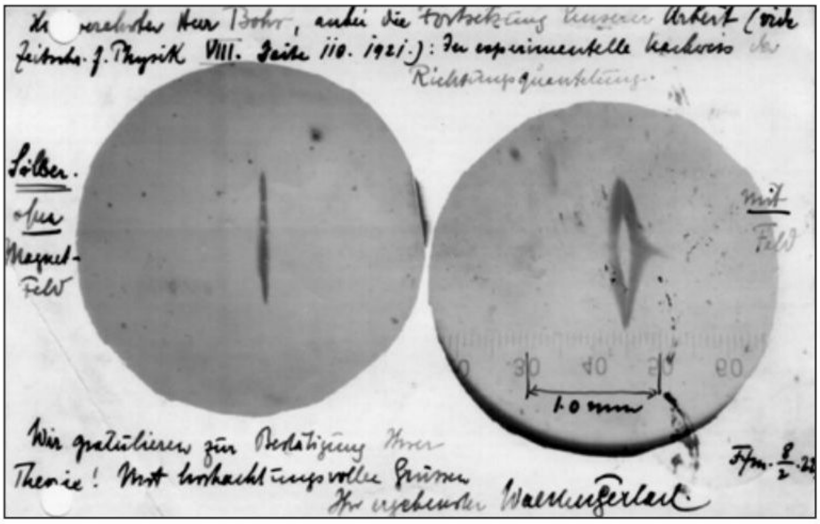

Postcard from Gerlach to Bohr. Image courtesy of Niels Bohr Archive, Copenhagen.

In the early 1920s physicists were still trying to explain the splitting of spectral lines in a magnetic field discovered by Pieter Zeeman. There were many models proposed, but most of them were unsatisfactory in explaining the experiment. A breakthrough was made by Wolfgang Pauli who conjectured that the splitting was due to an intrinsic property of the electron interacting with magnetic field: a classically indescribable two-vlauedness of the electron - as he wrote in the first of his two 1925 Zeitschrift fur Physik papers.

Later that year Pauli introduced the 'exclusion principle' - two electrons cannot be in the same quantum state. Using this principle Pauli could derive the exact structure of the atomic shell. Pauli two-valuedness of the electron can be imagined as a rotation of the electron about its own axis with one half-unit of angular momentum, the spin.

It was first suggested to Pauli by Ralph Kronig who also made calculations for level splittings, his results were factor of two different from the experiment. In 1926 Llewellyn H. Thomas could recover the missing factor of two using theory of relativity to describe electron rotation.

Pauli incorporated the spin of the electron in quantum mechanics by including two wave functions in the Schroedinger equation accounting for two possible spin orientations of the electron. Why should nature have chosen this particular model for the electron, instead of being satisfied with a point charge? Trying to answer this question, a young post doc in the University of Cambridge, Paul Dirac, discovered a correct quantum equation for a particle with spin $\frac{1}{2}$. He was able to show that the spin is a natural consequence of the correct application of special relativity to quantum mechanics of the electron. The Dirac equation is valid for any point-like charged object with spin $\frac{1}{2}$ - the quarks and leptons.

In 1932 Werner Heisenberg was puzzled by the fact that the proton and neutron had almost the same mass. Despite their different charges they behaved similar under the strong forces that dominate within the atomic nucleus. Using the same mathematics, Pauli used to describe the electron spin, Heisenberg postulated that proton and neutron were two states of the same particle the nucleon. These states differed only in a quantity analogous to spin - the ísotopic spin. In 1937 Wigner using the idea of isospin symmetry of proton and neutron predicted correctly the energies of all nuclei up to atomic number 42.

In 1935 Hideki Yukawa described the strong force by the exchange of light particles. Isospin conservation demanded three such particles, which later would be discovered, the π-mesons (π^+, π^-, π^0).

In his 1940 paper Pauli made an important connection between the spin of the particle and its quantum statistics. According to Pauli particles of half-integer spin obey Fermi-Dirac statistics, and those of integer spin obey Bose-Einstein statistics. The spin-statistics theorem explains the Pauli exclusion principle for electrons, and the absence of the exclusion principle for bosons (many bosons can occupy same state) as it happens in the Bose-Einstein condensate.

In 1970s the idea of spin and corresponding symmetries was generalized even more when the idea of supersymmetry was introduced. According to this idea all particles in the universe have their spin counterparts (superpartner). A fermion has a bosonic partner, and a boson has a fermion partner. Since none of the superssymmetric partners of normal particles have been observed so far, they have to be much more massive then their normal partners. Supersymmetry is often used in Grand Unified Theories.

2.2 Quantum Mechanics of Spin

2.2.1 Pauli equation

The Schroedinger wave equation is the basis of quantum mechanics. For the mechanical system composed of one electron it has the following form if we neglect the spin:

$$\left[H_0 + \frac{\hbar}{i}\frac{\partial}{\partial t}\right]\psi(x) = 0 \tag{2.1}$$

where

$$H_0 = \frac{1}{2m}\overline{p}^2 + V(\overline{x}) \tag{2.2}$$

$$p = (p_x, p_y, p_z) = \left(\frac{\hbar}{i}\frac{\partial}{\partial x}, \frac{\hbar}{i}\frac{\partial}{\partial y}, \frac{\hbar}{i}\frac{\partial}{\partial z}\right)$$

$\overline{x} = (x, y, z)$
(2.3)

and $\psi(x)$ is the wave function of the electron.

Pauli's problem was to modify this equation to include the electron spin. It results in two components of the wave function:

$$\psi(\overline{x}, s_z), \qquad s_z = +\frac{1}{2}, -\frac{1}{2} \tag{2.4}$$

The probability density of the electron in the point x with its spin up or down is given by:

$$\left|\psi(\overline{x}, \pm\frac{1}{2})\right| \tag{2.5}$$

To include the spin into Schroedinger's equation, we should add the energy of the spin to the full energy of the system H_0. To describe the Zeeman effect, a Hamiltonian of interaction between spin and external magnetic field has to be included Schrodinger equation:

$$H_1 = \frac{e\hbar}{2mc}[\overline{H}(\overline{l} + g_0\overline{s})] \tag{2.6}$$

Here H is an external magnetic field and l is the orbital angular momentum in units of $\hbar$

$$l_x = \frac{1}{i}(y\frac{\partial}{\partial z} - z\frac{\partial}{\partial y}), \tag{2.7}$$
$$l_y = \frac{1}{i}(z\frac{\partial}{\partial x} - x\frac{\partial}{\partial z}), \tag{2.8}$$
$$l_z = \frac{1}{i}(x\frac{\partial}{\partial y} - y\frac{\partial}{\partial x}), \tag{2.9}$$

and **s** is the spin angular momentum.

Furthermore we have to add an interaction Hamiltonian (H_2) between the internal magnetic field (caused by angular motion of the electron) and the spin magnetic moment:

$$H_2 = (g_0 - 1)\frac{e\hbar}{2mc}(\overline{H}_{int}\overline{s}) \tag{2.10}$$

The internal magnetic field can be written as:

$$\overline{H}_{int} = \frac{Ze\hbar}{mc}\frac{1}{r^3}\bar{l} \tag{2.11}$$

The operator for the spin satisfies the following commutation relations (just as any angular momentum in QM)

$$s_x s_y - s_y s_x = i s_z, \tag{2.12}$$
$$s_y s_z - s_z s_y = i s_x, \tag{2.13}$$
$$s_z s_x - s_x s_z = i s_y, \tag{2.14}$$
$$\tag{2.15}$$

The eigenvalue of the square is:

$$|\overline{s}^2| = \frac{1}{2}(\frac{1}{2} + 1) = \frac{3}{4} \tag{2.16}$$

Pauli introduced a set of 2×2 matrices to construct the operator of the spin:

$$\sigma_x = \begin{pmatrix} 0 & 1 \\ 1 & 0 \end{pmatrix}, \sigma_y = \begin{pmatrix} 0 & -i \\ i & 0 \end{pmatrix}, \sigma_z = \begin{pmatrix} 1 & 0 \\ 0 & -1 \end{pmatrix}, \tag{2.17}$$

$$s_x = \frac{1}{2}\sigma_x, \qquad s_y = \frac{1}{2}\sigma_y, \qquad s_z = \frac{1}{2}\sigma_z \tag{2.18}$$

The wave function of the electron has a two component structure:

$$\psi = \begin{pmatrix} \psi(x, +\frac{1}{2}) \\ \psi(x, -\frac{1}{2}) \end{pmatrix}, \tag{2.19}$$

The Pauli equation for the electron with spin:

$$\left[H_0 + H_1 + H_2 + \frac{\hbar}{i}\frac{\partial}{\partial t}\right]\psi(\overline{x}, s_z) = 0 \tag{2.20}$$

is a set of simultaneous differential equations for the two functions $\psi(x, +\frac{1}{2})$ and $\psi(x, -\frac{1}{2})$. For a stationary state ψ is given by:

$$\psi = \phi e^{-\frac{iEt}{\hbar}} \tag{2.21}$$

Using the Pauli equation, we can determine the energy of the stationary state by solving:

$$\left[H_0 + H_1 + H_2 - E\right]\psi(\overline{x}, s_z) = 0 \tag{2.22}$$

Pauli could calculate the level intervals within the doublet term and the anomalous Zeeman effect. Pauli noted himself that his theory is non-relativistic, since the spin degree of freedom is expressed as s_x, s_y, s_z which is a vector in (x, y, z)-space only. In order to obtain a relativistic theory, Pauli had to introduce an antisymmetric tensor in Minkowski space. Since the electron has only a magnetic moment in its rest frame, half of the six elements are zero and the remaining three correspond to Paulis spin vector. Pauli gave up creating a relativistic theory of electron, saying that its extremely difficult to apply such a condition to the spin degree of freedom. Pauli's theory introduces the electron spin angular momentum of $\frac{1}{2}$ and g_0 factor of 2 into H_1 and H_2 arbitrary. For this reasons Pauli's theory was incomplete.

2.2.2 Dirac equation

The correct relativistic theory of the electron, solving all the problems of Pauli's theory, was discovered by Paul Dirac. He could explain, why the electron has spin $\frac{1}{2}$, from basic principles of quantum mechanics and the theory of relativity.

Attempts to develop a relativistic mechanics have been made before Dirac by Schroedinger, O.Klein and W.Gordon. They arrived at the equation:

$$\frac{1}{c^2}\frac{\partial^2\psi}{\partial t^2} = \left(\frac{\partial^2\psi}{\partial x^2} + \frac{\partial^2\psi}{\partial y^2} + \frac{\partial^2\psi}{\partial z^2}\right) - \frac{m^2c^2\psi}{\hbar^2} \tag{2.23}$$

which is the simplest equation for a free particle which can reproduce the de Broglie-Einstein relation:

$$\nu^2 - (\frac{c}{\lambda})^2 = (\frac{mc^2}{h})^2, \qquad E = h\nu, p = \frac{h}{\lambda}. \tag{2.24}$$

Here ν is the frequency of the de Broglie wave and λ its wavelength. Schroedinger tried to use this relativistic equation to describe the hydrogen atom but could not obtain Sommerfelds formula for fine structure. Schroedinger conjectured that the spin of the electron has to be taken into account.

In an external field the Klein-Gordon equation has the following form:

$$\left[(-\frac{\hbar}{i}\frac{\partial}{c\partial t}+\frac{e}{c}A_0)^2-\sum_{r=1}^{3}(\frac{\hbar}{i}\frac{\partial}{\partial x_r}+\frac{e}{c}A_r)-m^2c^2\right]x\psi(x,y,z,t)=0 \quad (2.25)$$

Here A_0 and A_r are the components of the four-vector potential of the external electromagnetic field. For a free particle the Klein-Gordon equation has a solution in form of a plane wave:

$$\psi(x,y,z,t)=e^{2\pi i(\frac{z}{\lambda}-\nu t)} \quad (2.26)$$

Dirac modified the Klein-Gordon equation demanding that all derivatives are of the first order. This way he could treat time and space on equal footing as follows from the theory of relativity:

$$\left[(-\frac{\hbar}{i}\frac{\partial}{c\partial t}+\frac{e}{c}A_0)-\sum_{r=1}^{3}\alpha_r(\frac{\hbar}{i}\frac{\partial}{\partial x_r}+\frac{e}{c}A_r)-\alpha_0 mc\right]\times\psi(x,y,z,t)=0 \quad (2.27)$$

There are additional coefficients of α_r and α_0 in Dirac equation which need to be determined.

Dirac requires the square of his equation:

$$\left[(-\frac{\hbar}{i}\frac{\partial}{c\partial t})^2-\sum_{r=1}^{3}\alpha_r^2(\frac{\hbar}{i}\frac{\partial}{\partial x_r})^2-\sum_{\mu<\nu}(\alpha_\mu\alpha_\nu+\alpha_\nu\alpha_\mu)(\frac{\hbar}{i})^2\frac{\partial^2}{\partial x_\mu\partial x_\nu-\alpha_0^2m^2c^2}\right]\psi=0 \quad (2.28)$$

to be equal to the Klein-Gordon equation. Thus he finds a system of equations for the coefficients α_r and α_0:

$$\alpha_\mu^2=1 \qquad (\mu=0,1,2,3) \quad (2.29)$$

$$\alpha_\mu\alpha_\nu+\alpha_\nu\alpha_\mu=0, \qquad (\mu\neq\nu;\mu,\nu=0,1,2,3) \quad (2.30)$$

This system has only nontrivial solutions, if the coefficients α are matrices. We introduce the unit and zero 2×2 matrices:

$$\mathbf{1}=\begin{pmatrix}1&0\\0&1\end{pmatrix},\mathbf{0}=\begin{pmatrix}0&0\\0&0\end{pmatrix} \quad (2.31)$$

The solution for Dirac matrices can be constructed by blocks from Pauli matrices, thus giving 4×4 matrices:

$$\alpha_0=\begin{pmatrix}\mathbf{1}&\mathbf{0}\\\mathbf{0}&\mathbf{-1}\end{pmatrix} \qquad \alpha_1=\begin{pmatrix}\mathbf{0}&\boldsymbol{\sigma_1}\\\boldsymbol{\sigma_1}&\mathbf{0}\end{pmatrix} \quad (2.32)$$

$$\alpha_2=\begin{pmatrix}\mathbf{0}&\boldsymbol{\sigma_2}\\\boldsymbol{\sigma_2}&\mathbf{0}\end{pmatrix} \qquad \alpha_3=\begin{pmatrix}\mathbf{0}&\boldsymbol{\sigma_3}\\\boldsymbol{\sigma_3}&\mathbf{0}\end{pmatrix} \quad (2.33)$$

$$(2.34)$$

It follows that the wave function of the electron has to have 4 components:

$$\psi = \begin{pmatrix} \psi_1 \\ \psi_2 \\ \psi_3 \\ \psi_4 \end{pmatrix} \tag{2.35}$$

Instead of one differential equation of second order Dirac introduces 4 ordinary differential equations of the first order. In modern notation the Dirac equation has a very short form:

$$(i\gamma^\mu \partial_\mu - m)\psi = 0 \tag{2.36}$$

The gamma matrices satisfy the anticommutation relation:

$$\{\gamma^\mu, \gamma^\nu\} = 2\eta^{\mu\nu} \tag{2.37}$$

and can be written as:

$$\gamma^0 = \begin{pmatrix} \mathbf{1} & \mathbf{0} \\ \mathbf{0} & -\mathbf{1} \end{pmatrix}, \qquad \gamma^i = \begin{pmatrix} \mathbf{0} & \sigma^i \\ -\sigma^i & 0 \end{pmatrix} \tag{2.38}$$

The Dirac equation describes correctly the hyperfine structure of the hydrogen atom. Dirac showed that the orbital angular momentum is not a conserved quantity and that a conserved quantity is obtained only when the spin of the electron is added. The Dirac equation predicts the spin of the electron to be $\frac{1}{2}$:

$$spin = \frac{1}{2} \begin{pmatrix} \sigma & \mathbf{0} \\ \mathbf{0} & \sigma \end{pmatrix} (in\ units\ of\ \hbar) \tag{2.39}$$

In case of an external magnetic field the Dirac equation squared does not yield the Klein-Gordon equation. The difference has the form of the interaction between the external field and the magnetic moment. In this case the magnetic moment is given by:

$$magnetic \qquad moment = -\begin{pmatrix} \sigma & \mathbf{0} \\ \mathbf{0} & \sigma \end{pmatrix} (in\ units\ of\ \frac{e\hbar}{2mc}) \tag{2.40}$$

predicting the correct value for the gyro-magnetic ratio $g_0 = 2$.

Chapter 3

The Proton

3.1 QCD basics

Quarks were introduced as an explanation of the $SU(3)_f$ flavour symmetry observed in the spectrum of the lowest-mass mesons and baryons. The wave function of quarks in the spin $\frac{3}{2}$ baryons is symmetrical in the space coordinates, the spin and $SU(3)_f$ degrees of freedom. Yet the Fermi-Dirac statistics of these baryons implies that the wave function has to be totally antisymmetric. The resolution was to introduce to quarks a new degree of freedom - color. The color degree of freedom has three possible values - red, green, blue for each quark. The total wave function of the baryon, including color, becomes antisymmetric, since the color part is totally antisymmetric. The requirement that only color singlet states exist in nature has to be imposed to have agreement with experiment.

The group of the color transformations is $SU(3)$. The quarks q_a transform according to the fundamental (3×3 unitary matrix) representation and the antiquarks $\overline{q}^a$ according to the complex conjugate representation. The basic color singlet states describe the mesons $q_a\overline{q}^a$ and the baryons $\epsilon^{abc}q_aq_bq_c$, where ϵ^{abc} is a totally antisymmetric tensor.

An experimental test of the correctness of the three color idea is provided by the rate of the decay $\pi^0 \to \gamma\gamma$. The decay proceeds by the coupling of the pion to a quark loop. The rate is determined by the matrix element:

$$\langle 0 \mid J_\alpha(x)J_\beta(y)\phi(0) \mid 0\rangle = \frac{1}{f_\pi m_\pi^2}\langle 0 \mid J_\alpha(x)J_\beta(y)\partial_\mu A^\mu(0) \mid 0\rangle \tag{3.1}$$

where J_α is the electromagnetic current. The field for the neutral pion ϕ can be replaced by the divergence of the axial current A using the Golberger-Treiman relation. The pion decay constant $f_{\pi\simeq 93MeV}$ is measured in the decay $\pi^- \to \mu^-\nu_\mu$

$$\langle\mid A^\mu(0) \mid \pi(p)\rangle = if_\pi p^\mu \tag{3.2}$$

The decay rate can be calculated from the diagram above:

$$\Gamma(\pi^0 \to \gamma\gamma) = \xi^2 (\frac{\alpha}{\pi})^2 \frac{1}{64\pi} \frac{m_\pi^3}{f_\pi^2} = 7.6\xi^2 \ eV \tag{3.3}$$

The experimental value is $7.7 \pm 0.6eV$ [c 3 E]. The electric charge and colour factor ϵ for three colours of quarks is:

$$\xi = 3\left[(\frac{2}{3})^2 - (\frac{1}{3})^2\right] = 1 \tag{3.4}$$

where the factor of 3 represents the number of colors. The original calculation done before the discovery of quarks used proton and neutron as constituents and gave:

$$\xi = [(1)^2 - (0)^2] = 1 \tag{3.5}$$

Another test of the quark hypothesis is provided by the ratio R of the e^+e^- total hadronic cross section to the cross section for muon production. The virtual photon excites only the u,d and s quarks, each of which occurs in three colors. The ratio R is given by:

$$R = 3\left[(\frac{2}{3})^2 + (-\frac{1}{3})^2 + (-\frac{1}{3})^2\right] = 2 \tag{3.6}$$

For the center-of-mass energy $E_{cm} \geq 10GeV$ c and b quarks contribute to the ratio:

$$R = 3\left[(2 \times \frac{2}{3})^2 + 3 \times (-\frac{1}{3})^2\right] = \frac{11}{3} \tag{3.7}$$

The experimental data on R is in an acceptable agreement with the prediction of the three color model.

3.2 Lagrangian of QCD

The Feynman rules of QCD can be derived from the Lagrangian:

$$L_{QCD} = L_{classical} + L_{gauge-fixing} + L_{ghost} \tag{3.8}$$

The classical Lagrangian density is given by:

$$L_{classical} = -\frac{1}{4} F^A_{\alpha\beta} F^{\alpha\beta}_A + \sum_{flavours} \overline{q}_a (i\gamma_\mu D^\mu - m)_{ab} q_b \tag{3.9}$$

It describes the interaction of spin $\frac{1}{2}$ quarks of mass m and massless spin 1 gluons. Spinor indices of γ_μ and q_a have been suppressed, metric is given by $g^{\alpha\beta} = diag(1, -1, -1, -1)$ and $\hbar = c = 1$

The field stress tensor $F^A_{\alpha\beta}$ is derived from gluon field A^A_α:

$$F^A_{\alpha\beta} = [\partial_\alpha A^A_\beta - \partial_\beta A^A_\alpha - g f^{ABC} A^B_\alpha A^C_\beta] \tag{3.10}$$

indices A, B, C run over the eight colour degrees of freedom of the gluon field.g is the coupling constant which defines the strength of the interaction between colored quanta, $f^{ABC}(A, B, C = 1, \ldots, 8)$ are the structure constants of the $SU(3)$ color group.

The third term on the right-hand side gives rise to triplet and quadratic gluon self-interactions and eventually to the property of asymptotic freedom.

Quark fields are in the triplet representation of the color group ($a = 1, 2, 3$) and D is a covariant derivative which has the form:

$$(D_\alpha)_{ab} = \partial_\alpha \delta_{ab} + ig(t^C A^C_\alpha)_{ab},\ (D_\alpha)_{AB} = \partial_\alpha \delta_{AB} + ig(T^C A^C_\alpha)_{AB} \tag{3.11}$$

where t and T are matrices in the fundamental and adjoint representations of the $SU(3)$ respectively:

$$[t^A, t^B] = if^{ABC} t^C,\ [T^A, T^B] = if^{ABC} T^C,\ (T^A)_{BC} = -if^{ABC} \tag{3.12}$$

Generators t^A can be written using Gell-Mann matrices, which are hermitian and traceless:

$$t^A = \frac{1}{2}\lambda^A \tag{3.13}$$

$$\lambda^1 = \begin{pmatrix} 0 & 1 & 0 \\ 1 & 0 & 0 \\ 0 & 0 & 0 \end{pmatrix}, \lambda^2 = \begin{pmatrix} 0 & -i & 0 \\ i & 0 & 0 \\ 0 & 0 & 0 \end{pmatrix}, \lambda^3 = \begin{pmatrix} 1 & 0 & 0 \\ 0 & -1 & 0 \\ 0 & 0 & 0 \end{pmatrix}$$
$$\lambda^4 = \begin{pmatrix} 0 & 0 & 1 \\ 0 & 0 & 0 \\ 1 & 0 & 0 \end{pmatrix}, \lambda^5 = \begin{pmatrix} 0 & 0 & -i \\ 0 & 0 & 0 \\ i & 0 & 0 \end{pmatrix}, \lambda^6 = \begin{pmatrix} 0 & 0 & 0 \\ 0 & 0 & 1 \\ 0 & 1 & 0 \end{pmatrix}$$
$$\lambda^7 = \begin{pmatrix} 0 & 0 & 0 \\ 0 & 0 & -i \\ 0 & i & 0 \end{pmatrix}, \lambda^8 = \tfrac{1}{\sqrt{3}} \begin{pmatrix} 1 & 0 & 0 \\ 0 & 1 & 0 \\ 0 & 0 & -2 \end{pmatrix}$$

The conventional normalization for the $SU(N)$ matrices is chosen to be
:

$$Tr t^A t^B = T_R \delta^{AB},\ T_R = \frac{1}{2} \tag{3.14}$$

According to this normalization the colour matrices have the following relations among each other:

$$\sum_A t^A_{ab} t^A_{bc} = C_F \delta_{ac},\ C_F = \frac{N^2-1}{2N} \tag{3.15}$$

$$TrT^C T^D = \sum_{A,B} f^{ABC} f^{ABD} = C_A \delta^{CD},\ C_A = N \tag{3.16}$$

For the specific case of $SU(3)$ we have

$$C_F = \frac{4}{3},\ C_A = 3 \tag{3.17}$$

In the fundamental representation the commutator for t matrices is :

$$t^A, t^B = \frac{1}{N} \delta^{AB} I + d^{ABC} t^C \tag{3.17}$$

$$\sum_{A,B} d^{ABC} d^{ABD} = \frac{N^2-4}{N} \delta^{CD},\ d^{AAC} \equiv 0 \tag{3.18}$$

3.3 Local gauge invariance

The Lagrangian of QCD is invariant under local gauge transformations. This transformation is defined as follows:

$$q_a(x) \to q'_a(x) = exp(it\theta(x))_{ab} q_b(x) \equiv \Sigma(x)_{ab} q_b(x) \tag{3.19}$$

The covariant derivative is transforming the same way as the quark field (color indices omitted):

$$D_\alpha q(x) \to D'_\alpha q'(x) \equiv \Sigma(x) D_\alpha q(x) \tag{3.20}$$

Using the substitutions above we can obtain the transformation rules for the gauge field A:

$$D'_\alpha q'(x) = (\partial_\alpha + igt \times A'_\alpha) \sigma(x) q(x) \tag{3.21}$$

$$\equiv (\partial_\alpha \Sigma(x)) q(x) + \Sigma(x) \partial_\alpha q(x) + igt \times A'_\alpha \Sigma(x) q(x) \tag{3.22}$$

$$t \times A_\alpha \equiv \sum_A t^A A^A_\alpha \tag{3.23}$$

Thus we find that the gluon field transforms as:

$$t \times A'_\alpha = \Sigma(x) t \times A_\alpha \Sigma^{-1}(x) + \frac{i}{g}(\partial_\alpha \Sigma(x))\Sigma^{-1}(x) \tag{3.24}$$

From this follows that the non-Abelian strength tensor should transform as:

$$t \times F_{\alpha\beta}(x) \to t \times F'_{\alpha\beta}(x) = \Sigma(x) t \times F_{\alpha\beta}(x) \Sigma^{-1}(x) \tag{3.25}$$

We can derive same result using the relation:

$$[D_\alpha, D_\beta] = igt \times F_{\alpha\beta} \tag{3.26}$$

The QCD field strength tensor is not gauge invariant because of the self-interaction of the gluons. The gluons are them selfs colored and can interact with one another, unlike the electrically neutral photon in QED.

There is no gauge invariant way to include a mass term for the gluon field. A mass term:

$$m^2 A^\alpha A_\alpha \tag{3.27}$$

is not gauge invariant. Mass terms for quarks are allowed since they obey local gauge invariance.

3.4 Feynman rules for QCD

It is impossible to use perturbation theory with the classical Lagrangian of QCD without a gauge fixing term, since the propagator for the gluon field cannot be defined without specifying the gauge. The choice:

$$L_{gauge-fixing} = -\frac{1}{2\lambda}(\partial^\alpha A^A_\alpha)^2 \tag{3.28}$$

fixes the class of covariant gauges with gauge parameter λ. In a non-Abelian theory such as QCD a gauge fixing term must be supplemented with a ghost Lagrangian, which is given by:

$$L_{ghost} = \partial_\alpha \eta^{A\dagger}(D^\alpha_{AB}\eta^B) \tag{3.29}$$

Here η^A is a complex fermionic field. The ghost Lagrangian can be derived using the Feynmann path integral formalism and the procedures due to Fadeev and Popov . The ghost fields are canceling unphysical degrees of freedom in covariant gauges.

The Feynmann rules are defined from the operator:

$$S = i\int L d^4x \tag{3.30}$$

We can separate the Lagrangian into two pieces, the free piece which has all the terms bilinear in the fields and the interaction piece which has higher derivatives of the fields:

$$S = S_0 + S_I,\ S_0 = i \int L_0 d^4x,\ S_I = i \int L_I d^4x \tag{3.31}$$

Using the free part L_0 of the QCD Lagrangian, one can obtain the quark and gluon propagators. The inverse fermion propagator in the momentum space can be found by identifying $\partial^\alpha = -ip^\alpha$ for an incoming field. In momentum space the two-point function of the quark field depends on a single momentum p :

$$\Gamma^2_{ab}(p) = -i\delta_{ab}(\gamma_\mu p^\mu - m) \tag{3.32}$$

is an inverse of the propagator shown in Fig NN. The inverse propagator of the gluon field is found to be:

$$\Gamma^{(2)}_{AB,\alpha\beta}(p) = i\delta_{AB}\left[p^2 g_{\alpha\beta} - (1 - \frac{1}{\lambda})p_\alpha p_\beta\right] \tag{3.33}$$

Without the gauge fixing term this function would have no inverse. The gluon propagator is given by:

$$\Gamma^{(2)}_{AB,\alpha\beta}(p)\Delta^{(2)}_{BC,\beta\gamma}(p) = \delta^C_A g^\gamma_\alpha \tag{3.34}$$

$$\Delta^{(2)}_{BC,\beta\gamma}(p) = \delta_{BC}\frac{i}{p^2}\left[- g_{\beta\gamma} + (1-\lambda)\frac{p_\beta p_\gamma}{p^2}\right] \tag{3.35}$$

Replacing derivatives with the appropriate momenta, equations 3.9 and 3.29 can be used to derive Feynman rules for QCD.

The introduction of the gauge fixing term explicitly brakes the gauge invariance. The gauge fixing term has one extra parameter λ which does not affect the physical results of the calculations. Thus different choice of the parameter is made to simplify particular calculations. Setting $\lambda = 1$ ($\lambda = 0$) in Eq (3.35) we obtain the Feynman gauge (Landau gauge).The Feynman gauge is convenient for many purposes, reducing the number of terms in gluon propagator and making calculations simpler.

Axial gauges are fixing the gauge using an additional arbitrary vector, here denoted by n

$$L_{gauge-fixing} = -\frac{1}{2\lambda}(n^\alpha A^A_\alpha)^2 \tag{3.36}$$

The benefit of the axial gauges is that ghost fields are not required. The price for that is an increased complexity of the gluon propagator. The two-point function is:

$$\Gamma^{(2)}_{AB,\alpha\beta}(p) = i\delta_{AB}\left[p^2 g_{\alpha\beta} - p_\alpha p_\beta + \frac{1}{\lambda}n_\alpha n_\beta\right] \tag{3.37}$$

The inverse gives the gluon propagator:

$$\Delta^{(2)}_{BC,\beta\gamma}(p) = \delta_{BC}\frac{i}{p^2}\left[- g_{\beta\gamma} + \frac{n_\beta p_\gamma + p_\beta n_\gamma}{np} - \frac{(n^2+\lambda p^2)p_\beta p_\gamma}{(np)^2}\right] \tag{3.38}$$

There are new singularities at $n \cdot p = 0$.

There are several properties which make this gauges interesting. In the case of $\lambda = 0, n^2 = 0$ (light-cone gauge), the propagator becomes:

$$\Delta^{(2)}_{BC,\beta\gamma}(p) = \delta_{BC}\frac{i}{p^2} d_{\beta\gamma}(p,n) \tag{3.39}$$

where

$$d_{\beta\gamma}(p,n) = -g_{\beta\gamma} + \frac{n_\beta p_\gamma + p_\beta n_\gamma}{np} \tag{3.40}$$

In the limit $p^2 \to 0$ we find that:

$$n^\beta d_{\beta\gamma}(p,n) = 0, p^\beta d_{\beta\gamma}(p,n) = 0 \tag{3.41}$$

Only two physical polarization states orthogonal to n and p, propagate. In the limit of $p^2 \to 0$ we may decompose the numerator of the propagator into a sum over two polarizations:

$$d_{\alpha\beta} = \sum_i \varepsilon^{(i)}_\alpha(p)\varepsilon^{(i)}_\beta(p) \tag{3.42}$$

3.5 Exact symmetries

Gauge invariance is the most important exact symmetry of the QCD Lagrangian. It is responsible for the renormalizability of the theory. In addition, the QCD Lagrangian is invariant under other discrete global symmetries: the operation of parity, charge conjugation and time reversal. These discrete symmetries are in agreement with experimental observation of strong interaction processes [see PDG].

The study of these symmetries at the quantum level of QCD is complicated due to the possibility of an additional term in the Lagrangian which is also gauge invariant:

$$L_\theta = \frac{\theta g^2}{32\pi^2} F^A_{\alpha\beta}\tilde{F}^{\alpha\beta}_A \tag{3.43}$$

where $\tilde{F}$ is the dual of the gluon field strength tensor:

$$\tilde{F}^{\alpha\beta}_A = \frac{1}{2}\epsilon_{\alpha\beta\gamma\delta}F^{\gamma\delta}_A \tag{3.44}$$

This term corresponds to an interaction $E \cdot B$ in QED. It would violate parity and time reversal symmetries, in contradiction to the observed properties of strong interactions.

The term 3.43 can be written as a total divergence:

$$F^A_{\alpha\beta}\tilde{F}^{\alpha\beta}_A = \partial_\alpha K^\alpha \quad (3.45)$$

$$K^\alpha = 2\epsilon^{\alpha\beta\gamma\delta}A^A_\beta \partial_\gamma A^A_\delta - \frac{2}{3} g f^{ABC} A^B_\gamma A^C_\delta \quad (3.46)$$

Thus it does not contribute to the results calculated in perturbation theory (since it contributes only a surface term to the action). A more sophisticated non-perturbative analysis shows that L_θ can give rise to a real physical effects. The vacuum of QCD can have a non-trivial topological structure and in this case the surface term can not be neglected.

The L_θ term gives rise to a violation of the CP. The limit on the size of the parameter θ coming from the measurements of the dipole moment of the neutron is $\theta < 10^{-9}$. It is usually assumed that it is exactly zero. The unexplained smallness of the parameter θ is the strong CP problem. However this problem has no impact on the validity of perturbative QCD.

3.6 Approximate symmetry

The Lagrangian of QCD also has several approximate symmetries. They are related to the properties of the quark mass matrix. These symmetries are very important, since they provide relations between masses and matrix elements which are holding even in the strong coupling regime, where perturbation theory is not valid.

Not all classical symmetries are preserved after the quantization of the theory. A well know example is the violation of the scale invariance, which is true for QCD without quark masses at the classical level. Quantum effects lead to a violation of the scale invariance. Here we will discuss symmetries which follow from the quark mass matrix.

Consider for simplicity just two quark flavors:

$$L = \sum_{j=u,d} \overline{q}_j (i\gamma_\mu D^\mu + m) q_j \quad (3.47)$$

A global phase redefinition of the up and down fields separately leaves the Lagrangian unchanged. This corresponds to the conservation of the quark number.

It is useful to introduce a matrix notation for quark field which incorporates all the flavours:

$$q = \begin{pmatrix} u \\ d \end{pmatrix} \quad (3.48)$$

In this notation the Lagrangian is:

$$L = \overline{q}(i\gamma_\mu D^\mu + M)q \tag{3.49}$$

where

$$M = \begin{pmatrix} m_u & 0 \\ 0 & m_d \end{pmatrix} \tag{3.50}$$

If we assume that $m_u - m_d$ is very much less then the typical hadronic mass, we can approximate the matrix M by a multiple of the unit matrix. In this case there is an additional symmetry of the Lagrangian. It becomes invariant under the U(2) rotations. The general form of this transformation is:

$$q' = exp(\sum_0^3 \alpha_i \sigma_i)q \tag{3.51}$$

where $\sigma_i (i = 1, 2, 3)$ are the Pauli matrices and σ_0 is the unit matrix.

The symmetry $U(2)_V$ can be decomposed into the product of $U(1) \oplus SU(2)_V$. The U(1) is the quark number symmetry and $SU(2)_V$ is an approximate isospin symmetry, which becomes exact if quarks have the same mass.

The Noether theorem relates a conserving current to this symmetry:

$$J^i_\mu = \overline{q}\gamma_\mu \sigma^i q \tag{3.52}$$

If we include strange quarks, the approximate isospin symmetry can be extended further, though the mass difference between strange and up and down quarks suggests that this symmetry should be less reliable then the original two flavour isospin symmetry. The SU(3) isospin symmetry provides a good classification of the mesons and baryons into flavour octets and decuplets.

The symmetry group becomes bigger is we assume the quark masses to be zero. It is convenient to introduce left- and right-handed projectors:

$$\gamma_L = \frac{1}{2}(1 - \gamma_5), \gamma_R = \frac{1}{2}(1 + \gamma_5) \tag{3.53}$$

which satisfy the relations $\gamma_L^2 = \gamma_L, \gamma_R^2 = \gamma_R$ and $\gamma_L \gamma_R = 0$. The quark fields may be decomposed into left and right-handed components, $q_L = \gamma_L q, q_{R=\gamma_R q}$. In the massless limit this gives positive and negative helicity states. The quark sector of the Lagrangian becomes the sum:

$$L = \overline{q}_L i\gamma_\mu D^\mu q_L + \overline{q}_R i\gamma_\mu D^\mu q_R \tag{3.54}$$

The is no term which mixes right and left handed fields, thus there is a possibility to rotate them independently, which gives an $U(2)_L(2)_R$ symmetry:

$$q'_L = exp(\sum_0^3 \alpha_i \sigma_i) q_L,\ q'_R = exp(\sum_0^3 \beta_i \sigma_i) q_R \tag{3.55}$$

This symmetry which acts separately on left and right-handed fields is called a chiral symmetry. The associated currents are:

$$L^i_\mu = \overline{q}\gamma_\mu \gamma_L \sigma^i q R^i_\mu = \overline{q}\gamma_\mu \gamma_R \sigma^i q \tag{3.56}$$

The chiral symmetry is not manifesting itself in the observed spectrum of QCD, otherwise every hadron would have a partner of opposite parity with the same mass. The chiral symmetry is believed to be spontaneously broken, leaving only the $SU(2) \oplus U(1)$ symmetry of isospin and baryon number conservation.

The spontaneous breaking of the symmetry occurs when the solutions of the theory do not exhibit some of the symmetries of the Lagrangian of the theory. One example: the ground state of the theory (vacuum) is not invariant under the full group of symmetry transformations. The QCD vacuum has a non-zero expectation value of the light quark operator $\overline{q}q$:

$$< 0|\overline{q}q|0 >=< 0|(\overline{u}u + \overline{d}d)|0 > \simeq (250MeV)^3 \tag{3.57}$$

This vacuum expectation value is called quark condensate. The condensate connects left and right-handed fields:

$$< 0|\overline{q}q|0 > \equiv < 0|\overline{q}_L q_R + \overline{q}_R q_L|0 > \tag{3.58}$$

thus breaking the chiral symmetry, while remaining invariant under the subgroup $SU(2) \oplus U(1)$

According to the Goldstone theorem a symmetry which is spontaneously broken gives rise to massless spin-zero particles called Goldstone bosons. The number of such particles is equal to the number of broken symmetry generators.

In case of chiral $SU(2)$ the three pions π^+, π_-, π_0 are identified with the Goldstone bosons. However they are not massless, this is due to approximate property of the chiral symmetry. The $U(1)_L \oplus U(1)_R$ symmetry is also broken down to $U(1)_V$, but the missing $U(1)_A$ is destroyed by the quantum anomaly and does not give rise to a Goldstone boson. This is related to the existence of the theta term (3.43) in the Lagrangian.

In reality the quark masses are not zero thus the chiral symmetry is not exact. Nevertheless they are small compare to hadron masses allowing for the use of perturbation theory. A perturbative approach used to extract quark masses from pion masses gives $m_u \simeq 4MeV, m_d \simeq 7MeV$. The chiral perturbation theory gives a remarkably good picture of the strong interaction at the energies smaller than the proton mass.

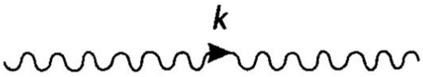

$$\frac{i}{k^2}\left[(1-\xi)\frac{k_\mu k_\nu}{k^2} - g_{\mu\nu}\right]\delta_{ab}$$

$$\frac{i}{k^2}\delta_{ab}$$

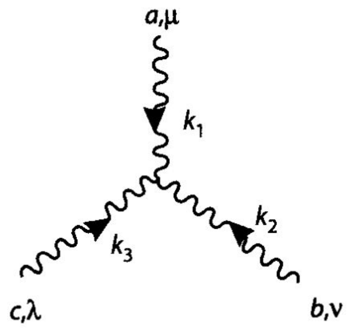

$$\begin{aligned} &gf^{abc}[g_{\mu\nu}(k_1-k_2)_\lambda \\ &\qquad + g_{\nu\lambda}(k_2-k_3)_\mu + g_{\lambda\mu}(k_3-k_1)_\nu] \end{aligned}$$

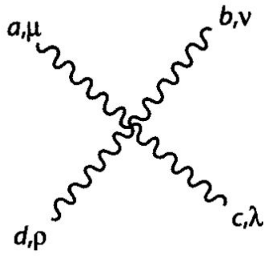

$$\begin{aligned} &-ig^2[f^{abe}f^{cde}(g_{\mu\lambda}g_{\nu\rho} - g_{\mu\rho}g_{\nu\lambda}) \\ &\quad + f^{ade}f^{cbe}(g_{\mu\lambda}g_{\nu\rho} - g_{\mu\nu}g_{\rho\lambda}) \\ &\quad + f^{ace}f^{bde}(g_{\mu\nu}g_{\lambda\rho} - g_{\mu\rho}g_{\nu\lambda})] \end{aligned}$$

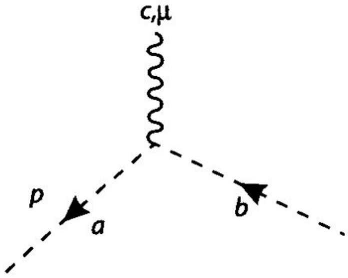

$$gf^{abc}p^\mu$$

Figure 3.1: Feynman rules for QCD, curly lines are gluons, solid lines are fermions and dotted lines are ghosts.

Chapter 4

The Spin of the Proton

4.1 Orbital angular momentum

In this subchapter we introduce methods to study the orbital angular momentum of quarks and gluons inside a nucleon. In QED without electrons the orbital angular momentum can be written as:

$$\vec{J} = \int d^3r\vec{x} \times \left(\vec{E} \times \vec{B}\right) = \int d^3r\vec{x}\times\left[\vec{E} \times \left(\vec{\bigtriangledown} \times \vec{A}\right)\right] \tag{4.1}$$

if we integrate by parts:

$$\vec{J} = \int d^3r\left[E^j\left(\vec{x} \times \vec{\bigtriangledown}\right)A^j + \left(\vec{x} \times \vec{A}\right)\vec{\bigtriangledown} \cdot \vec{E} \times \vec{A}\right] \tag{4.2}$$

We disregard the second term (due to the equation of motion $\vec{\bigtriangledown} \cdot \vec{E} = 0$) and obtain $\vec{J} = \vec{L} + \vec{S}$, where:

$$\vec{L} = \int d^3rE^j\left(\vec{x} \times \vec{\bigtriangledown}\right)A^j \qquad \vec{S} = \int d^3r\vec{E} \times \vec{A} \tag{4.3}$$

$\vec{L}$ and $\vec{S}$ are not separately gauge invariant

In QED with electrons there is additional term:

$$\vec{J}_\gamma = \int d^3r\vec{r} \times \left(\vec{E}\vec{B}\right) = \int d^3r\vec{r}\times\left[\vec{E} \times \left(\vec{\bigtriangledown} \times \vec{A}\right)\right] =$$

$$\int d^3r\left[E^j\left(\vec{r} \times \vec{\bigtriangledown}\right)A^j - \vec{r} \times \left(\vec{E} \cdot \vec{\bigtriangledown}\right)\vec{A}\right] =$$

$$\int d^3r\left[E^j\left(\vec{r} \times \vec{\bigtriangledown}\right)A^j + \left(\vec{r} \times \vec{A}\right)\vec{\bigtriangledown} \cdot \vec{E} + \vec{E} \times \vec{A}\right] \tag{4.4}$$

Replacing the second term with the equation of motion ($\vec{\bigtriangledown} \times \vec{E} = ej^0 = e\psi^\dagger\psi$), we get:

$$\vec{J}_\gamma = \int d^3r\left[\psi^\dagger\vec{r} \times e\vec{A}\psi + E^j\left(\vec{x} \times \vec{\bigtriangledown}\right)A^j + \vec{E} \times \vec{A}\right] \tag{4.5}$$

$\psi^\dagger \vec{r} \times e\vec{A}\psi$ cancells similar term in electron orbital angular momentum $\psi^\dagger \vec{r} \times (\vec{p} - e\vec{A})\psi$

Decomposing $\vec{J}_\gamma$ into spin and orbital parts shifts the angular momentum from photons to electrons.

The total angular momentum of the isolated system is uniquely defined. Ambiguities arise when $\vec{J}$ is decomposed into contributions from different constituents. Changing the gauge can also shift the angular momentum between various degrees of freedom. Decomposition of the angular momentum in general depends on the gauge and quantization schemes.

One has to always keep the same decomposition scheme in all parts of the analysis. Possible decomposition schemes for the proton spin are the Ji , Jaffe-Manohar, Chen-Goldman decompositions.

Ji decomposition:

$$J = L_q + \frac{1}{2}\Delta\Sigma + J_g \tag{4.6}$$

Jaffe-Manohar decomposition:

$$J = L_q + L_g + \Delta G + \frac{1}{2}\Delta\Sigma \tag{4.7}$$

Only the quark spin term $\frac{1}{2}\Delta\Sigma$ is common for both decompositions.

The angular momentum tensor is:

$$M^{\mu\nu\rho} = x^\mu T^{\nu\rho} - x^\nu T^{\mu\rho} \tag{4.8}$$

Conservation of angular momentum:

$$\partial_\rho M^{\mu\nu\rho} = 0 \tag{4.9}$$

implies:

$$j^i = \frac{1}{2}\epsilon^{ijk} \int d^3 r M^{jk0} \tag{4.10}$$

The total angular momentum operator contains two types of terms: the ones which has the structure $'\vec{x} \times Operator'$ and can be identified with the orbital angular momentum and the terms where the factor $\vec{x}\times$ does not appear. These terms can be identified with spin of quarks.

4.2 Ji decomposition

The spin of the proton is given by:

$$\vec{J} = \int d^3x \left[\psi^\dagger \vec{\Sigma}\psi + \psi^\dagger \vec{x} \times \left(i\vec{\partial} - g\vec{A}\right)\psi + \vec{x} \times \left(\vec{E} \times \vec{B}\right)\right] \tag{4.11}$$

where:

$$\Sigma^i = \frac{i}{2}\epsilon^{ijk}\gamma^j\gamma^k \tag{4.12}$$

Ji does not integrate the gluon term by parts, and does not identify the gluon spin/OAM separately. The Ji decomposition is valid for all components of $\vec{J}$, but usually only applied to $\vec{z}$ component, where the quark spin term has a partonic interpretation.

The advantage of such a decomposition is the manifest gauge invariance of all terms.
Deep virtual Compton scattering can be used to probe $\vec{J_q} = \vec{S_q} + \vec{L_q}$
The disadvantage is a presence of interactions in the quark orbital angular momentum.
Thus only the quark spin has a partonic interpretation as a single particle density.

Ji decomposes the proton spin as:

$$\frac{1}{2} = \sum_q J_q + J_g = \sum_q \left(\frac{1}{2}\Delta q + L_q\right) + J_g \tag{4.13}$$

$$\frac{1}{2}\Delta q = \frac{1}{2}\int d^3x \langle P, S|q^\dagger(\vec{x})\Sigma^3 q(\vec{x})|P, S\rangle \qquad \Sigma^3 = i\gamma^1\gamma^2 \tag{4.14}$$

$$L_q = \int d^3x \langle P, S|q^\dagger(\vec{x})\left(\vec{x} \times i\vec{D}\right)^3 q(\vec{x})|P, S\rangle \tag{4.15}$$

$$J_g = \int d^3x \langle P, S|\left[\vec{x}\left(\vec{E} \times \vec{B}\right)\right]^3 |P, S\rangle \tag{4.16}$$

where:

$$i\vec{D} = i\vec{\partial} - g\vec{A} \qquad P^\mu = (M, 0, 0, 1), S^\mu = (0, 0, 0, 1) \tag{4.17}$$

Δq can be accessed from polarized DIS, $J_q = \frac{1}{2}\Delta q + L_q$ can be obtained from exp/lattice (GPDs). L_q is independently defined as a matrix element of $q^{\dagger(\vec{r}\times i\vec{D})q}$. In practice it is easier to obtain it by subtraction $L_q = J_q - \frac{1}{2}\Delta q$. J_q is usually defined through $J_q = \frac{1}{2} - J_q$, but can be defined through the gluon GPDs. Ji makes no further decomposition of J_g into intrinsic (spin) and extrinsic (OAM) piece.

4.3 Jaffe-Manohar decomposition

According to Jaffe and Manohar the orbital angular momentum can be defined on a light-like hypersurface rather than a space-like hypersurface.

$$J^3 = \int d^2x_\perp \int dx^- M^{12+} \tag{4.18}$$

where

$$x^- = \frac{1}{\sqrt{2}}(x^0 - x^-) \tag{4.19}$$

and $M^{12+} = \frac{1}{\sqrt{2}}(M^{120} + M^{123})$

Since $\partial_\mu M^{12\mu} = 0$, we find:

$$\int d^2x_\perp \int dx^- M^{12+} = \int d^2x_\perp \int dx^3 M^{120} \tag{4.20}$$

In a light-cone framework and light-cone gauge $A^+ = 0$ one finds:

$$J^z = \int dx^- d^2r_\perp M^{+xy}\frac{1}{2} = \frac{1}{2}\Delta\Sigma + \sum_q L_q + \Delta G + L_g \tag{4.21}$$

In terms of matrix elements we have (here $\gamma^+ = \gamma^0 + \gamma^z$)

$$L_q = \int d^3r \langle P,S|\vec{q}(\vec{r})\gamma^+ \left(\vec{r} \times i\vec{\partial}\right)^z q(\vec{r})|P,S\rangle \tag{4.22}$$

$$\Delta G = \epsilon^{+-ij} \int d^3r \langle P,S|TrF^{+i}A^j|P,S\rangle \tag{4.23}$$

$$L_g = 2\int d^3r \langle P,S|TrF^{+j} \left(\vec{x} \times i\vec{\partial}\right)^z A^j|P,S\rangle \tag{4.24}$$

$\Delta\Sigma = \sum_q \Delta q$ can be found from polarized DIS (or lattice), ΔG can be accessed from proton-proton collisions and from polarized DIS evolution. ΔG is a gauge invariant and local operator only in the light-cone gauge. Moments of the gluon spin can be also described by a local gauge invariant operators. L_q, L_g are independently defined but there is no experiment proposed to access them, also they are not accessible in lattice simulations.

4.4 Chen-Goldman et al. decomposition

Chen, Goldman et al. integrate by parts in J_g only for term involving A_{phys}, where:

$$A = A_{phys} + A_{pure} \qquad with \qquad \bigtriangledown A_{phys} = 0 \qquad \bigtriangledown \times A_{pure} = 0 \tag{4.25}$$

$$\frac{1}{2} = \sum_q J_q + J_g = \sum_q (\frac{1}{2}\Delta q + L'_q) + S'_g + L'_g \tag{4.26}$$

Here Δq is the same as in the JM and Ji decompositions.

$$L'_q = \int d^3x \langle P,S|q(\vec{x}) \left(\vec{x} \times i\vec{D}_{pure}\right)^3 q(\vec{x})|P,S\rangle \tag{4.27}$$

$$S'_g = \int d^3x \langle P,S| \left(\vec{E} \times \vec{A}_{phys}\right)^3 |P,S\rangle \tag{4.28}$$

$$L'_g = \int d^3x \langle P,S|E^i \left(\vec{x} \times \vec{\bigtriangledown}\right)^3 A^i_{phys}|P,S\rangle \tag{4.29}$$

where $i\vec{D}_{pure} = i\vec{\partial} - g\vec{A}_{pure}$. In this decomposition only $\frac{1}{2}\Delta q$ is accessible experimentally.

4.5 The axial anomaly

The naive parton model interpretation of the EMC experiment is treating the flavour singlet axial current as the quark spin-density operator. This leads to a small contribution to the proton spin from the quark spins, $a_0 = 2S_z^{quarks} \simeq 0$, in contradiction with the Quark Model.

Proton spin in field theory

The operator $J^0_{5\mu}$ for the singlet axial current, containing quark field operators only, is the quark spin density operator for free fields. It measures the total quark spin in the initial parton state. $J^0_{5\mu}$ is not a conserved current. Its expectation value in the nucleon state where the partons interact strongly with each other is not the same as the expectation value in the initial state of free partons. In the naive parton model we ignore these interactions setting the expectation values in the nucleon and free parton states equal. Only the total J_z , not S_z, is generally conserved. There is a reason why non-conservation of $J^0_{5\mu}$ is important. From the equations of motion $J^0_{5\mu}$ is conserved for massless quarks. The non-conservation is anomalous when one works with massless quarks.

There is an important consequence of the non-conservation of $J^0_{5\mu}$. Consider the proton matrix element $\langle P|J^0_{5\mu}|P\rangle$ in the Heisenberg picture. Inserting a sum over free parton states, we have:

$$\langle P|J^0_{5\mu}|P\rangle = \int \sum |\langle k_1...k_n|P\rangle|^2 \; \langle k_1...k_n|J^0_{5\mu}|k_1...k_n\rangle \, . \tag{4.30}$$

Matrix elements like $\langle k_1...k_n|\hat{O}|k_1...k_n\rangle$ will, in general, depend on the renormalization scale μ^2. Only in case where the operator $\hat{O}$ is conserved one can show that the matrix elements are independent of μ^2. This is true for $J^3_{5\mu}$ and $J^8_{5\mu}$ with massless quarks. The expectation value of a non-conserved operator cannot have any simple physical significance. We should not think of the expectation value of $J^0_{5\mu}$ as "the physical spin of the parton" – it is not a fixed number. It depends on the value of μ^2 and it can have any value. To avoid this one should always indicate the renormalization scale, i.e. write $\langle k_1...k_n|J^0_{5\mu}|k_1...k_n\rangle_{\mu^2}$. Thus the contradiction between the proton spin measurements and theory is a property of to the naive parton model.

QCD, the Quark Model and the Naive Parton Model

Since the expectation value of $J^0_{5\mu}$ depends upon the renormalization scale μ^2, it is important to know if there is a value of μ^2 at which the expectation value agrees with the quark model result, i.e. corresponds to the physical spin of free quarks. This should happen as $\mu^2 \to 0$. There are several arguments from the perturbative domain to support this assumption.

The quark model does not contain gluons. The dynamics is given by the quark degrees of freedom. The quark momentum operator and the gluon momentum operator are not conserved in QCD, only their sum is. The momentum fractions of a hadron carried by quarks or by gluons depend on the renormalization scale. At large μ^2, where $\alpha_s(\mu^2)$ is small and perturbation theory can be trusted, the momentum fraction carried by the gluons increases to the limit 16/25 at $\mu^2 \to \infty$. Thus the gluons play a smaller role in the momentum sum rule at smaller μ^2. Similarly, the spin at scale μ carried by the gluons increases without limit as $\mu^2 \to \infty$, so that gluons contribute less in the angular momentum sum rule at lower μ^2.

These examples suggest that one is approaching the quark model as $\mu^2 \to 0$. At the other end of the scale we have the partonic picture which was invented to explain Bjorken scaling which holds as $Q^2 \to \infty$, which in the present context corresponds to $\mu^2 \to \infty$. Since $\alpha_s(\mu^2) \to 0$ as $\mu^2 \to \infty$ one does usually obtain the relationships of the naive parton model in this limit, but one has to use Q^2-dependent parton distributions.

An important exception to this rule is the gluonic contribution to the first moment of $g_1(x, Q^2)$. Here a QCD correction proportional to $\alpha_s(Q^2)$ contributes, multiplied by the gluon spin at scale Q^2, which increases like $\ln Q^2$. The logarithmic decrease of $\alpha_s(Q^2)$ as $Q^2 \to \infty$ is compensated by the increase in the gluon spin, leaving a finite, non-zero contribution as $Q^2 \to \infty$. This is linked directly to the existence of the axial anomaly in QCD.

The axial anomaly

Consider the axial current

$$J^f_{5\mu} = \bar{\psi}_f(x)\, \gamma_\mu \gamma_5\, \psi_f(x) \tag{4.31}$$

bilinear in the quark operators of definite flavour f (colour summation implied). From the free Dirac equation of motion one finds that

$$\partial^\mu J^f_{5\mu} = 2im_q \bar{\psi}_f(x)\, \gamma_5\, \psi_f(x) \tag{4.32}$$

where m_q is the mass of the quark of flavour f.

In the chiral limit $m_q \to 0$ we find that $J^f_{5\mu}$ is conserved. If this were true, there would be a symmetry between left and right-handed quarks, and as a consequence there would be a parity degeneracy of the hadron spectrum: there would exist two protons of opposite parity. As shown originally by Adler, and by Bell and Jackiw [84] (in the context of QED) the formal argument from the free equations of motion is not reliable and there is an anomalous contribution arising from the triangle diagram shown in Fig. 4.5.

This leads to a nonconservation of the axial current when $m_q = 0$. For the QCD case one has [H.Fritzsch, M.Gell-Mann and H.Leutwyler, Phys. Lett. 47B, 365 (1973)]:

$$\partial^\mu J^f_{5\mu} = \frac{\alpha_s}{4\pi} G^a_{\mu\nu} \widetilde{G}^{\mu\nu}_a = \frac{\alpha_s}{2\pi} \mathrm{Tr}\,[\boldsymbol{G}_{\mu\nu}\, \widetilde{\boldsymbol{G}}^{\mu\nu}] \tag{4.33}$$

where $\widetilde{G}^a_{\mu\nu}$ is the dual field tensor

$$\widetilde{G}^a_{\mu\nu} \equiv \frac{1}{2}\, \varepsilon_{\mu\nu\rho\sigma} G^{\rho\sigma}_a \tag{4.34}$$

and where a field vector or tensor without a colour label stands for a matrix. In this case

$$\boldsymbol{G}_{\mu\nu} \equiv \left(\frac{\boldsymbol{\lambda}_a}{2}\right) G^a_{\mu\nu}\,. \tag{4.35}$$

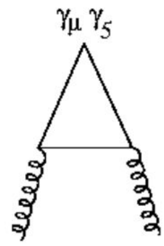

Figure 4.1: Triangle diagram giving rise to the axial anomaly.

The result (4.33), which represents a calculation of the triangle diagram (Fig. 4.5) using $m_q = 0$ and the gluon virtuality $k^2 \neq 0$, is a particular limit of a highly non-uniform function. If we take $m_q \neq\ 0,\ k^2 \neq 0$ the right hand side of (1.3.3) is multiplied by

$$T(m_q^2/k^2) = 1 - \frac{2m_q^2/k^2}{\sqrt{1 + 4m_q^2/k^2}}\ \ln\left(\frac{\sqrt{1 + 4m_q^2/k^2} + 1}{\sqrt{1 + 4m_q^2/k^2} - 1}\right). \tag{4.36}$$

This anomaly corresponds to $T \to 1$ for $(m_q^2/k^2) \to 0$. For on-shell gluons, $k^2 = 0$, and $m_q \neq 0$, i.e. in the limit $(m_q^2/k^2) \to \infty$, the terms cancel, and there is no anomaly.

The anomaly induces a pointlike interaction between $J^0_{5\mu}$ and gluons.

Using Adler's expression [84] for the triangle diagram, modified to QCD, we can write for the forward gluonic matrix element of the flavour f current ($\varepsilon_{0123} = 1$)

$$\begin{aligned} \langle k, \lambda | J^f_{5\mu} | k, \lambda\rangle &= \frac{i\alpha_s}{2\pi}\, \varepsilon_{\mu\nu\rho\sigma}\, k^\nu \varepsilon^{*\rho}(\lambda) \varepsilon^\sigma(\lambda)\, T(m_q^2/k^2) \\ &= -\frac{\alpha_s}{2\pi}\, S^g_\mu(k,\lambda)\, T(m_q^2/k^2) \end{aligned} \tag{4.37}$$

where λ is the gluon helicity and

$$S^g_\mu(k,\lambda) \approx \lambda k_\mu \tag{4.38}$$

is the covariant spin vector for almost massless gluons.

It possible to compute the gluonic contributions to the hadronic expectation value $\langle P,S|J^0_{5\mu}|P,S\rangle$. Since the gluons are bound, they will be slightly off-shell i.e. $k^2 \neq 0$, but small. The full triangle contribution involves a sum over all quark flavours. We take m_u, m_d and m_s to be $\ll k^2$, m_c, m_b and m_t are $\gg k^2$. The function $T(m_q^2/k^2)$ thus takes the values:

$$\begin{aligned} T &= 1 \quad \text{for} \quad u,\ d,\ s \\ T &= 0 \quad \text{for} \quad c,\ b,\ t \end{aligned} \tag{4.39}$$

and the gluon contribution is then given by

$$\begin{aligned} a_0^{gluons}(Q^2) &= -3\,\frac{\alpha_s}{2\pi}\int_0^1 dx\ \Delta g(x,Q^2) \\ &= -3\,\frac{\alpha_s}{2\pi}\,\Delta g(Q^2) \end{aligned} \tag{4.40}$$

or from (4.2.1)

$$\Gamma_{1p}^{gluons}(Q^2) = -\frac{1}{3}\,\frac{\alpha_s}{2\pi}\,\Delta g(Q^2)\,. \tag{4.41}$$

$\Delta g(x,Q^2)$ is the difference between the number density of gluons with the same helicity as the nucleon and those with opposite helicity. Its integral $\Delta g(Q^2)$ is the total helicity carried by the gluons. If N_f massless quark flavours contribute in the anomalous triangle, then on the right hand side of (4.41) we find:

$$1/3 \rightarrow N_f\langle e_f^2\rangle/2$$

where $\langle e_f^2\rangle$ is the mean of the squared charges.

Even though (4.33) was derived perturbatively to order α_s, it is believed to be an exact result. It was shown by Adler [84] that the anomaly is not influenced by higher order corrections at the 2-loop level. These results remain true in QCD for the matrix elements of (4.33). Further, it has been argued by Jackiw [85] that (4.33) is true even outside the perturbative domain of QCD.

The result (4.40) tells us that the naive parton model formula for a_0 (and for Γ_1^p in terms of the Δq_f) is incorrect:

$$a_0 = \Delta\Sigma \equiv \int_0^1 dx\ \Delta\Sigma(x) \tag{4.42}$$

.

Instead we have:

$$a_0 = \Delta\Sigma - 3\,\frac{\alpha_s}{2\pi}\,\Delta g \tag{4.43}$$

This means that the small measured value of a_0 does not necessarily imply that $\Delta\Sigma$ is small.

The axial gluon current $\boldsymbol{K^\mu}$ and the gluon spin

We consider the axial gluon current

$$
\begin{aligned}
K^\mu &= \frac{1}{2}\,\varepsilon^{\mu\nu\rho\sigma} A^a_\nu \left(G^a_{\rho\sigma} - \frac{g}{3}\, f_{abc} A^b_\rho A^c_\sigma \right) \\
&= \varepsilon^{\mu\nu\rho\sigma} \mathrm{Tr} \left\{ \boldsymbol{A}_\nu \left(\boldsymbol{G}_{\rho\sigma} + \frac{i}{3}\, g[\boldsymbol{A}_\rho, \boldsymbol{A}_\sigma] \right) \right\}
\end{aligned} \tag{4.44}
$$

$$
\boldsymbol{A}_\rho = \frac{\boldsymbol{\lambda}_a}{2} A^a_\rho \tag{4.45}
$$

We find:

$$
\partial_\mu K^\mu = \frac{1}{2}\, G^a_{\mu\nu} \widetilde{G}^{\mu\nu}_a = \mathrm{Tr}\,(\boldsymbol{G}_{\mu\nu}\, \widetilde{\boldsymbol{G}}^{\mu\nu})\,. \tag{4.46}
$$

If $m_q = 0$, the modified current

$$
\widetilde{J}^f_{5\mu} \equiv J^f_{5\mu} - \frac{\alpha_s}{2\pi}\, K_\mu \tag{4.47}
$$

is conserved: $\partial^\mu \widetilde{J}^f_{5\mu} = 0$.

The matrix elements of the modified singlet axial current

$$
\widetilde{J}^0_{5\mu} \equiv J^0_{5\mu} - N_f\, \frac{\alpha_s}{2\pi}\, K_\mu \tag{4.48}
$$

are independent of the renormalization scale and should correspond to the value obtained in the Quark Model (no gluons; approximately $SU(6)$ quark wave function) i.e.

$$
\langle P,S|\widetilde{J}^0_{5\mu}|P,S\rangle = 2M\tilde{a}_0 S^\mu\,, \tag{4.49}
$$

We expect $\tilde{a}_0$ independent of Q^2 and thus $\tilde{a}_0 \simeq 1$.

Many of the operators corresponding to standard dynamical observables are not gauge-invariant in a local gauge theory. In the gauge $A^a_0(x) = 0$ the gluon spin operator $\hat{\boldsymbol{S}}^g$ becomes

$$
\hat{S}^g_i = -\varepsilon_{ijk} A^j_a \partial^0 A^k_a\,. \tag{4.50}
$$

In this gauge the cubic term vanishes for the spatial components of the vector K^μ and one finds

$$
K_i = -\hat{S}^g_i \qquad (\text{gauge } A^0_a = 0)\,. \tag{4.51}
$$

We consider the hadronic expectation value of K^μ in the gauge $A_0 = 0$. We find,

$$
\langle P,S|K^\mu|P,S\rangle = -2M\, S^\mu(P)\,\Delta g\,. \tag{4.52}
$$

We should consider the question of the gauge dependence of this relation. The current K^μ is not gauge invariant. In QED there is no cubic term (since it is an Abelian theory), and the gauge transformation induced in K^μ as a consequence of

$$A_\mu(x) \to A_\mu(x) + \partial_\mu \Lambda(x) \tag{4.53}$$

can be written in the form

$$K_\mu(x) \to K_\mu(x) - \frac{1}{2}\,[\partial^\nu \Lambda(x)]\,\varepsilon_{\mu\nu\rho\sigma} F^{\rho\sigma}(x) \tag{4.54}$$

Here we use the fact that $F^{\mu\nu}$ is gauge invariant in QED. Though $K_\mu(x)$ changes, its forward matrix elements, or expectation values do not, since the expectation value of $F^{\rho\sigma}(x)$ vanishes. In QED $F^{\rho\sigma}$ is related to $A_\mu(x)$ via derivatives, and one may use $[\hat{P}_\mu, f(x)] = -i\partial f/\partial x^\mu$.

In QCD, using

$$\boldsymbol{A}_\mu \to \boldsymbol{U}\boldsymbol{A}_\mu\boldsymbol{U}^{-1} + \frac{i}{g}(\partial_\mu \boldsymbol{U})\boldsymbol{U}^{-1} \tag{4.55}$$

one has

$$\boldsymbol{G}_{\mu\nu} \to \boldsymbol{U}\boldsymbol{G}_{\mu v}\boldsymbol{U}^{-1} \tag{4.56}$$

One obtains:

$$\begin{aligned} K_\mu \quad &\to \quad K_\mu + \frac{2i}{g}\,\varepsilon_{\mu\nu\alpha\beta}\,\partial^\nu \mathrm{Tr}(\boldsymbol{A}^\alpha \boldsymbol{U}^{-1}\partial^\beta \boldsymbol{U}) \\ &+ \quad \frac{2}{3g^2}\,\varepsilon_{\mu\nu\alpha\beta}\,\mathrm{Tr}\{\boldsymbol{U}^{-1}(\partial^\nu \boldsymbol{U})\boldsymbol{U}^{-1}(\partial^\alpha \boldsymbol{U})\boldsymbol{U}^{-1}(\partial^\beta \boldsymbol{U})\}\,. \end{aligned} \tag{4.57}$$

The second term in the right hand side of (4.57) is a total divergence and gives zero contribution to the expectation value of K_μ. The third term can also be shown to be a divergence [86]. It cannot be discarded because of the non-trivial topological structure of QCD. We may ignore the last term for “small" gauge transformations, i.e. those continuously connected to the unit transformation $\boldsymbol{U} = \boldsymbol{I}$, but it is not possible to ignore it for “large" (topologically non-trivial) gauge transformations.

4.6 Experiments studying the spin structure

Bjorken considered it very difficult to test his sum rule when he first derived it 40 year ago, since the experimental technology needed to test it was not available. In late 70s the first experiments at SLAC [21, 22, 23, 24] using polarized electrons seemed to confirm the expectations of the naive quark parton model. The range in x covered was rather limited, and the data had large errors and were taken at fairly low Q^2. These experiments started the exploration of the nucleon spin structure, not only in the DIS region, but also in the region of the nucleon resonances [23].

The EMC collaboration [9] used the polarized muon beam at CERN, with much higher beam energy then the SLAC experiments, together with a polarized proton target. The EMC experiment extended the x-range down to significantly lower $x \approx 0.01$. Combined with the earlier SLAC data, their result seemed to indicate that the proton spin was not due to the helicities of the quarks. This violated the Ellis-Jaffe sum rule [10] within the simple quark-parton picture assuming that SU(3) is a good symmetry and the strange (sea) quark contribution to the nucleon spin could be ignored.

This puzzling result lead to the development of several new experiments that had to verify the data on the proton with greater precision and test the Bjorken sum rule [12] by probing the spin structure of the neutron as well. This required the use of targets containing polarized neutrons.

The Spin Muon Collaboration used large dynamically polarized cryogenic deuteron [28] and proton [29] targets to extract information on the neutron and to improve on the statistics of the EMC result. SMC pioneered the use of semi-inclusive data, where a leading hadron is identified in coincidence with the scattered lepton, to get more information on the contribution of various quark flavors to the nucleon spin [30]. The complete data set collected by the SMC resulted in precise inclusive results both at the highest momentum transfer Q^2 [31] and at the lowest quark momentum fraction x accessible to fixed target experiments [32].

The E142 collaboration at SLAC was the first to use a ^{3}He gas target with high luminosity to directly access the neutron spin structure functions g_1^n and g_2^n [33, 34]. Together with the EMC and SMC experiments, the data showed that the Bjorken sum rule including QCD corrections appeared to be valid. E142 was followed by a series of additional experiments at SLAC that used all three nuclear targets (proton, deuteron and ^{3}He) to accumulate a highly precise data set on the spin structure functions in the deep inelastic region. Instrumental for achieving ever higher precision was a significant improvement in the polarization (to over 80%) and intensity of available electron beams from strained GaAs cathodes irradiated with circularly polarized laser light. By using several electron beam energies and a set of up to 3 spectrometers, the E143 [35, 36, 37] and the E155 [38, 39] collaborations collected data on the proton and the deuteron over a wide range of momentum trans-

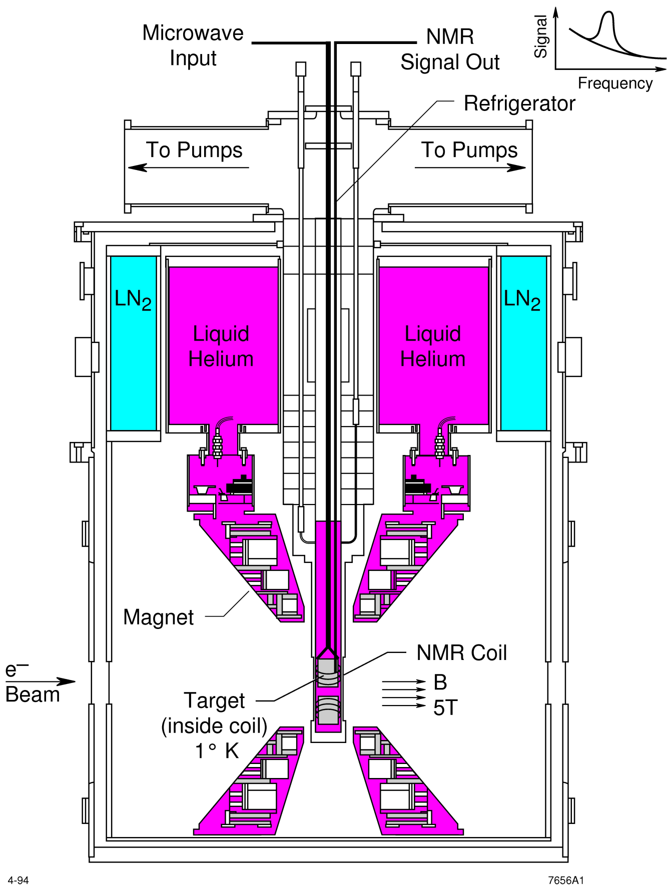

Figure 4.2: Solid state polarized proton or deuteron target for electron scattering experiments. The part containing the frozen ammonia ($^{15}\mathrm{N}\vec{\mathrm{H}}_3$ or $^{15}\mathrm{N}\vec{\mathrm{D}}_3$) is at the center of a Helmholtz-type magnet creating a magnetic field of about 5 T. A ^{4}He evaporation refrigerator (a liquid helium bath in a low-pressure environment) cools the target material to about 1 K. 140 GHz microwaves irradiate the target material to dynamically polarize the hydrogen nuclei. The polarization is measured by a resonant NMR circuit (the obtained signal vs. frequency is showed in the top right). Polarized targets for muon beams are typically much longer and can be cooled to lower temperatures.

fer Q^2 at several values of x, which were used to study scaling violations for polarized structure functions. The E154 collaboration [40, 41] added more neutron data at similar kinematics, using a polarized ^{3}He target. The E143

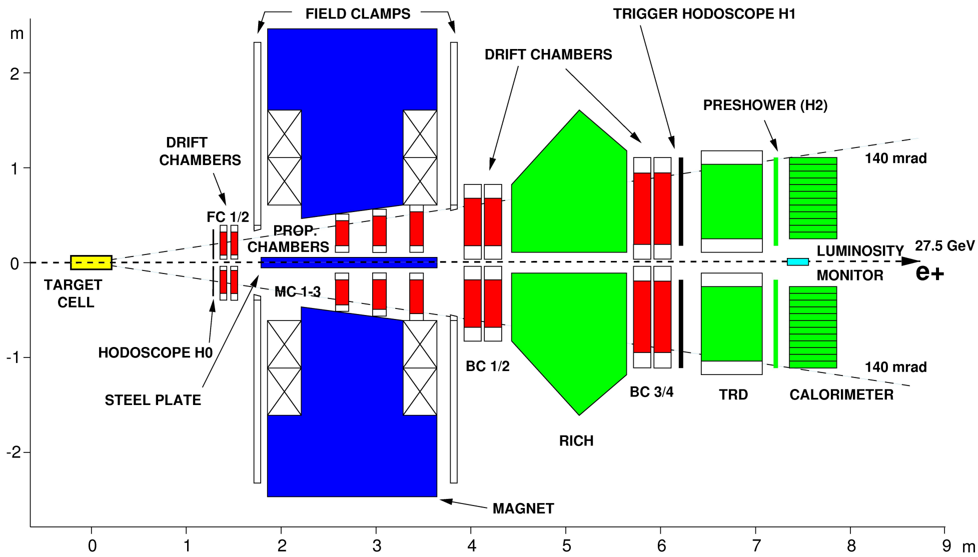

Figure 4.3: HERMES experiment at HERA/Desy (Hamburg, Germany). The electron or positron beam traverses an open storage cell supported by an atomic beam source with polarized H, D or ^{3}He. Leptons (and leading hadrons) are detected in a large acceptance spectrometer using wire chambers, scintillator hodoscopes, ring-imaging Cherenkov (RICH) and transition-radiation (TRD) detectors, and an electromagnetic calorimeter.

collaboration also published the first precision results at lower Q^2 and in the nucleon resonance region ($W \leq 2$GeV) [42]. The spin structure functions $g_2^{p,n,d}$ were measured with high precision by rotating the target polarization for all 4 experiments from a longitudinal to a perpendicular orientation to the beam [37, 43, 44].

The HERMES collaboration developed an innovative approach to measure DIS structure functions (see Fig. 4.3). They used positrons or electrons circulating in one of the HERA rings at DESY together with internal low–density gas targets supplied directly from atomic beam sources [45, 46]. Atoms in the target are polarized using hyperfine transitions induced by radio frequency fields and Stern-Gerlach type separation with magnetic sextupoles. The atomic beam is injected into a thin, windowless tube through which the beam circulates. This method provides a pure polarized target without any dilution from unpolarized materials. The beam is polarized by utilizing the Sokolov-Ternov effect (the spontaneous vertical polarization through spin-dependent synchrotron radiation of leptons in a storage ring). Spin rotators turn the polarization into the longitudinal direction at the target. The scattered electrons, as well as hadrons produced in coincidence, are detected by a large spectrometer. This setup allowed the HERMES collaboration to independently measure the inclusive spin structure functions g_1 and g_2 (for final results see [47]), but also semi-inclusive structure functions for flavor–tagging [48]. HERMES collected a large data set on related reactions of interest, from Deeply Virtual Compton Scattering (DVCS) [49] and transverse spin structure functions [50] to a first direct measurement of the gluon polarization [51].

Currently there are three laboratories left where experiments studying the spin structure of the nucleon continue: CERN, with the SMC-successor experiment "COMPASS"; BNL (on Long Island, NY) with the polarized proton-proton collision program at RHIC; and the Thomas Jefferson National Accelerator Facility ("Jefferson Lab" or JLab) in Newport News, Virginia, with an ongoing program of electron scattering in all 3 experimental halls.

The COMPASS experiment (see Fig. 4.4) uses the secondary muon beam at CERN together with large polarized deuteron and hydrogen targets to extend the kinematic reach and precision of SMC. Its main purpose is to extract information on the gluon polarization. This goal has been pursued by measuring both the production of hadron pairs with high transverse momentum [13] and by detecting charmed mesons in the final state (which are predominantly produced via photon-gluon fusion). Indirect information on the gluon contribution to the nucleon spin also comes from NLO analyses of inclusive DIS data, where the large kinematic lever arm offered by COMPASS makes an important contribution. The first results on the deuteron have been published [52, 53, 54] and the COMPASS experimental program will continue in the foreseeable future.

High-energy collisions of counter-circulating proton beams in the Relativistic Heavy Ion Collider (RHIC) at Brookhaven National Lab (BNL, Long Island, NY) are used to study the spin structure of the nucleon. Polarized protons are injected into a series of accelerators that finally fill both RHIC rings, where energies up to 100 GeV (250 GeV in the future) can be reached (see Fig. 4.5). Siberian snakes rotate the proton spins to avoid depolarizing resonances, while spin rotators can select the desired spin direction at the interaction points.

Currently, there are two large experiments (PHENIX and STAR) that use polarized proton collisions to study the gluon helicity contribution ΔG to the nucleon spin. The observables include meson production with high transverse momentum p_T as well as jet production, both probing the gluons through quark-gluon and gluon-gluon interactions in the initial state. Results from these experiments have been published in [55, 56, 57, 58] By orienting the proton spins perpendicular to the beam direction, both experiments can

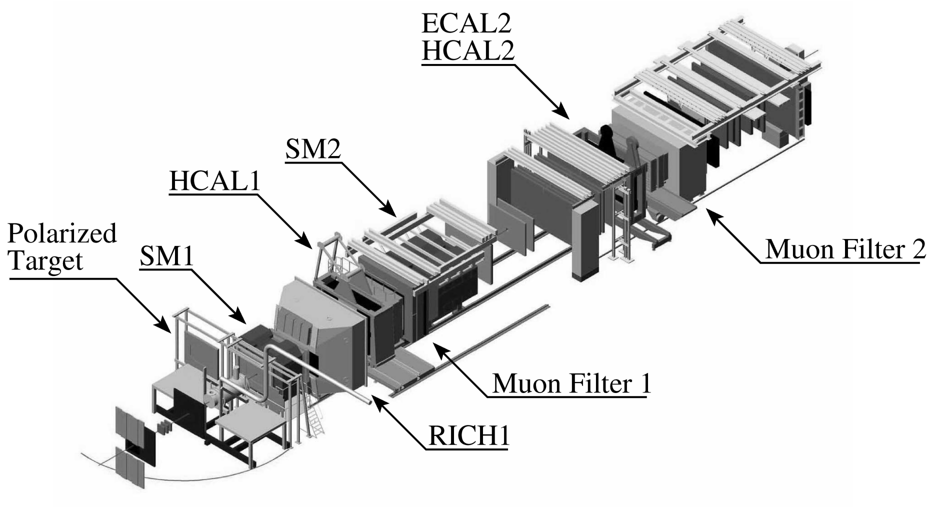

Figure 4.4: Layout of the COMPASS experiment at CERN (Geneva, Switzerland).

also study reactions sensitive to transverse spins.

In the last 10 years a large program using electron scattering to study the spin structure of nucleons has been underway at Jefferson Lab (JLab).

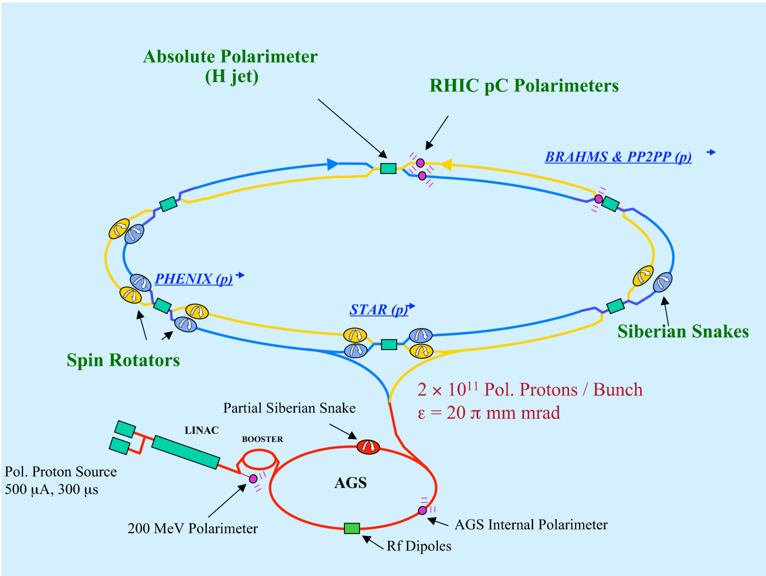

Figure 4.5: Layout of the RHIC accelerator complex at BNL (Long Island, NY).

JLab used the highest polarization electron beams (over 85%) with energies from 0.8 GeV to close to 6 GeV and all three species of polarized targets (p, d, and ^{3}He) to study spin-dependent structure functions both in the DIS regime as well as in the nucleon resonance region. This program is ongoing in all three experimental halls and will be continued, once the energy upgrade to 12 GeV of the JLab accelerator is completed in 2014. In the following we give some of the experimental details for all three halls.

JLab's Hall A is focused on the spin structure of the neutron, using a polarized ^{3}He target as an effective polarized neutron target. Measurements of polarized cross-sections and asymmetries in the two orthogonal directions allow a direct extraction of g_1, g_2, A_1 and A_2. A series of high precision experiments [59, 60, 61, 62, 63, 64, 65, 66, 67, 68] measured g_1 and g_2 in a wide range of kinematics, from very low Q^2 (≈ 0.01 GeV^2) up to 5 GeV^2 and from the elastic peak to the DIS region ($W \approx 3$ GeV). A pair of High Resolution Spectrometers (HRS) are used to detect the scattered electrons. The HRS have angular acceptances of ≈ 6 msr and momentum acceptances of $\approx 9\%$. Their angular range is 12.5° to 160° and can reach as low as 6° with the addition of a septum magnet. The high luminosity of 10^{36} cm^{-2}s^{-1} allowed for precision measurements at numerous HRS momentum and angular settings to cover a wide area in the (Q^2,W)-plane. The electron detector package consists of vertical drift chambers (for momentum analysis and vertex reconstruction), scintillation counters (for data acquisition trigger), gas Cherenkov counters and lead-glass shower calorimeters (for particle identification). The HRS optical property and acceptance have been carefully studied. Absolute cross sections are measured to a level of 2-3% precision. Asymmetries are measured to a level of 4-5% precision, mostly due to the uncertainties from the beam and target polarization measurements. The spin structure functions g_1 and g_2 are extracted using polarized cross section differences in which contributions from unpolarized materials, such as target windows and nitrogen, cancel. Corrections for the two protons in ^{3}He are still needed since they are slightly polarized due to the D state (8%) and S$'$ state (1.5%) of the ^{3}He wave function [69]. Corrections for binding and Fermi motion are applied using state-of-the-art ^{3}He calculations [70, 71]. Uncertainties due to the nuclear corrections have been studied [70]. In the region of DIS and for the extraction of moments, the uncertainties are usually small, typically less than 5%.

In JLab's Hall B the EG1–EG4 series of experiments has as its goal to map out the asymmetry A_1 and the spin structure function g_1 of both nucleons over the largest, continuous kinematic range accessible. It uses the CEBAF Large Acceptance Spectrometer (CLAS) in Hall B that covers an angular range of about 6 degrees to over 140 degrees in polar angle and nearly 2π in azimuth [72]. Geometry and the toroidal magnetic field (maintained by 6 superconducting coils evenly distributed in azimuth), allows to simultaneously detect scattered electrons over a wide kinematic range, as well as secondary produced hadrons (nucleons, pions and kaons) for semi-inclusive or exclusive channels. Combining runs with several different beam energies from 1 to 6 GeV, a continuous coverage in Q^2 from 0.015 to 5 GeV^2 and in final state mass W, from the elastic peak ($W = 0.94$ GeV) to the DIS region ($W \approx 3$ GeV), has been achieved. Inclusive results from the EG1 experiment have been published [73, 74, 75, 76].

So far, only targets polarized along the beam direction have been utilized (because of the difficulty to combine a large transverse magnetic field with the open geometry of CLAS), which necessitates (minor) corrections of the measured asymmetries for the unobserved contribution from A_2 . A fit to the world data on A_2 and on unpolarized structure functions R and F_1 [77, 78] is used to extract the desired spin structure function information from the measured asymmetries. In addition to the structure function $g_1(x, Q^2)$, the CLAS data have also yielded new results on resonance excitation and decay (via exclusive π^+, π^0 and π^- channels) [79, 80], on deeply virtual Compton scattering [81], and on single and double spin asymmetries in semi-inclusive hadron production [82].

The experiment completed in Hall C used a standard DNP ammonia target ($^{15}NH_3$ and $^{15}ND_3$) and the existing high momentum spectrometer (HMS) for a detailed look at the resonance region at intermediate $Q^2 \approx 1.3$

GeV^2. This is the only experiment at JLab on the proton and the deuteron where both longitudinal and transverse double spin asymmetries were measured, allowing an unambiguous separation of the structure functions A_1 and A_2 or g_1 and g_2 up to a final state missing mass of $W \approx 2$ GeV. The first results have been published [83].

4.7 Polarized lepton-nucleon DIS

4.7.1 The one photon exchange approximation

In this section we outline the general formalism used to describe inelastic scattering of polarized leptons on polarized nucleons. We use the following notation - m: the lepton mass, k (k'): the initial (final) lepton four-momentum, s (s'): its covariant spin four-vector, defined by $s \cdot k = 0$ ($s' \cdot k' = 0$) and $s \cdot s = -1$ ($s' \cdot s' = -1$). The nucleon mass is M and the nucleon four-momentum and spin four-vector are, respectively, P and S.

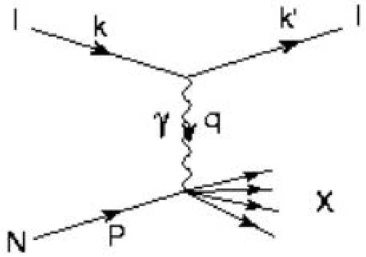

Figure 4.6: One photon approximation

Using the one photon exchange approximation (see Fig.[?]) , the differential cross-section for detecting the final polarized lepton in the solid angle $d\Omega$ and in the final energy range (E', $E' + dE'$) in the laboratory frame, $P = (M, \mathbf{0})$, $k = (E, \boldsymbol{k})$, $k' = (E', \boldsymbol{k}')$, can be written as

$$\frac{d^2\sigma}{d\Omega\, dE'} = \frac{\alpha^2}{2Mq^4}\, \frac{E'}{E}\, L_{\mu\nu}\, W^{\mu\nu}\,, \tag{4.58}$$

$q = k - k'$, α : fine structure constant.

In Eq. (4.58) the leptonic tensor $L_{\mu\nu}$ is given by

$$L_{\mu\nu}(k, s; k', s') = [\bar{u}(k', s')\ \gamma_\mu\ u(k, s)]^*\ [\bar{u}(k', s')\ \gamma_\nu\ u(k, s)] \tag{4.59}$$

It can be separated into symmetric (S) and antisymmetric (A) parts under μ, ν interchange:

$$\begin{aligned} L_{\mu\nu}(k, s; k', s') &= L^{(S)}_{\mu\nu}\ (k; k') + iL^{(A)}_{\mu\nu}\ (k, s; k') \\ &+ L'^{(S)}_{\mu\nu}\ (k, s; k', s') + iL'^{(A)}_{\mu\nu}\ (k; k', s') \end{aligned} \tag{4.60}$$

where

$$
\begin{aligned}
L^{(S)}_{\mu\nu}\ (k;k') &= k_\mu k'_\nu + k'_\mu k_\nu - g_{\mu\nu}\ (k\cdot k' - m^2) && (4.61)\\
L^{(A)}_{\mu\nu}\ (k,s;k') &= m\ \varepsilon_{\mu\nu\alpha\beta}\ s^\alpha\ (k-k')^\beta && (4.62)\\
L'^{(S)}_{\mu\nu}(k,s;k',s') &= (k\cdot s')\ (k'_\mu s_\nu + s_\mu k'_\nu - g_{\mu\nu}\ k'\cdot s) && \\
&- (k\cdot k' - m^2)\ (s_\mu s'_\nu + s'_\mu s_\nu - g_{\mu\nu}\ s\cdot s') && (4.63)\\
&+ (k'\cdot s)(s'_\mu k_\nu + k_\mu s'_\nu) - (s\cdot s')(k_\mu k'_\nu + k'_\mu k_\nu) && \\
L'^{(A)}_{\mu\nu}\ (k;k',s') &= m\ \varepsilon_{\mu\nu\alpha\beta}\ s'^\alpha (k-k')^\beta\,. && (4.64)
\end{aligned}
$$

The usual unpolarized leptonic tensor $2L^{(S)}_{\mu\nu}$ can be obtained by summing Eq. 4.61 over s' and taking an average over s. Taking a sum over s', yields $2L^{(S)}_{\mu\nu} + 2iL^{(A)}_{\mu\nu}$.

The hadronic tensor (describing the unknown structure of the nucleon) $W_{\mu\nu}$ is defined in terms of four structure functions as [137, 138, 139].

$$
W_{\mu\nu}(q;P,S) = W^{(S)}_{\mu\nu}(q;P) + i\ W^{(A)}_{\mu\nu}(q;P,S) \tag{4.65}
$$

with

$$
\begin{aligned}
\frac{1}{2M}\ W^{(S)}_{\mu\nu}(q;P) &= \left(-g_{\mu\nu} + \frac{q_\mu q_\nu}{q^2}\right)\ W_1(P\cdot q, q^2) && \\
&+ \left[\left(P_\mu - \frac{P\cdot q}{q^2}\ q_\mu\right)\left(P_\nu - \frac{P\cdot q}{q^2}\ q_\nu\right)\right]\ \frac{W_2(P\cdot q,q^2)}{M^2} && (4.66)\\
\frac{1}{2M}\ W^{(A)}_{\mu\nu}(q;P,S) &= \varepsilon_{\mu\nu\alpha\beta}\ q^\alpha \Bigg\{ M S^\beta G_1(P\cdot q, q^2) && \\
&+ [(P\cdot q)S^\beta - (S\cdot q)P^\beta]\ \frac{G_2(P\cdot q,q^2)}{M}\Bigg\}. && (4.67)
\end{aligned}
$$

For differential cross-section one obtains:

$$
\begin{aligned}
\frac{d^2\sigma}{d\Omega\ dE'} &= \frac{\alpha^2}{2Mq^4}\ \frac{E'}{E}\ \Big[L^{(S)}_{\mu\nu}\ W^{\mu\nu(S)} + L'^{(S)}_{\mu\nu}\ W^{\mu\nu(S)} \\
&- L^{(A)}_{\mu\nu}\ W^{\mu\nu(A)} - L'^{(A)}_{\mu\nu}\ W^{\mu\nu(A)}\Big]\,. \qquad (4.68)
\end{aligned}
$$

Each term in the square brackets can be separately studied by looking at cross-sections or differences between cross-sections with specific initial and final polarizations [140]. These terms are, at least in principle, measurable quantities which are either a function of the two spin-averaged structure functions W_1 and W_2 (terms containing $W^{(S)}_{\mu\nu}$) or of the two spin-dependent structure functions G_1 and G_2 (terms containing $W^{(A)}_{\mu\nu}$). The usual unpolarized cross-section is proportional to $L^{(S)}_{\mu\nu}\ W^{\mu\nu(S)}$

$$\begin{aligned}\frac{d^2\sigma^{unp}}{d\Omega\ dE'}\left(k,P;k'\right) &= \frac{1}{4}\sum_{s,s',S}\frac{d^2\sigma}{d\Omega\ dE'}\ (k,s,P,S;k',s') \\ &= \frac{\alpha^2}{2Mq^4}\ \frac{E'}{E}\ 2L^{(S)}_{\mu\nu}\ W^{\mu\nu(S)}\,, \end{aligned} \tag{4.69}$$

The differences of cross-sections with opposite target spins single out the $L^{(A)}_{\mu\nu}\ W^{\mu\nu(A)}$ term:

$$\begin{aligned}&\sum_{s'}\left[\frac{d^2\sigma}{d\Omega\ dE'}\ (k,s,P,-S;k',s') - \frac{d^2\sigma}{d\Omega\ dE'}\ (k,s,P,S;k',s')\right] \\ &\qquad = \frac{\alpha^2}{2Mq^4}\ \frac{E'}{E}\ 4L^{(A)}_{\mu\nu}\ W^{\mu\nu(A)}\,. \end{aligned} \tag{4.70}$$

Bjorken scaling

The cross-section for the inelastic scattering of unpolarized leptons on unpolarized nucleons in the laboratory frame can be written explicitly, using above equations and neglecting the lepton mass, as

$$\frac{d^2\sigma^{unp}}{d\Omega\ dE'} = \frac{4\alpha^2 E'^2}{q^4}\left[2W_1\sin^2\frac{\theta}{2} + W_2\cos^2\frac{\theta}{2}\right] \tag{4.71}$$

where θ is the laboratory scattering angle of the lepton. Its measurement gives information on the unpolarized structure functions $W_1(P\cdot q, q^2)$ and $W_2(P\cdot q, q^2)$.

In the Bjorken limit, or deep inelastic scattering (DIS) regime,

$$-q^2 = Q^2 \to \infty \qquad \nu = E - E' \to \infty \qquad x = \frac{Q^2}{2P\cdot q} = \frac{Q^2}{2M\nu}\,,\ \text{fixed} \tag{4.72}$$

the structure functions show a scaling behaviour:

$$\begin{aligned}\lim_{Bj}\ MW_1(P\cdot q, Q^2) &= F_1(x) \\ \lim_{Bj}\ \nu W_2(P\cdot q, Q^2) &= F_2(x)\,, \end{aligned} \tag{4.73}$$

where $F_{1,2}$ vary very slowly with Q^2 at fixed x.

Similarly, for cross-section difference , one has

$$\sum_{s'}\left[\frac{d^2\sigma}{d\Omega\ dE'}(k,s,P,S;k',s') - \frac{d^2\sigma}{d\Omega\ dE'}(k,s,P-S;k',s')\right] \equiv$$

$$\equiv \frac{d^2\sigma^{s,S}}{d\Omega\ dE'} - \frac{d^2\sigma^{s,-S}}{d\Omega\ dE'} \quad = \tag{4.74}$$

$$= \frac{8m\alpha^2 E'}{q^4 E}\left\{\left[(q\cdot S)(q\cdot s) + Q^2(s\cdot S)\right] MG_1 + Q^2\Big[(s\cdot S)(P\cdot q) - (q\cdot S)(P\cdot s)\Big]\frac{G_2}{M}\right\}$$

which yields information on the polarized structure functions $G_1(P\cdot q, q^2)$ and $G_2(P\cdot q, q^2)$. They also are expected to scale approximately:

$$\begin{aligned} \lim_{Bj} \frac{(P\cdot q)^2}{\nu}\ G_1(P\cdot q, Q^2) &= g_1(x) \\ \lim_{Bj}\ \nu\ (P\cdot q)\ G_2(P\cdot q, q^2) &= g_2(x)\,. \end{aligned} \tag{4.75}$$

In terms of $g_{1,2}$ the expression for $W^{(A)}_{\mu\nu}$ becomes

$$W^{(A)}_{\mu\nu}(q;P,s) = \frac{2M}{P\cdot q}\,\varepsilon_{\mu v\alpha\beta}\, q^\alpha\left\{S^\beta g_1(x,Q^2) + \left[S^\beta - \frac{(S\cdot q)\,P^\beta}{(P\cdot q)}\right] g_2(x,Q^2)\right\}. \tag{4.76}$$

Cross-section differences

To gather information on the polarized structure functions G_1 and G_2, we can use Eq. (4.74) and consider specific spin configurations.

In the case of longitudinally polarized leptons (initial lepton with spin along ($\rightarrow$) or opposie($\leftarrow$) the direction of motion) the nucleons at rest are polarized along (S) or opposite ($-S$) an arbitrary direction $\hat{\boldsymbol{S}}$. We can write:

$$\begin{aligned} s^\mu_{\rightarrow} &= -\,s^\mu_{\leftarrow} = \frac{1}{m}\ (|\boldsymbol{k}|,\ \hat{\boldsymbol{k}}E) \qquad \hat{\boldsymbol{k}} = \frac{\boldsymbol{k}}{|\boldsymbol{k}|} \\ S^\mu &= (0, \hat{\boldsymbol{S}})\,. \end{aligned} \tag{4.77}$$

We take the z-axis along the incoming lepton direction and define

$$\begin{aligned} k^\mu &= (E,0,0,|\boldsymbol{k}|) \simeq E(1,0,0,1) \\ k'^\mu &= (E', \boldsymbol{k}') \simeq E'(1, \hat{\boldsymbol{k}}') \\ &= E'(1, \sin\theta\cos\varphi,\ \sin\theta\sin\varphi,\ \cos\theta) \\ \hat{\boldsymbol{S}} &= (\sin\alpha\cos\beta,\ \sin\alpha\sin\beta,\ \cos\alpha)\,. \end{aligned} \tag{4.78}$$

From Eqs. (4.74) we obtain (at leading order in m/E)

$$\begin{aligned} \frac{d^2\sigma^{\rightarrow,S}}{d\Omega\ dE'} \ - \ \frac{d^2\sigma^{\rightarrow,-S}}{d\Omega\ dE'} &= -\frac{4\alpha^2}{Q^2}\ \frac{E'}{E} \\ \times \ \Big\{[E\cos\alpha + E'\cos\Theta]MG_1 &+ 2EE'[\cos\Theta - \cos\alpha]\ G_2\Big\}\,. \end{aligned} \tag{4.79}$$

α is the polar angle of the nucleon spin direction, i.e. the angle between $\hat{\boldsymbol{k}}$ and $\hat{\boldsymbol{S}}$, and Θ is the angle between the outgoing lepton direction, $\hat{\boldsymbol{k}}'$, and $\hat{\boldsymbol{S}}$:

$$\begin{aligned} \cos\Theta &= \sin\theta\cos\varphi\sin\alpha\cos\beta \\ &+ \sin\theta\sin\varphi\sin\alpha\sin\beta + \cos\theta\cos\alpha \\ &= \sin\theta\sin\alpha\cos\phi + \cos\theta\cos\alpha \end{aligned} \tag{4.80}$$

where $\phi = \beta - \varphi$ is the azimuthal angle between the $(\hat{\boldsymbol{k}}, \hat{\boldsymbol{k}}')$ scattering plane and the $(\hat{\boldsymbol{k}}, \hat{\boldsymbol{S}})$ polarization plane

For nucleons polarized along ($\Rightarrow$) or opposite ($\Leftarrow$) the initial lepton direction of motion one has $\alpha = 0$, $\Theta = \theta$, and Eq. (4.79) gives

$$\frac{d^2\sigma^{\overrightarrow{\Rightarrow}}}{d\Omega\ dE'} - \frac{d^2\sigma^{\overleftarrow{\Rightarrow}}}{d\Omega\ dE'} = -\frac{4\alpha^2}{Q^2}\ \frac{E'}{E}\left[(E + E'\cos\theta)MG_1 - Q^2 G_2\right]. \tag{4.81}$$

If the nucleons are transversely polarized (the nucleon spin is perpendicular to the direction of the incoming lepton) $\alpha = \pi/2$ and Eqs. (4.79, 4.80) yield

$$\frac{d^2\sigma^{\rightarrow\Uparrow}}{d\Omega\ dE'} - \frac{d^2\sigma^{\rightarrow\Downarrow}}{d\Omega\ dE'} = -\frac{4\alpha^2}{Q^2}\ \frac{E'^2}{E}\ \sin\theta\cos\phi\ (MG_1 + 2EG_2)\,. \tag{4.82}$$

If the nucleon spin is perpendicular to the scattering plane ($\alpha = \phi = \pi/2$), the cross-section difference in Eq. (4.82) is zero. Such a difference has its maximum absolute value when $\phi = 0$ or π, that is when the nucleon spin vector, perpendicular to $\hat{\boldsymbol{k}}$, lies in the scattering plane.

Above we assumed longitudinally polarized leptons. Dealing with transversely polarized leptons is more complicated. For transversely polarized incoming leptons we have

$$s = (0, \hat{\boldsymbol{s}})\,, \tag{4.83}$$

with the unit vector $\hat{\boldsymbol{s}}$ orthogonal to $\hat{\boldsymbol{k}}$, $\hat{\boldsymbol{s}} \cdot \hat{\boldsymbol{k}} = 0$. Contrary to the case of longitudinally polarized leptons, Eq. (4.77) has no factor E/m to cancel the factor m/E which appears in the cross-section differences (4.74), and the latter turn out to be vanishingly small in the large energy limit ($m/E \to 0$).

Information on the unpolarized structure functions W_1 and W_2 can be obtained by looking at lepton spin asymmetries in the initial and final states [140]; this requires measurement of the scattered lepton polarization, which is difficult to achieve.

Measurement of g_1 and g_2 on nucleon targets

Cross-section differences with particular lepton and nucleon spin configurations give information on the polarized structure functions G_1 and G_2 or on the scaling functions g_1 and g_2, Eq. (4.75).

A single difference measurement provides information on a combination of G_1 and G_2, rather than on the separate structure functions. Extracting from the data values of G_1 or G_2 requires an additional approximation.

a) Longitudinally polarized target

Most of the experiments [141, 142, 143, 144, 145, 146, 147, 148] measured the longitudinal spin-spin asymmetry in $\ell p \to \ell X$,

$$A_{\parallel} \equiv \frac{d\sigma^{\rightleftarrows} - d\sigma^{\rightrightarrows}}{d\sigma^{\rightrightarrows} + d\sigma^{\rightleftarrows}} \,, \tag{4.84}$$

Here $d\sigma$ stands for $d^2\sigma/(d\Omega\, dE')$ and the denominator is twice the unpolarized cross-sections. From Eqs. (4.71) and (4.81) we have

$$A_{\parallel} = \frac{Q^2\ [(E + E'\cos\theta)MG_1 - Q^2 G_2]}{2EE'\ [2W_1 \sin^2(\theta/2) + W_2\cos^2(\theta/2)]} \,. \tag{4.85}$$

The asymmetry $A_{\parallel}$ is usually expressed in terms of virtual Compton scattering asymmetries $A_{1,2}$ [LEA 85],

$$A_{\parallel} = D(A_1 + \eta A_2)\,, \tag{4.86}$$

here D and η are known coefficients (they can be found in original experimental papers cited above). To a good approximation one find the expressions

$$A_{\parallel} \approx DA_1 \tag{4.87}$$

and

$$g_1(x) \approx \frac{A_{\parallel}}{D}\ \frac{F_2(x)}{2x[1 + R(x)]} \,, \tag{4.88}$$

where $F_2(x)$ is the unpolarized scaling structure function, Eq. (4.73). R is the ratio of the longitudinal to transverse cross-section

$$R = \frac{W_2}{W_1}\left(1 + \frac{\nu^2}{Q^2}\right) - 1\,. \tag{4.89}$$

Approximations involved in the simplifications can be shown to be suitable when measuring g_1 [144, 145]. One can show that

$$|A_2| \leq \sqrt{R} \tag{4.90}$$

R is known to be small.

From (4.71, 75 and 85) we have

$$\frac{M\nu Q^2 E}{2\alpha^2 E'(E + E'\cos\theta)}\ \frac{d^2\sigma^{unp}}{d\Omega\ dE'}\ A_{\parallel} = g_1 - \frac{2xM}{E + E'\cos\theta}\ g_2 \tag{4.91}$$

This can be rewritten

$$g_1 - \kappa g_2 = 2K \; d\sigma^{unp} \; A_{\|} \tag{4.92}$$

with

$$\kappa = \frac{2xM}{E + E'\cos\theta} \approx \frac{xM}{E - Q^2/(4Mx)}$$

$$K = \frac{M\nu Q^2 E}{4\alpha^2 E'(E + E'\cos\theta)} = \frac{EE' \; \cos^2(\theta/2)}{2x\sigma_{Mott} \; (E + E'\cos\theta)} \tag{4.93}$$

where

$$\sigma_{Mott} = \left[\frac{\alpha\cos(\theta/2)}{2E\sin^2(\theta/2)}\right]^2 .$$

The right hand side of Eq. (4.92) is obtained directly from experiment, with no need of additional data analysis in order to extract F_2 and R, as required in Eq. (4.88).

The single measurement of $A_{\|}$ (and $d\sigma^{unp}$) provides us information on the combination $g_1 - \kappa g_2$, and not on g_1 or g_2 alone. The usual argument [141, 142, 143] is that the g_2 term in Eq. (4.92) can be neglected because of the kinematical coefficient κ which, in the large energy limit, is very small, as can be seen from Eqs. (4.93). This was confirmed by a more detailed analysis of the g_2 term [149]. The measurement of the quantities on the RHS of Eq. (4.92) provides a direct measurement of the polarized scaling structure function g_1.

To obtain data on $g_1(x, Q^2)$ we should use eq (4.92). It would be important to obtain $g_1(x, Q^2)$ over the entire x-range $0 \leq x \leq 1$ at the same Q^2. Experimentally this is not possible. The kinematics of the experiment puts a constraint on smaller values of x which will correspond to a smaller range of accessible Q^2.

The experimentalists have to extrapolate the data in Q^2 at fixed x. The question is: which quantities vary most smoothly and slowly in Q^2? According to the experiments $A_{\|}(x, Q^2)/D$ varies only slowly with Q^2. Experimentalists prefer to express their measurements in terms of data on $A_{\|}(x, Q^2)$ via (4.88). Another assumption is that $A_{\|}(x, Q^2)/D$ is independent of Q^2 and the value of $g_1(x, \langle Q^2\rangle)$ quoted. For an experiment with mean value of Q^2 equal to $\langle Q^2\rangle$ one finds:

$$g_1(x, \langle Q^2\rangle) \equiv \left(\frac{A_{\|}(x)}{D}\right) \frac{F_2(x, \langle Q^2\rangle)}{2x[1 + R(x, \langle Q^2\rangle)]} \, . \tag{4.94}$$

The approximations leading to (4.88) are safe if one is trying to evaluate $g_1(x)$. The perpendicular asymmetry $A_{\perp}$ is used to measure a combination of g_1 and g_2 in order to extract g_2. g_2 is expected to be much smaller than

g_1 and special attention has to be paid when using an approximate version of $g_1(x)$.

b) Transversely polarized target

Information on g_2 must be obtained from other spin-spin asymmetries. By scattering longitudinally polarized leptons on transversely polarized nucleons, one can measure the quantity

$$A_\perp \equiv \frac{d\sigma^{\rightarrow\Downarrow} - d\sigma^{\rightarrow\Uparrow}}{d\sigma^{\rightarrow\Uparrow} + d\sigma^{\rightarrow\Downarrow}} \tag{4.95}$$

$d\sigma$ stands for $d^2\sigma/(d\Omega\ dE')$, and the denominator is twice the unpolarized cross-section $d\sigma^{unp}$.

From Eqs. (4.71) and (4.82) one obtains

$$A_\perp = \frac{Q^2 \sin\theta (MG_1 + 2EG_2)}{2E\,[2W_1 \sin^2(\theta/2) + W_2 \cos^2(\theta/2)]} \cos\phi \tag{4.96}$$

where ϕ is the difference between the azimuthal angles of $\hat{\boldsymbol{S}}$ and $\hat{\boldsymbol{k}}'$, $\phi = \beta - \varphi$

Repeating for g_2 the same direct procedure, Eqs. (4.91–93), and use Eqs. (4.71, 75 and 96) (with $\phi = 0$) to write

$$g_2 + \frac{\nu}{2E}\, g_1 = \left(\frac{\nu}{E}\right) K'\ d\sigma^{unp}\ A_\perp \tag{4.97}$$

where

$$K' = \frac{Q^2 E M \nu}{4\alpha^2 E'^2 \sin\theta} = \frac{E\cos^2(\theta/2)}{2x\sigma_{Mott}\ \sin\theta} \tag{4.98}$$

and σ_{Mott} is given in Eqs. (4.93).

A measurement of $A_\perp$ gives direct information on the structure function combination $g_2 + \nu/(2E)\, g_1$. The coefficient of g_1 is not negligible. To isolate g_2 one must have knowledge of g_1 obtained from the $A_\parallel$ measurement. If the values of Q^2 and x are fixed, the only dependence on the beam energy E in the left hand side of (4.92) is in the coefficient of $g_2(x)$. Looking at the energy variation of the right hand side of (4.91) allows to obtain information about $g_2(x)$. The coefficient of $g_2(x)$ is small, thus it is not clear whether this method is useful or not.

The measurement of $A_\perp$ at different beam energies E allows the isolation of $g_2(x)$ from (4.97). Measurements at $E = E_1$ and E_2 yield

$$(E_1 - E_2)\ g_2(x) = [\nu K'\ d\sigma^{unp}\ A_\perp]_{E=E_1} - [\nu k'\ d\sigma^{unp}\ A_\perp]_{E=E_2}\,. \tag{4.99}$$

Equations (4.91, 98) provide the most direct access to g_2 , assuming that the knowledge of g_1 is accurate enough. If we want to obtain the data at fixed Q^2 over the entire range of x, a different strategy is required, which we now describe.

c) Combined analysis using $A_\parallel$ and $A_\perp$

The longitudinal polarization data can be used to extrapolate $A_\parallel/D$ smoothly in Q^2 at fixed x. Taking this together with the perpendicular polarization data, where it is measured, one can construct

$$A' \equiv \frac{\sqrt{Q^2}}{2M}\, A_2 = \frac{\sqrt{Q^2}}{2M(1+\xi\eta)}\left\{\xi\frac{A_\parallel}{D} + \frac{A_\perp}{d}\right\} \tag{4.100}$$

at the values of the $A_\perp$ experiment. A' should vary slowly with Q^2 because

$$g_1(x,Q^2) + g_2(x,Q^2) = \frac{F_2(x,Q^2)}{2x^2[1+R(x,Q^2)]}\, A'(x,Q^2) \tag{4.101}$$

Equation (2.1.44) can be used to estimate g_1+g_2 over the entire x, Q^2 range.

Using A' extrapolated to the relevant Q^2, one can obtain an improved evaluation of $g_1(x,Q^2)$ using

$$g_1(x,Q^2) = \frac{F_2(x,Q^2)}{2x[1+R(x,Q^2)]}\cdot\frac{1}{1+4M^2x^2/Q^2}\cdot\left\{\frac{A_\parallel}{D} - \frac{2M}{\sqrt{Q^2}}\left(\eta - \frac{2Mx}{\sqrt{Q^2}}\right)A'\right\}. \tag{4.102}$$

The formulae (4.101) and (4.102) are exact. They are expressed in terms of the functions $A'(x,Q^2)$ and $A_\parallel/D$ which should both be slowly varying functions of Q^2 at fixed x.

d) The problem of extrapolating in Q^2

In section a) above we mentioned that

$$A_1(x,Q^2) = \frac{A_\parallel(x,Q^2)}{D} \tag{4.103}$$

is taken to be independent of Q^2 in the experimental evaluation of $g_1(x,\langle Q^2\rangle)$ via (4.94). No assumption has been made for the error in extrapolating from the measured region of Q^2 for the x involved to the required value $\langle Q^2\rangle$. A linear parametrization $a + b\,Q^2$ or $a + b\ln Q^2$ for A_1 will not work, since a best fit will yield a very small value of b, but with very large errors, leading to unrealistic error estimates on $g_1(x,\langle Q^2\rangle)$.

There is no rigorous theoretical solution proposed for this experimental problem, but the following approximate procedure should lead to an improved estimate of $g_1(x,\langle Q^2\rangle)$ and its error.

We define a zeroth order approximation to $g_1(x,\langle Q^2\rangle)$ for each x_i via (4.94), i.e.

$$g_1^{(0)}(x_i,\langle Q^2\rangle) \equiv A_1(x_i,Q_i^2)F_1(x_i,\langle Q^2\rangle) \tag{4.104}$$

where

$$F_1 = \frac{F_2}{2x[1+R]} \tag{4.105}$$

An improved estimate of $g_1(x, \langle Q^2 \rangle)$ for each x_i is

$$g_1(x_i, \langle Q^2 \rangle) \equiv A_1(x_i, \langle Q^2 \rangle) F_1(x_i, \langle Q^2 \rangle) \tag{4.106}$$

where $A_1(x_i, \langle Q^2 \rangle)$ is obtained using

$$A_1(x_i, \langle Q^2 \rangle) \approx A_1(x_i, Q_i^2) + b(x_i, Q_i^2) \ln(\langle Q^2 \rangle / Q_i^2) \tag{4.107}$$

and $b(x_i, Q_i^2)$ is estimated from

$$\begin{aligned} b(x_i, Q_i^2) &= \frac{1}{F_1(x_i, Q_i^2)} \left. \frac{\partial g_1(x_i, Q^2)}{\partial \ln Q^2} \right|_{Q^2=Q_i^2} \\ &- \frac{A_1(x_i, Q_i^2)}{F_1(x_i, Q_i^2)} \left. \frac{\partial F_1(x_i, Q^2)}{\partial \ln Q^2} \right|_{Q^2=Q_i^2} . \end{aligned} \tag{4.108}$$

Terms on the right hand side of (4.108) are known from experiment except for the derivative of g_1. This term can be approximately calculated from the evolution equation, if we use the experimental fact, that the flavour singlet part of g_1 is much smaller than the non-singlet part. We consider the evolution as if it were purely non-singlet, i.e. we compute

$$\left. \frac{\partial g_1(x_i, Q^2)}{\partial \ln Q^2} \right|_{Q^2=Q_i^2} \approx \frac{\alpha_s(Q_i^2)}{2\pi} \int_{x_i}^1 \frac{dy}{y}\, g_1(y, Q_i^2)\, \Delta P_{qq} \left(\frac{x_i}{y} \right) , \tag{4.109}$$

where ΔP_{qq} is the non-singlet polarized splitting function. For the non-singlet case polarized and unpolarized splitting functions are equal [151],

$$\Delta P_{qq}(x) = P_{qq}(x) = \frac{4}{3} \left(\frac{1+x^2}{1-x} \right)_+ . \tag{4.110}$$

In the convolution integral in (4.109) we approximate g_1 by its known zeroth order estimate (4.104). The approximate formula is

$$\left. \frac{\partial g_1(x_i, Q^2)}{\partial \ln Q^2} \right|_{Q^2=Q_i^2} \approx \frac{\alpha_s(Q_i^2)}{2\pi} \int_{x_i}^1 \frac{dy}{y}\, g_1^{(0)}(y, Q_i^2)\, \Delta P_{qq} \left(\frac{x_i}{y} \right) . \tag{4.111}$$

This provides an estimate for the value of b in (4.108) and for the error on it.

Measurement of $g_{1,2}$ on nuclear targets

A spin 1 target is deuterium, and a spin 1/2 target is ^{3}He. The following asymmetries are the analogues of (4.84 and 95) and are defined for the nucleus A by

$$A_\parallel^A = \frac{d\sigma_A^{\overset{\rightarrow}{\leftarrow}} - d\sigma_A^{\rightrightarrows}}{d\sigma_A^{\overset{\rightarrow}{\leftarrow}} + d\sigma_A^{\rightrightarrows}} \tag{4.112}$$

$$A_{\perp}^{A} = \frac{d\sigma_A^{\rightarrow\Downarrow} - d\sigma_A^{\rightarrow\Uparrow}}{d\sigma_A^{\rightarrow\Downarrow} + d\sigma_A^{\rightarrow\Downarrow}} \tag{4.113}$$

where $\sigma_A^{\Rightarrow}$, $\sigma_A^{\Leftarrow}$ means $J_z = \pm 1/2$ for a spin $1/2$ target, but $J_z = \pm 1$ for a spin one target longitudinally polarized.

The constituents of the nucleons are assumed to contribute independently to the scattering. Shadowing and Fermi motion are neglected.

For unpolarized scattering on deuterium this implies taking

$$\sigma_d = \sigma_p + \sigma_n \,, \tag{4.114}$$

This is good approximation for σ_d but it can be misleading when differences of cross-section are being studied. The Gottfried sum rule requires the combination $\sigma_p - \sigma_n$ for which the approximation $2\sigma_p - \sigma_d$ may be dangerous, because the subtraction of comparable quantities magnifies the error [152].

A test of the Bjorken sum rule requires the quantity $g_1^p - g_1^n$, and it can be difficult obtaining g_1^n from nuclear data on the basis of independent scattering. Because g_1^p and g_1^n are expected to be rather different in magnitude, this approach should be reliable [153].

The nuclear cross-section difference is given by

$$d\sigma_A^{\Rightarrow} - d\sigma_A^{\Leftarrow} = 2\,[Z d\sigma_p\,\mathcal{P}_p\,A_{\parallel}^p + N d\sigma_n\,\mathcal{P}_n\,A_{\parallel}^n]\,, \tag{4.115}$$

where Z is number of protons, N is number of neutrons, $d\sigma_{p,n}$ are the unpolarized nucleon cross-sections, $A_{\parallel}^{p,n}$ the nucleon longitudinal asymmetries and $\mathcal{P}_{p,n}$ the longitudinal polarization of the nucleons in the nuclear state with $J_z = 1/2$ or 1.

The asymmetry defined in (4.112) is

$$A_{\parallel}^A = f_p \mathcal{P}_p\,A_{\parallel}^p + f_n \mathcal{P}_n\,A_{\parallel}^n \tag{4.116}$$

where

$$f_p = \frac{Z d\sigma_p}{Z d\sigma_p + N d\sigma_n} \qquad f_n = \frac{N d\sigma_n}{Z d\sigma_p + N d\sigma_n} \tag{4.117}$$

are the fractions of events originating on protons and neutrons respectively.

A similar result holds for $A_{\perp}^A$.

Equation (4.116) is the main formula used to extract $A_{\parallel}^n$ from $A_{\parallel}^A$ and a knowledge of $A_{\parallel}^p$.

Because of the D-state admixture for deuterium we obtain,

$$\mathcal{P}_p^d = \mathcal{P}_n^d = (1 - \frac{3}{2}\,\omega_D) \tag{4.118}$$

where $\omega_D = 0.058$ is the D-state probability.

For the fractions $f_{p,n}$ one finds :

$$f_p^d = \frac{F_2^p/(1+R^p)}{2F_2^d/(1+R^d)} \qquad f_n^d = \frac{F_2^n/(1+R^n)}{2F_2^d/(1+R^d)} \tag{4.119}$$

where F_2^d is the deuteron F_2 per nucleon.

Often one defines g_1^d per nucleon via (4.87, 88)

$$g_1^d(x, Q^2) \equiv \frac{A_\parallel^d}{D} \frac{F_2^d(x, Q^2)}{2x[1 + R^d(x, Q^2)]} \tag{4.120}$$

so that (4.116) becomes

$$g_1^d\ (x, Q^2) = \frac{(1 - \frac{3}{2}\omega_D)}{2} \left\{ g_1^p(x, Q^2) + g_1^n(x, Q^2) \right\}. \tag{4.121}$$

For spin 1/2 targets with degree of longitudinal polarization $\mathcal{P}$ we can generalize:

$$A_\parallel = \frac{1}{\mathcal{P}} \left\{ \frac{d\sigma^{\rightarrow}(-\mathcal{P}) - d\sigma^{\rightarrow}(\mathcal{P})}{d\sigma^{\rightarrow}(-\mathcal{P}) + d\sigma^{\rightarrow}(\mathcal{P})} \right\} = \frac{1}{\mathcal{P}} \frac{d\sigma^{\rightarrow}(-\mathcal{P}) - d\sigma^{\rightarrow}(\mathcal{P})}{2\, d\sigma} \tag{4.122}$$

where $d\sigma$ is the unpolarized cross-section. A similar result holds for $A_\perp$.

The result for spin 1 targets is more complicated. If $p_+,\ p_-,\ p_0$ are the probabilities of finding states with $J_z = 1,\ -1,\ 0$ in the target, then the degree of polarization is [154]

$$\mathcal{P} = p_+ - p_- \tag{4.123}$$

and the alignment is

$$\mathcal{A} = 1 - 3p_0\,. \tag{4.124}$$

Then one has

$$d\sigma^{\rightarrow}(-\mathcal{P}) - d\sigma^{\rightarrow}(\mathcal{P}) = \mathcal{P} \left\{ d\sigma^{\overset{\rightarrow}{\Leftarrow}} - d\sigma^{\overset{\rightarrow}{\Rightarrow}} \right\}, \tag{4.125}$$

but

$$d\sigma^{\rightarrow}(-\mathcal{P}) + d\sigma^{\rightarrow}(\mathcal{P}) = 2d\sigma + \frac{\mathcal{A}}{3}[d\sigma_+ + d\sigma_- - 2\, d\sigma_0] \tag{4.126}$$

where $d\sigma$ is the unpolarized cross-section for the spin 1 target.

It follows that for a spin 1 target

$$A_\parallel = \frac{1}{\mathcal{P}} \frac{d\sigma^{\rightarrow}(-\mathcal{P}) - d\sigma^{\rightarrow}(\mathcal{P})}{2\, d\sigma + (\mathcal{A}/3)[d\sigma_+ + d\sigma_- - 2\, d\sigma_0]} \tag{4.127}$$

This is equal to

$$\frac{1}{\mathcal{P}} \frac{d\sigma^{\rightarrow}(-\mathcal{P}) - d\sigma^{\rightarrow}(\mathcal{P})}{2\, d\sigma} \tag{4.128}$$

if the alignment $\mathcal{A}$ is known to be zero.

In principle it should be possible to check the assumption of independent scattering by experimentally testing (4.126).

The ^{3}He wave-function is almost entirely an S-state with the two protons having opposite spins. The spin is carried by the neutron, but there is some mixing in the wave-function [156, 155], and one estimates

$$\mathcal{P}_n^{^3He} = (87 \pm 2)\% \qquad \mathcal{P}_p^{^3He} = (-2.5 \pm 0.3)\%\,. \tag{4.129}$$

For the fractions $f_{p,n}$ the following approximation can be used:

$$\begin{aligned} f_n^{^3He} &= \frac{F_2^n/(1+R^n)}{3F_2^{^3He}/(1+R^{^3He})} \\ f_p^{^3He} &= \frac{2F_2^p/(1+R^p)}{3F_2^{^3He}/(1+R^{^3He})} \end{aligned} \tag{4.130}$$

where $F_2^{^3He}$ is the helium-3 F_2 per nucleon.

Defining $g_1^{^3He}$ per nucleon via (4.88),

$$g_1^{^3He}\,(x,Q^2) = \frac{A_\parallel^{^3He}}{D}\;\frac{F_2^{^3He}(x,Q^2)}{2x[1+R^{^3He}(x,Q^2)]}\,, \tag{4.131}$$

one obtains

$$g_1^{^3He}\,(x,Q^2) = \frac{1}{3}\left[(0.87\pm 0.02)\; g_1^n(x,Q^2) - (0.050\pm 0.006)\; g_1^p(x,Q^2)\right]\,. \tag{4.132}$$

The analysis above is based on an independent scattering from the constituent nucleons. This assumption is reasonable at high Q^2, but it is probably not a good approximation in the experiments which have low momentum transfer.

4.8 Sum rules

The fundamental properties of the nucleon structure such as the total momentum fraction carried by the quarks or the contribution of the quark spins to the spin of the nucleon can be studied by investigating the moments of the structure functions. Moments of the structure functions can be measured in the experiments and then directly compared to theoretical results - sum rules, lattice QCD calculations and chiral perturbation theory. The proton spin puzzle originated directly from a discrepancy between the data and an approximate "sum rule" by Ellis and Jaffe [10]. A detailed measurement of the Q^2–evolution of the Bjorken sum rule [12] provides a significant test of perturbative QCD in the spin sector.

Using Operator Product Expansion (OPE) the moments of $g_{1,2}$ can be related to hadronic matrix elements of current operators. The moments can be written as a sum, ordered according to the *twist* $\tau =$ (dimension $-$ spin) of the current operators, starting with the lowest twist $\tau = 2$. Additional units of τ produces a factor of order $\frac{\Lambda_{QCD}}{Q}$, and are less important in the high Q^2 region. The higher twist terms are mixed with correction terms of order $\frac{M^2}{Q^2}$ of kinematic origin (target mass corrections), which can be calculated exactly, giving access to the HT terms which are of dynamic origin. Some of the twist 2 terms can be directly measured in other processes. Twist 3 and higher terms can sometimes be determined from combinations of measured quantities.

It is possible to express the n^{th} moment $\int_0^1 dx\, x^{n-1}\, g_1(x, Q^2)$ for $n = 1, 3, 5......$ of g_1 and the n^{th} moment $\int_0^1 dx\, x^{n-1}\, g_2(x, Q^2)$ for $n = 3, 5, 7......$ of g_2, in terms of hadronic matrix elements of local operators.

The most important case is the first moment, $n = 1$, of g_1. The operators used here are the octet of axial-vector currents which control the neutron and hyperon β-decay:

$$J^i_{5\mu} = \bar{\boldsymbol{\psi}}\gamma_\mu\gamma_5 \left(\frac{\boldsymbol{\lambda}_i}{2}\right)\boldsymbol{\psi} \qquad (i = 1, 2, ..., 8), \tag{4.133}$$

where the $\boldsymbol{\lambda}_j$ are Gell-Mann matrices and $\boldsymbol{\psi}$ is a column vector in flavor space

$$\boldsymbol{\psi} = \begin{pmatrix} \psi_u \\ \psi_d \\ \psi_s \end{pmatrix}. \tag{4.134}$$

The flavor singlet current, which does not play a role in β-decay, is

$$J^0_{5\mu} = \bar{\boldsymbol{\psi}}\gamma_\mu\gamma_5\boldsymbol{\psi}\,. \tag{4.135}$$

The relation between hadronic matrix elements and the first moments $a_3 \equiv g_A$, a_8, a_0 of the flavor combinations of quark densities is

$$\begin{aligned}\langle P,S|J^3_{5\mu}|P,S\rangle &= Ma_3S_\mu\\ \langle P,S|J^8_{5\mu}|P,S\rangle &= \frac{M}{\sqrt{3}}\,a_8S_\mu\\ \langle P,S|J^0_{5\mu}|P,S\rangle &= 2Ma_0(Q^2)S_\mu.\end{aligned}\tag{4.136}$$

The Q^2 dependence of a_0 depends on the choice of the renormalization scale, which we take to be Q^2.

The expression for $\Gamma_1^{p,n}$, valid for $Q^2 \gg M^2$, is given by:

$$\Gamma_1^{p,n} = \frac{1}{12}\big[\big(\pm a_3 + \frac{1}{3}\,a_8\big)E_{NS}(Q^2) + \frac{4}{3}\,a_0(Q^2)E_S(Q^2)\big],\tag{4.137}$$

The coefficient functions are given, for 3 active flavors, by

$$E_{NS}(Q^2) = 1 - \big(\frac{\alpha_s}{\pi}\big) - 3.58\,\big(\frac{\alpha_s}{\pi}\big)^2 - 20.22\big(\frac{\alpha_s}{\pi}\big)^3...\tag{4.138}$$

In the $\overline{MS}$ scheme we have:

$$E_S(Q^2) = 1 - \big(\frac{\alpha_s}{\pi}\big) - 1.096\,\big(\frac{\alpha_s}{\pi}\big)^2....\tag{4.139}$$

There are several important sum rules for the moments of $g_{1,2}$.

- *The Bjorken sum rule.* Bjorken [12] showed that as $Q^2 \to \infty$,

$$\int_0^1 dx\,[g_1^p(x,Q^2) - g_1^n(x,Q^2)] = \frac{g_A}{6}\,\big[1 - \big(\frac{\alpha_s}{\pi}\big) - 3.58\big(\frac{\alpha_s}{\pi}\big)^2 - 20.22\big(\frac{\alpha_s}{\pi}\big)^3\cdots\big],\tag{4.140}$$

  where the square bracket on the RHS contains the perturbative corrections Eq. 4.138, for 3 active flavors, to Bjorken's original result $g_A/6$.

- *The Efremov-Leader-Teryaev sum rule* . The ELT sum rule [18] follows from the OPE and states that

$$\int_0^1 dx\,x\,[g^V_{1,f}(x) + 2g^V_{2,f}(x)] = 0,\tag{4.141}$$

  where V is the *valence* contribution and the result is valid for each flavor f. Originally is was assumed that the sea-quark densities are the same in protons and neutrons, in which case Eq. 4.141 can be written as an analogue to the Bjorken sum rule

$$\int_0^1 dx\,x\,[g_2^p(x) - g_2^n(x)] = \frac{1}{2}\int_0^1 dx\,x\,[g_1^n(x) - g_1^p(x)].\tag{4.142}$$

  The above assumption about see-quark densities is equivalent to assuming $\Delta\bar{u} = \Delta\bar{d}$ in a proton, which for the *unpolarized* antiquark densities, is not a good approximation. For further sum rules of this type see [116, 90].

- *Higher twist corrections.*

  At lower values of Q^2 higher twist contributions become important. $\Gamma_1(Q^2)$ can be expanded, for $Q^2 > \Lambda^2_{QCD}$, in inverse powers of Q^2 (twist expansion)

$$\Gamma_1(Q^2) = \mu_2(Q^2) + \frac{\mu_4(Q^2)}{Q^2} + \frac{\mu_6(Q^2)}{Q^4} + ... \tag{4.143}$$

  with μ_2, the leading twist term, given by Eq. (4.137).

  The evolution in Q^2 of the $\mu_n(Q^2)$ can, in principle, be calculated in perturbative QCD, but the results are known only for μ_2 . The Q^2 dependence of $\mu_{4,6}$ is usually ignored. The functions μ_n are related to matrix elements of operators of twist $\tau \leq n$; presence of operators with twist lower than n is a kinematic effect, a consequence of target mass corrections.

  We consider the structure of the higher twist (i.e., $1/Q^2$) corrections to $\Gamma_1(Q^2)$ as defined in Eq. 4.143. $\mu_4(Q^2)$ contains both target mass (TM) corrections and dynamical higher twist contributions. The TM corrections for $g_{1,2}(x, Q^2)$ are given in [115]. For the first moment they are

$$\mu_4^{TM}(Q^2) = \frac{2M^2}{9} \int_0^1 dx\, x^2\, [5g_1(x, Q^2) + 6g_2(x, Q^2)]. \tag{4.144}$$

  g_2 contains a twist-2 (and kinematic twist-3) part, g_2^{WW}, is given by:

$$g_2^{WW}(x, Q^2) = -g_1(x, Q^2) + \int_x^1 \frac{g_1(y, Q^2)}{y} dy \tag{4.145}$$

  and a dynamic twist-3 part given by $g_2 - g_2^{WW}$. Writing

$$g_2 = g_2^{WW} + (g_2 - g_2^{WW}) \tag{4.146}$$

  one finds :

$$\mu_4^{TM}(Q^2) = \frac{2M^2}{9} \Big\{ \int_0^1 dx\, x^2\, g_1(x, Q^2) + 6 \int_0^1 dx\, x^2\, [g_2(x, Q^2) - g_2^{WW}(x, Q^2)] \Big\}. \tag{4.147}$$

  The twist-2 combination of moments is usually referred to as a_2 and the twist-3 as d_2:

$$a_2(Q^2) \equiv 2 \int_0^1 dx\, x^2\, g_1(x, Q^2) \qquad d_2(Q^2) \equiv 3 \int_0^1 dx\, x^2\, [g_2(x, Q^2) - g_2^{WW}(x, Q^2)]. \tag{4.148}$$

  There is a twist-4 contribution to μ_4, written as $\frac{4M^2}{9} f_2$:

$$\mu_4(Q^2) = \frac{M^2}{9}[a_2(Q^2) + 4d_2(Q^2) + 4f_2(Q^2)]. \tag{4.149}$$

The twist-4 part f_2 cannot be written in terms of moments of the scaling functions. In terms of operator matrix elements it is defined by

$$f_2(Q^2)M^3S^\mu = \frac{1}{2}\sum_{flavors} e_f^2\langle P,S\,|\,g\bar{\psi}_f\,\tilde{G}^{\mu\nu}\,\gamma_\nu\,\psi_f\,|P,S\,\rangle \tag{4.150}$$

where $\tilde{G}^{\mu\nu} = (1/2)\epsilon^{\mu\nu\alpha\beta}G_{\alpha\beta}$ with the sign convention $\epsilon^{0123} = +1$.

The first expressions for d_2 and f_2 were given by Ji and Unrau [88] and by Ehrnsperger, Mankiewicz and Schäfer [91].

Since μ_4, a_2 and d_2 can be measured, Eq. 4.149 gives a measurement of the twist-4 matrix element f_2. Both d_2 and f_2 can then be compared to non-perturbative QCD calculations.

It is of some interest also to consider the color electric and color magnetic polarizabilities of the nucleon [92]. They are defined by

$$\chi_E 2M^3\boldsymbol{S} = \langle\, N,\boldsymbol{S}\,|\,\boldsymbol{j}_a{\times}\boldsymbol{E}_a\,|N,\boldsymbol{S}\,\rangle \qquad \chi_B 2M^3\boldsymbol{S} = \langle\, N,\boldsymbol{S}\,|\,j_a^0\boldsymbol{B}_a\,|N,\boldsymbol{S}\,\rangle \tag{4.151}$$

where $\boldsymbol{S}$ is the rest frame spin vector of the nucleon and j_a^μ is the quark current. $\boldsymbol{E}_a$ and $\boldsymbol{B}_a$ are the color electric and magnetic fields respectively. The color polarizabilities can be expressed in terms of d_2 and f_2 as

$$\chi_E = \frac{2}{3}(2d_2 + f_2) \qquad \chi_M = \frac{1}{3}(4d_2 - f_2). \tag{4.152}$$

- *Extrapolation to low Q^2: the Gerasimov, Drell, Hearn sum rule.*

The twist expansion does not converge for very small Q^2. To study polarized structure functions in the low Q^2 region, it is necessary to make a connection with soft, non-perturbative physics i.e. to study the relation to Compton scattering with *real* photons. In this region one has to be careful in defining moments of the structure functions. Relations between moments of structure functions and matrix elements of operators are only valid if the moments include the elastic contributions, located at $x = 1$. In the *deep* inelastic region the elastic contributions are negligible and are not included in experimental estimates of the moments, but at low Q^2, in the resonance region, the distinction is important. Thus moments in the latter region, without an elastic contribution, will be labeled $\bar{\Gamma}$.

The GDH sum rule [93, 94] is related to Compton scattering with real photons, i.e., with $Q^2 = 0$. It is derived from the fact, that the value of the forward spin-flip amplitude, $f_2(\nu)$, at $\nu = 0$, calculated to order

e^2, is given by low energy theorems, and from the assumption that the dispersion relation for it does not require subtractions. This gives

$$\int_0^\infty \frac{d\nu}{\nu}\left[\sigma_A(\nu)-\sigma_P(\nu)\right] = -\frac{2\pi^2\alpha}{M^2}\,\kappa^2 \tag{4.153}$$

where κ is the anomalous magnetic moment of the nucleon. The $\sigma_{A,P}$ are the total cross-sections for the absorption of a circularly polarized photon by a proton polarized with spin antiparallel/parallel to the photon spin.

To order e^2, the cross-sections are zero below pion production threshold ν_0 . Eq. 4.153 can be written in the form

$$I(0) \equiv \int_{\nu_0}^\infty \frac{d\nu}{\nu}\left[\sigma_A(\nu)-\sigma_P(\nu)\right] = -\frac{2\pi^2\alpha}{M^2}\kappa^2. \tag{4.154}$$

In the DIS formalism the above cross-section difference is referred to as σ_{TT}, and Eq. 4.154, generalized to non-zero Q^2, is usually written

$$\lim_{Q^2\to 0}\bar{I}_{TT}(Q^2) = -\kappa^2/4 \tag{4.155}$$

where

$$\bar{I}_{TT}(Q^2) = M^2\int_{\nu_0(Q^2)}^\infty \frac{d\nu}{\nu^2}\left[\nu M G_1(\nu,Q^2) - Q^2 G_2(\nu,Q^2)\right] \tag{4.156}$$

$$= \frac{2M^2}{Q^2}\bar{\Gamma}_{TT}(Q^2) \tag{4.157}$$

with

$$\nu_0(Q^2) = \frac{Q^2+m_\pi(2M+m_\pi)}{2M} \tag{4.158}$$

and where $\bar{\Gamma}_{TT}(Q^2)$ is the *inelastic* portion of the first moment

$$\bar{\Gamma}_{TT}(Q^2) \equiv \int_0^{x_0(Q^2)} dx\,\left[g_1(x,Q^2) - \frac{4M^2x^2}{Q^2}g_2(x,Q^2)\right] \tag{4.159}$$

and $x_0(Q^2)$ is the threshold for pion production,

$$x_0 = \frac{Q^2}{Q^2+m_\pi(2M+m_\pi)}. \tag{4.160}$$

The generalization of $I(0)$ in Eq. 4.154 to arbitrary Q^2 is then given by

$$I(Q^2) = \frac{8\pi^2\alpha}{M^2}\,\bar{I}_{TT}(Q^2). \tag{4.161}$$

The importance of Eqs. 4.155 and 4.157 to deep inelastic scattering was first pointed out by Anselmino, Ioffe and Leader [95], who noted that the first moment $\bar{\Gamma}^p_{TT}(Q^2)$, which is a positive function in the DIS region, would have to change drastically in order to satisfy Eq. 4.155 at small Q^2. However [95] could not distinguish between the full moment $\Gamma^p_{TT}(Q^2)$ and its inelastic version $\bar{\Gamma}^p_{TT}(Q^2)$, and Ji [87] pointed out that there is a significant difference between the extrapolation to $Q^2 = 0$ of the full and the inelastic moments . The reason is a non-uniformity of the limits $\nu \to 0$ and $Q^2 \to 0$ in the generalization of $f_2(\nu)$ to $Q^2 \neq 0$, namely,

$$\lim_{Q^2\to 0} \lim_{\nu\to 0} f_2(\nu, Q^2) \neq \lim_{\nu\to 0} \lim_{Q^2\to 0} f_2(\nu, Q^2). \tag{4.162}$$

The RH limit does not include an elastic contribution from the Born terms in Compton Scattering, but the LH one does. Since the integrals involved in the moments above correspond to $\nu = 0$ in $f_2(\nu, Q^2)$, it is the LH limit which must be used in the extrapolation to $Q^2 = 0$. For the *full* moment Eq. 4.155 is changed to

$$\lim_{Q^2\to 0} I_{TT}(Q^2) = \frac{M^2}{Q^2}[F_1^{el}(Q^2) + F_2^{el}(Q^2)]^2 - \kappa^2/4 \tag{4.163}$$

where $F^{el}_{1,2}$ are the Dirac and Pauli *elastic* from factors normalized to

$$F^{el}_{1p}(0) = 1 \qquad F^{el}_{1n}(0) = 0 \qquad F^{el}_{2p,n}(0) = \kappa_{p,n}. \tag{4.164}$$

Using similar arguments one can generalize the spin-dependent Compton amplitudes $S_{1,2}$ to arbitrary Q^2 [87]. They are normalized:

$$Im S_{1,2}(\nu, Q^2) = 2\pi\, G_{1,2}(\nu, Q^2). \tag{4.165}$$

For S_1 one obtains the dispersion relation

$$S_1(\nu, Q^2) = 4\int_{\nu_0(Q^2)}^{\infty} \frac{G_1(\nu', Q^2)\nu' d\nu'}{\nu'^2 - \nu^2}. \tag{4.166}$$

Then

$$\begin{aligned} \frac{M^3}{4} S_1(0, Q^2) = \bar{I}_1(Q^2) &\equiv M^2 \int_{\nu_0(Q^2)}^{\infty} \frac{d\nu}{\nu} M G_1(\nu, Q^2) && (4.167) \\ &= \frac{2M^2}{Q^2}\bar{\Gamma}_1(Q^2) && (4.168) \end{aligned}$$

where $\bar{\Gamma}_1(Q^2)$ is the *inelastic* portion of the first moment $\Gamma_1(Q^2)$

$$\bar{\Gamma}_1(Q^2) \equiv \int_0^{x_0(Q^2)} dx\, g_1(x, Q^2) \tag{4.169}$$

and

$$\lim_{Q^2\to 0} \bar{I}_1(Q^2) = -\kappa^2/4. \tag{4.170}$$

For the full moment we obtain:

$$\lim_{Q^2\to 0} I_1(Q^2) = \frac{M^2}{Q^2} F_1^{el}(Q^2)\,[F_1^{el}(Q^2) + F_2^{el}(Q^2)] - \kappa^2/4. \tag{4.171}$$

The elastic contribution to the moments is totally negligible in the DIS region. In the extrapolation down through the resonance region towards $Q^2 = 0$ it is important to distinguish between the two cases.

The Compton amplitude $S_2(\nu)$ is the basis of the BC sum rule. If one assumes that $S_2(\nu, Q^2)$ satisfies a superconvergence relation, i.e., that it vanishes as $\nu \to \infty$ fast enough so that both S_2 and νS_2 satisfy unsubtracted dispersion relations, then it is possible to show that

$$\int_0^\infty ImS_2(\nu, Q^2)d\nu = 2\pi \int_0^\infty G_2(\nu, Q^2)d\nu = 0 \tag{4.172}$$

which leads to $\int_0^1 dx\, g_2(x) = 0$ for the full moment. From the elastic terms in $S_2(0, Q^2)$ one obtains an expression for the inelastic integral

$$\bar{I}_2(Q^2) \equiv \frac{2M}{Q^2} \int_0^{x_0(Q^2)} g_2(x, Q^2)dx = \frac{1}{4} F_2^{el}(Q^2)[F_1^{el}(Q^2) + F_2^{el}(Q^2)]. \tag{4.173}$$

- *Generalization of the GDH approach.*

  The analysis based on the dispersion relations for $f_2(\nu, Q^2), S_{1,2}(\nu Q^2)$, has been generalized to all the amplitudes in virtual Compton scattering by Drechsel, Pasquini and Vanderhaeghen [97]. At very small energies, $\nu < \nu_0(Q^2)$, the amplitudes can be expanded in powers of ν^2. The coefficients of the next-to-leading terms are called generalized forward spin polarizabilities of the nucleon. They can be expressed in terms of moments of the structure functions and can be measured. This coefficients reflect soft, non-perturbative aspects of the nucleon structure and can be approximately calculated, using various forms of chiral perturbation theory and lattice methods, providing good tests for these theories. We give here the expressions for experimentally relevant polarizabilities, for details of the amplitudes etc, see [97].

$$\gamma_0(Q^2) = \frac{16\alpha M^2}{Q^6} \int_0^{x_0} x^2 \left[g_1(x, Q^2) - \frac{4M^2x^2}{Q^2} g_2(x, Q^2)\right] dx$$

$\delta_0(Q^2) = \frac{16\alpha M^2}{Q^6} \int_0^{x_0} x^2 \left[g_1(x, Q^2) + g_2(x, Q^2)\right] dx$

4.9 Gluon spin in the Proton

We consider the integral of the polarized gluon distribution,

$$\Gamma(Q^2) = \int_0^1 dx\, \Delta g(x, Q^2) = \int_0^1 dx (g_\uparrow(x, Q^2) - g_\downarrow(x, Q^2)) \tag{4.174}$$

Γ is defined in terms of the matrix element of products of gluon vector potentials and field strengths *in the nucleon rest frame and in $A^+ = 0$ gauge*,

$$\Gamma(Q^2) = \frac{1}{2M} \langle \hat{e}_3 | \, 2\, \mathrm{Tr}\{(\vec{E} \times \vec{A})^3 + \vec{A}_\perp \cdot \vec{B}_\perp\}\Big|_{Q^2} | \hat{e}_3 \rangle \tag{4.175}$$

where $\perp$ means the direction transverse to the $\hat{e}_3$ axis, defined by the target spin, and Q^2 is the renormalization scale of the operators.

Operator Description of the Gluon Spin

It is possible to measure the polarized gluon distribution function, $\Delta g(x, Q^2)$, in deep inelastic lepton scattering. Δg measures the net polarization of gluons in the direction of the nucleon spin. The operator representation of the polarized gluon distribution function is

$$\begin{aligned} \Delta g(x, Q^2) &= \frac{i}{4x\pi P^+} \int d\xi^- e^{-ix\xi^- P^+} \langle P, \hat{e}_3 | \, \mathrm{Tr}\, \{F^{+\alpha}(\xi^-, \vec{0}) \mathcal{I}(\xi^-, 0) \tilde{F}_\alpha{}^{+}(0)\}\Big|_{Q^2} | P, \hat{e}_3 \rangle \\ &+ \ (x \to -x), \end{aligned} \tag{4.176}$$

where F (and A) are matrices ($F \equiv \sum_{a=1}^{8} F^a \lambda^a$, *etc.*). $\{F^a\}$ describe the adjoint, and $\{\lambda^a\}$ the triplet representation (with $\mathrm{Tr}\{\lambda^a \lambda^b\} = \frac{1}{2}\delta^{ab}$). $\xi^\pm, \vec{\xi}^\perp$ are light-cone coordinates and $(\xi^-, \vec{0})$ denotes the point $\xi^-, \xi^+ = \vec{\xi}^\perp = 0$. The label Q^2 is a reminder that the tower of local matrix elements in the Taylor expansion of $F\tilde{F}$ are understood to be renormalized at the factorization scale Q^2. $\mathcal{I}$ is the Wilson-line integral,

$$\mathcal{I}(\xi^-, 0) = \mathcal{P}\mathrm{exp}\left(ig \int_0^{\xi^-} dy^- A^+(y^-, \vec{0}) \right). \tag{4.177}$$

The usual parton interpretation follows from eq. (4.176) if we choose $A^+ = 0$ gauge and introduce the momentum decomposition of the fields F and $\tilde{F}$ quantized at $\xi^+ = 0$.

To integrate eq. (4.176) over x we should study the apparent singularity at $x = 0$. $\Delta g(x, Q^2)$ is not expected to diverge as fast as $1/x$, so the ξ^-–integral must vanish as $x \to 0$. The singularity at $x = 0$ is integrable. We can interchange the x and ξ^- integrations and, because Δg is symmetric in

x, we can use the principal value prescription at $x=0$, $\fint \frac{dx}{x} e^{-i\alpha x} = -i\pi\varepsilon(\alpha)$. We obtain

$$\Gamma(Q^2) = \frac{1}{2P^+} \int d\xi^- \varepsilon(\xi^-) \langle P, \hat{e}_3 | \operatorname{Tr} \{ F^{+\alpha}(\xi^-) \mathcal{I}(\xi^-, 0) \tilde{F}_\alpha{}^+(0) \} \Big|_{Q^2} | P, \hat{e}_3 \rangle. \tag{4.178}$$

Using the $A^+ = 0$ gauge $\mathcal{I} = 1$ and $F^{+\alpha} = \frac{\partial}{\partial \xi^-} A^\alpha$, we may perform the ξ^- integration. The terms at $\xi^- = \pm\infty$ vanish, because the integral in eq. (4.176) converges for $x = 0$. Only the local ($\xi^- = 0$) contribution survives. We choose the rest frame for P and obtain:

$$\begin{aligned} \Gamma(Q^2) &= \frac{1}{\sqrt{2}M} \langle P, \hat{e}_3 | 2 \operatorname{Tr} \{ A^1 F^{+2} - A^2 F^{+1} \} \Big|_{Q^2} | P, \hat{e}_3 \rangle \\ &= \frac{1}{2M} \langle P, \hat{e}_3 | 2 \operatorname{Tr} \{ (\vec{E} \times \vec{A})^3 + \vec{A}_\perp \cdot \vec{B}_\perp \} \Big|_{Q^2} | P, \hat{e}_3 \rangle, \end{aligned} \tag{4.179}$$

where $E^i = F^{i0}$, and $B^i = -\frac{1}{2}\varepsilon^{ijk} F^{jk}$. The choice of $A^+ = 0$ gauge was essential for this derivation. Otherwise Γ does not appear to be associated with a *local* operator.

Eq. (4.179) can be related directly to the gluon spin term in the angular momentum tensor density in QCD. It is described by a rank-3 Lorentz tensor, $M^{\mu\nu\lambda}$:

$$\begin{aligned} M^{\mu\nu\lambda}_{QCD} &= \frac{i}{2} \bar{\psi} \gamma^\mu \left(x^\lambda \partial^\nu - x^\nu \partial^\lambda \right) \psi + \frac{1}{2} \epsilon^{\mu\nu\lambda\sigma} \bar{\psi} \gamma_\sigma \gamma_5 \psi \\ &- 2 \operatorname{Tr} \{ F^{\mu\alpha} \left(x^\nu \partial^\lambda - x^\lambda \partial^\nu \right) A_\alpha \} + 2 \operatorname{Tr} \{ F^{\mu\lambda} A^\nu + F^{\nu\mu} A^\lambda \} \\ &- \frac{1}{2} \operatorname{Tr} F^2 \left(x^\nu g^{\mu\lambda} - x^\lambda g^{\mu\nu} \right), \end{aligned} \tag{4.180}$$

The second term in eq. (4.180) measures the quark spin. The first and third terms look like the quark and gluon orbital angular momentum respectively, because they have the standard form of orbital angular momentum in a field theory, $\Pi^\dagger (\vec{x} \times \vec{\nabla}) \Phi$, where Π and Φ are canonical coordinate and momentum respectively. The last term contributes only to boosts. The fourth term is a candidate for the gluon spin.

Let us define

$$M^{\mu\nu\lambda}_\Gamma \equiv 2 \operatorname{Tr} \{ F^{\mu\nu} A^\lambda + F^{\lambda\mu} A^\nu \}. \tag{4.181}$$

Comparison with eq. (4.179) shows that

$$\Gamma(Q^2) = \frac{1}{2S^+} \langle P, \hat{e}_3 | M^{+12}_\Gamma \Big|_{Q^2} | P, \hat{e}_3 \rangle, \tag{4.182}$$

in the $A^+ = 0$ gauge. This restriction does not make Γ gauge dependent: There is a corresponding operator definition of Γ in any gauge.

4.10 The Gluon Spin in Quark Models

There are two general classes of quark models for the hadrons : non-relativistic quark models, where the quarks are described by the Schroedinger equation and bag models, where relativistic quarks move in some confining background field. Both cases give good explanations of the mass spectrum of the lightest hadrons (pseudoscalar and vector mesons, and octet and decuplet baryons). A major role is played by color mediated, spin dependent forces. The gluons responsible for these spin splittings are *anti-aligned* with the nucleon spin ($\Gamma < 0$). This is a particular consequence of the non-abelian nature of the QCD interactions.

The quantity we want to evaluate is

$$\Gamma(\mu_0^2) = \langle T, \hat{e}_3| \int d^3x\, 2\mathrm{Tr}\,\{\left(\vec{E}(\vec{x}) \times \vec{A}(\vec{x})\right)^3 + \vec{A}_\perp(\vec{x})\cdot\vec{B}_\perp(\vec{x})\}|T, \hat{e}_3\rangle \quad (4.183)$$

The color-electric fields are given by the gradient of a time-independent function of the quark degrees of freedom, $\vec{E}^a(\vec{x}) = -\vec{\nabla}\Phi^a(\vec{x})$, with

$$\Phi^a(\vec{x}) = \frac{g}{4\pi}\sum_i \lambda_i^a \mathcal{G}(\vec{x}, \vec{x}_i) \quad (4.184)$$

The magnetic field $\vec{B}^a(\vec{x})$ can be written as the *curl* of a time independent function of the quark variables, $\vec{B}^a(\vec{x}) = \vec{\nabla} \times \vec{U}^a(\vec{x})$, with

$$\vec{U}^a(\vec{x}) = \frac{g}{4\pi}\sum_i \lambda_i^a \vec{\sigma}_i \times \vec{\mathcal{G}}(\vec{x}, \vec{x}_i). \quad (4.185)$$

The operators Φ and $\vec{U}$ are not yet the appropriate scalar and vector potentials for the gluon field, since they do not satisfy the $A^+ = 0$ gauge condition. Suitable potentials can be easily constructed. Define

$$\begin{aligned} A^{0a}(\vec{x}) &= \Phi^a(\vec{x}) \\ \vec{A}^a(\vec{x}) &= \vec{U}^a(\vec{x}) - \vec{\nabla}\int_0^z d\zeta \Phi^a(x, y, \zeta) \end{aligned} \quad (4.186)$$

These potentials generate $\vec{E}^a$ and $\vec{B}^a$ in the usual way and satisfy the gauge constraint $A^{0a} + A^{3a} = 0$. The choice of time independent potentials as well as the lower limit on the ζ integration correspond to the residual gauge freedom, available in the $A^+ = 0$ gauge.

Substituting the operator definitions of A^{0a} and $\vec{A}^a$ into eq. (4.183) we have

$$\begin{aligned} \Gamma(\mu_0^2) &= \sum_{i\neq j}\sum_{a=1}^{8}\int d^3x \langle T, \hat{e}_3|\{\left[\vec{E}_i^a(\vec{x}) \times \vec{U}_j^a(\vec{x})\right]^3 + \left[\vec{E}_i^a(\vec{x}) \times \vec{\nabla} f_j^a(\vec{x})\right]^3 \\ &+ \vec{U}_{\perp i}^a(\vec{x}) \cdot \vec{B}_{\perp j}^a(\vec{x}) + \vec{\nabla}_\perp f_i^a(\vec{x}) \cdot \vec{B}_{\perp j}^a(\vec{x})\}|T, \hat{e}_3\rangle \end{aligned} \quad (4.187)$$

where we have separated the contributions from individual quarks i and j to each of the field operators. We have dropped the $i = j$ terms.

The second and third terms in eq. (4.187) vanish. The second term vanishes after integration by parts because $\vec{\nabla} \times \vec{E}_j^a = 0$. There is no associated surface term. The third term vanishes for spatially symmetric quark wavefunctions.

Consider now the fourth term and write out the space components explicitly (suppressing the color (a) and quark (i, j) labels, and bras and kets):

$$
\begin{aligned}
\Gamma_4 &= \int d^3x \left(\frac{\partial f}{\partial y} \frac{\partial U_1}{\partial z} - \frac{\partial f}{\partial x} \frac{\partial U_2}{\partial z} \right) \\
&= \int d^3x \, (E_1 U_2 - E_2 U_1) \\
&+ \oint_{S_R} d^2 s \hat{e}_3 \cdot \hat{r} \left(U_1(\vec{x}) \int_0^z d\zeta E_2(x, y, \zeta) - U_2(\vec{x}) \int_0^z d\zeta E_1(x, y, \zeta) \right)
\end{aligned}
$$

where the surface integral is over a sphere at large distance (for unconfined gluons) or the bag surface (for bag-like models). The first term in eq. (4.188) is identical to the first term in eq. (4.187).

We combine these results and substitute the parameterizations of $\vec{E}$ and $\vec{U}$. We obtain:

$$
\Gamma = \frac{8}{9} \alpha \int_0^R dr r Q(r)(h(R) - 2h(r)), \tag{4.188}
$$

where the r-integration goes to infinity in generic non-relativistic quark models, but ends at $r = R$, the bag surface in the bag model. The term proportional to $-2h(r)$ is the volume integral of $\vec{E} \times \vec{U}$, and the $h(R)$-term is the surface contribution left over from integration by parts. In reaching eq. (4.188) we have used $\sum_{a=1}^{8} \lambda_i^a \lambda_j^a = -2/3$ for $i \neq j$.

Now we consider quark potential models where quarks are confined. The gluon field strengths fall off at large distances like abelian multipoles. The non-relativistic vector potential, $\vec{U} = \vec{m} \times \vec{r}/r^3$, corresponds to $h(r)_{NQM} \propto 1/2m_q r^3$. At large R, $Q(R) \to 1$, so the surface term in eq. (4.188) vanishes. Eq. (4.188) reduces to

$$
\begin{aligned}
\Gamma_{NQM}(\mu_0^2) &= -\frac{8}{9m_q} \alpha_{NQM}(\mu_0^2) \int_0^\infty dr r |\psi(r)|^2 \\
&= -\frac{8}{9m_q} \alpha_{NQM}(\mu_0^2) \langle \frac{1}{r} \rangle,
\end{aligned} \tag{4.189}
$$

where we have restored the quark model renormalization scale μ_0^2 to indicate that this value pertains to some low scale at which the model is formulated.

The parameters m_q, $\langle \frac{1}{r} \rangle$ and $\alpha_{NQM}(\mu_0^2)$ are model dependent. $m_q \approx 0.3 GeV$ reproduces the nucleon magnetic moments. Another constraint comes from the $\Delta - N$ mass difference, which is given by

$$\Delta M = \frac{8\pi}{3}\frac{\alpha_{NQM}(\mu_0^2)}{m_q^2}\langle\delta^3(\vec{r})\rangle \tag{4.190}$$

in the non-relativistic quark model.

Static bag model calculations of hadron spin splittings were carried out by explicit construction of color electric and magnetic fields.We can use results from that work to evaluate eq. (4.188). The color magnetic field is calculated from the QCD generalization of Maxwell's equation, $\vec{\nabla} \times \vec{B}^a = g\psi^\dagger\vec{\alpha}\lambda^a\psi$, taking into account the boundary condition $\hat{r} \times \vec{B}^a = 0$ at $r = R$. A short calculation gives:

$$\begin{aligned} Q(r) &= \int_0^r dr' r'^2 \left(f^2(r') + g^2(r')\right) \\ h(r) &= \{\frac{1}{2}\frac{\mu(R)}{R^3} + \frac{\mu(r)}{r^3} + \int_r^R dr' \frac{\mu'(r')}{r'^3}\}, \quad \text{where} \\ \mu(r) &= \int_0^r dr' \frac{8\pi}{3} r^3 f(r) g(r) \end{aligned} \tag{4.191}$$

where $f(r) \propto j_0(x_0 r/R)$ and $g(r) \propto j_1(x_0 r/R)$. [$x_0$ is the lowest solution to the eigenvalue condition $\tan x = x/1 - x \quad (x_0 = 2.0428)$.] Substituting the explicit wavefunctions we find

$$\Gamma_{bag}(\mu_0^2) = -0.1\alpha_{bag}(\mu_0^2) \tag{4.192}$$

Standard bag model calculations of baryon spin splittings require $\alpha_{QCD} \approx 2$. We find $\Gamma_{bag} \sim -0.2$ at the renormalization scale of the model.

4.11 Quarks with internal structure

A possible solution to proton spin crisis is proposed by Fritzsch and Eldahoumi which is of interest for us.

The experimental data and theoretical analysis of the proton spin crisis suggest that we can consider the constituent quarks as composite systems, consisting of a valence quark, surrounded by a cloud of gluons and quark-antiquark pairs. The effective mass of a constituent quark is dynamically generated and is due to the cloud of gluons and pairs, surrounding the constituent quark.

The constituent quarks are denoted by the capital letters U, D and S. The internal structure of the U-quark is given by the following quark and gluon distribution functions:

$$u(x)\ ,\ \bar{u}(x)\ ,\ d(x)\ ,\ \bar{d}(x)\ ,\ etc.\ ,\ G(x) \tag{4.193}$$

Thus a constituent U-quark depends on 7 functions. The constituent D-quark is obtained after the interchange of u and d. The proton consists of *2*U-quarks and one D-quark: $P = (UUD)$. The current quark distribution functions of the proton are obtained as follows:

$$\begin{aligned} u_p(x) &= 2\ u(x) + d(x) \\ d_p(x) &= 2\ d(x) + u(x) \\ \bar{u}_p(x) &= 2\ \bar{u}(x) + \bar{d}(x) \\ \bar{d}_p(x) &= 2\ \bar{d}(x) + \bar{u}(x) \\ s_p(x) &= 3\ s(x) \\ \bar{s}_p(x) &= 3\ \bar{s}(x) \\ g_p(x) &= 3\ G(x) \end{aligned} \tag{4.194}$$

The current quark distributions of the U-quark have to obey the following sum rules:

$$\begin{aligned} \int_0^1 dx(u-\bar{u}) &= 1 \\ \int_0^1 dx(d-\bar{d}) &= 0 \\ \int_0^1 dx(s-\bar{s}) &= 0 \end{aligned} \tag{4.195}$$

Using the relations (2), we find for the current quark distributions of the

U-quark:

$$\begin{aligned}
u(x) &= \frac{1}{3}\ (2u_p(x) - d_p(x)) \\
\bar{u}(x) &= \frac{1}{3}\ (2\bar{u}_p(x) - \bar{d}_p(x)) \\
d(x) &= \frac{1}{3}\ (2d_p(x) - u_p(x)) \\
\bar{d}(x) &= \frac{1}{3}\ (2\bar{d}_p(x) - \bar{u}_p(x)) \\
s(x) &= \frac{1}{3}\ s_p(x) \\
\bar{s}(x) &= \frac{1}{3}\ \bar{s}_p(x) \\
G(x) &= \frac{1}{3}\ g_p(x)
\end{aligned} \tag{4.196}$$

The sum of the contributions of the (anti)quarks to the nucleon momentum is about 48% (ref.5):

$$\int_0^1 x[(u_p + \bar{u}_p) + (d_p + \bar{d}_p) + (s_p + \bar{s}_p)]dx \cong 0.48 \tag{4.197}$$

It follows that the contributions of the gluons to the nucleon momentum must be about 52%:

$$\int_0^1 xG(x)dx \cong 0.52 \tag{4.198}$$

A constituent quark contributes 33% to the momentum of a nucleon. For the distribution functions of the constituent quarks u, d, etc. we find:

$$\begin{aligned}
&\int_0^1 x[u + \bar{u} + d + \bar{d} + s + \bar{s}]dx \cong 0.16 \\
&\int_0^1 xG(x)dx \cong 0.17
\end{aligned} \tag{4.199}$$

Neglecting the strange quarks in the nucleon, and assuming that the u and d antiquarks are the same, we can express the distribution functions of the proton as follows:

$$\begin{aligned}
u_p &= 2u + d \\
d_p &= 2d + u \\
\bar{u}_p &= \bar{d}_p - \bar{u}_p = 3u
\end{aligned} \tag{4.200}$$

Thus the quark distribution functions of the U-quark are given by:

$$\begin{aligned} u &= \frac{1}{3}(2u_p - d_p) \\ d &= \frac{1}{3}(2d_p - u_p) \\ \bar{u}_p &= \bar{d}_p = 3d \end{aligned} \qquad (4.201)$$

We consider the spin structure of the constituent quarks and relate it to the spin structure of the nucleon. We introduce the spin-dependent distribution functions u_+, u_-, etc. The index "+" or "-" denotes the helicity of the corresponding quark or antiquark in a polarized U-quark with positive helicity. Especially we consider the integrals:

$$\int_0^1 dx[(q_+ + \bar{q}_+) - (q_- + \bar{q}_-)] = I_q \qquad (4.202)$$
$$(q = u\ ,\ d\ ,\ s)$$

The difference $(I_u - I_d)$ is the analogue of the Bjorken sum rule:

$$I_u - I_d = g_a \qquad (4.203)$$

(g_a: axial vector coupling constant, given by the isotriplet axialvector current. We also introduce the sum:

$$I_u + I_d + I_s = \triangle\Sigma \qquad (4.204)$$

This sum has been measured:

$$\triangle\Sigma \cong 0.30 \pm 0.1 \qquad (4.205)$$

Thus the quarks contribute only about 30% to the nucleon spin.

The nucleon spin can be decomposed into a quark contribution $\triangle\Sigma$, a gluon contribution $\triangle G$ and an orbital contribution $\triangle L$:

$$\frac{1}{2} = \frac{1}{2}\triangle\Sigma + \triangle G + \triangle L \qquad (4.206)$$

If we take $\triangle L = 0$, $\triangle G$ would have to be about 0.35.

A polarized constituent quark depends on the four functions u_+, u_-, G_+ and G_-. If we identify the constituent and current quarks and use a SU(6) wave function, we obtain:

$$\begin{aligned} u_+ &= \delta(1-x) \\ u_- &= G_+ = G_- = 0 \end{aligned} \qquad (4.207)$$

4.12 Quarks with orbital angular momentum

In the case of the moving proton we can no longer use the static classification group SU(3) of constituent quarks, were no $L \neq 0$ states contribute. Instead we shall use current quark group which can be obtained from static SU(3) by means of a specific unitary transformation (which physically represents a boost). This group is called SU(6) of quark currents. In this group $L \neq 0$ states are present, since the operator representing the boost transformation mixes states with $L \neq 0$ and $L = 0$. We can write:

$$|p\rangle = \frac{1}{\sqrt{2}}\cos\theta\left[|p\rangle_S|\uparrow\rangle_{\frac{1}{2},S} + |p\rangle_A|\uparrow\rangle_{\frac{1}{2},A}\right]_{L=0} +$$
$$\frac{1}{\sqrt{2}}\sin\theta\left(\left[|p\rangle_A|\downarrow\rangle_{\frac{1}{2},A} - \frac{1}{2}|p\rangle_S|\downarrow\rangle_{\frac{1}{2},S} + \frac{\sqrt{2}}{3}|p\rangle_S|\downarrow\rangle_{\frac{3}{2},S}\right]_{L=1} + \left[\sqrt{\frac{2}{3}}|p\rangle_S|\uparrow\rangle_{\frac{3}{2},S}\right]_{L=-1}\right)$$

Here the part in front of cosine is an usual S-wave state and the second part represents the contribution from P-wave. The indices S and A represent symmetric and antisymmetric parts of the wave function. The ratio $\frac{g_A}{g_V}$ is related to the matrix element $I_3\sigma_z$ (which is a coefficient of $\overline{\psi}\gamma_3\gamma_5\psi$) between proton states. After some algebra we obtain:

$$\frac{g_A}{g_V} = \langle p|I_3\sigma_z|p\rangle = \frac{5}{3}(\cos^2\theta - \sin^2\theta) = \frac{5}{3}\cos 2\theta$$

Taking into account the experimental number for the ratio, we can get the value of a mixing angle. It appears to be about $\sin^2\theta = \frac{1}{8}$.

We want to calculate how much of the proton spin is carried by the angular motion of the quarks.

The total angular momentum of the proton is the spin of the quarks S plus their orbital angular momentum L:

$$J = S + L$$

We can compute S and L using the wavefunction written above. For the spin part of the proton we have:

$$S = \frac{1}{2}\cos^2\theta + \frac{1}{2}\sin^2\theta\left(-\frac{1}{2} - \frac{1}{8} - \frac{2}{9}\frac{3}{2} + \frac{2}{9}\frac{3}{2}\right) \approx \frac{7}{16} - \frac{1}{26} \approx 0.4 = 80\%$$

Calculating the orbital momentum of the quarks L we find:

$$L = 0 + \frac{1}{2}\sin^2\theta\left(1 + \frac{1}{4} + \frac{2}{9} - \frac{2}{9}\right) = \frac{1}{16}\frac{5}{4} \approx 0.1 = 20\%$$

4.13 Gluon contribution to the proton spin

The total gluon contribution to the proton spin is given by the integral $\Delta G = \int_0^1 dx \Delta g(x)$. There are two main questions - what is the value of the ΔG and how does the structure function $g(x)$ depend on the Feynman momentum x? The operator ΔG is not related directly to the matrix element of a local, gauge-invariant operator. It can not be directly calculated in the lattice QCD simulations.

There are several ways to access ΔG in experiment:

- from the evolution of the structure function $g_1(x, Q^2)$ with the Q^2. This method is not precise since the range of the Q^2 is very limited.
- ΔG can be also accessed in $c\bar{c}$ production, assuming there is no charm in the proton. This production involves $\gamma - gluon$ fusion.

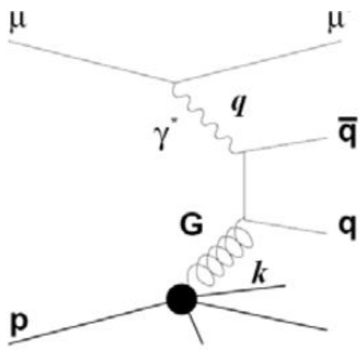

Figure 4.7: Open charm production from the gluon

- Effects of ΔG can be found in single particle production in the polarized proton-proton collisions, for example at RHIC.

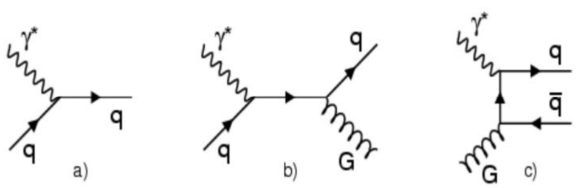

Figure 4.8: Leading contributions at COMPASS a) DIS LO, b) QCD Compton scattering, c) Photon-Gluon fusion

The distributions for $\Delta g(x)$ are sensitive to assumptions during data analysis, such as if $\Delta g(x)$ is changing the sign in x. It is important therefore to be able to estimate the ΔG from proton models.

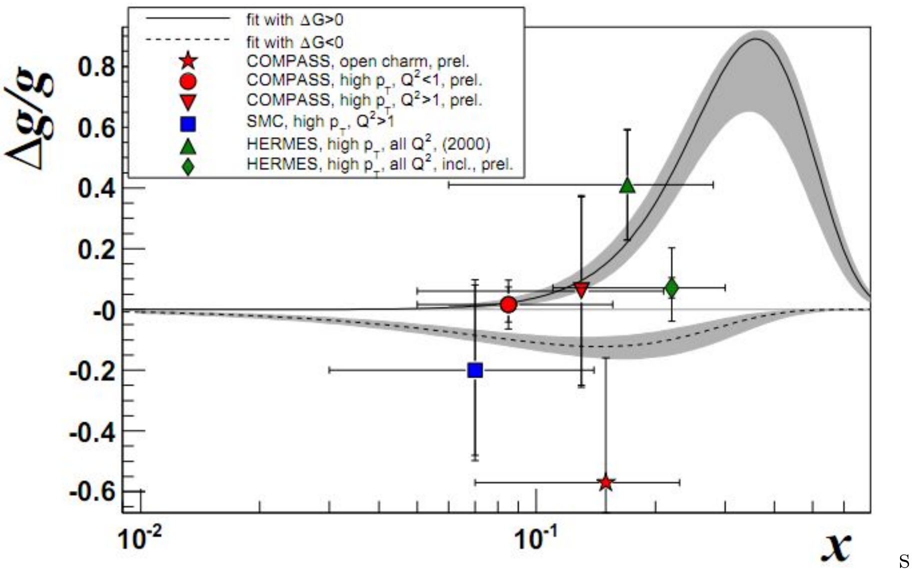

Figure 4.9: COMPASS, HERMES and SMC data on $\Delta g(x)$ together with the COMPASS fits for $\Delta g(x)/g(x)$ at $Q^2 = 3$ GeV^2

The current experimental status of the ΔG is listed in Table 4.1 and shown in Figure 4.9 for $x_g \sim 0.1$.

Table 4.1: Polarized gluon measurements from deep inelastic experiments.

Experiment	process	$\langle x_g \rangle$	$\langle \mu^2 \rangle$ (GeV^2)	$\Delta g/g$
HERMES	hadron pairs	0.17	~ 2	$0.41 \pm 0.18 \pm 0.03$
HERMES	inclusive hadrons	0.22	1.35	$0.071 \pm 0.034^{+0.105}_{-0.127}$
SMC	hadron pairs	0.07		$-0.20 \pm 0.28 \pm 0.10$
COMPASS	hadron pairs, $Q^2 < 1$	0.085	~ 3	$0.016 \pm 0.058 \pm 0.054$
COMPASS	hadron pairs, $Q^2 > 1$	0.082	~ 3	$0.08 \pm 0.10 \pm 0.05$
COMPASS	open charm	0.11	13	$-0.49 \pm 0.27 \pm 0.11$

4.14 $\Delta g(x)$ in quark models

$\Delta g(x)$ is represented by the non-local operator [170]

$$\Delta g(x) = -\frac{i}{x}\int_{-\infty}^{\infty}\frac{d\lambda}{2\pi}e^{-i\lambda x}\langle P|F^{+\alpha}(\lambda n)W\tilde{F}^{+}{}_{\alpha}(0)|P\rangle \ ,$$

where $|P\rangle$ is the proton state wavefunction, n is a light-like vector conjugating to an infinite momentum frame P. $F^{\mu\nu}$ is the gluon field tensor and W is a gauge link along the direction n connecting the two gluon field tensors. We ignore effects of nonlinear interaction and assume that the gluon fields behave as 8 independent Abelian fields. Leaving out the gauge link we obtain (inserting a complete set of intermediate states between the gluon field tensors):

$$\begin{aligned}\Delta g(x) &= -i\int\frac{d^4k}{(2\pi)^4}\frac{1}{V_4}\epsilon_{\perp}^{\alpha\beta}(k^+g^{\alpha\mu}g^{\beta\nu}-k^{\alpha}g^{+\mu}g^{\beta\nu}-k^{\beta}g^{+\nu}g^{\alpha\mu})\delta(x-k\cdot n)\\ &\quad\times\sum_m\langle\tilde{P}|A_\mu^*(k)|m\rangle\langle m|A_\nu(k)|\tilde{P}\rangle(V_3\cdot 2P^+)\ ,\end{aligned}$$

m sums over all possible intermediate states, and V_3 and V_4 are the space and space-time volumes, respectively.

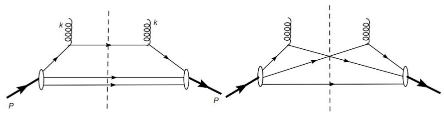

Figure 4.10: The polarized gluon operator in the quark models of the proton: one-body and two-body contributions are to the left and right respectively.

The one-body term with excited intermediate quark states provides the leading contribution. Using free-space gluon propagator the matrix element is:

$$\langle m|A_\nu(k)|\tilde{P}\rangle = 2\pi\delta\big(k^0-(\epsilon_f-\epsilon_i)\big)\frac{-i}{k^2}(-igt^a)\langle m|j_\nu(k)|\tilde{P}\rangle\ ,$$

j_ν is the color current.

Divergencies should be regulated by cut-offs. The excitation energy of the intermediate states is taken as a cut-off.

The result of the calculations for the MIT bag model is shown in Fig[4.11] with different cut-offs [168].

4.15 Δg from QCD evolution of g_1

$\Delta g(x, Q^2)$ can be measured by investigating scaling violations of the spin-dependent proton structure function $g_1(x, Q^2)$. The Q^2-dependence of the

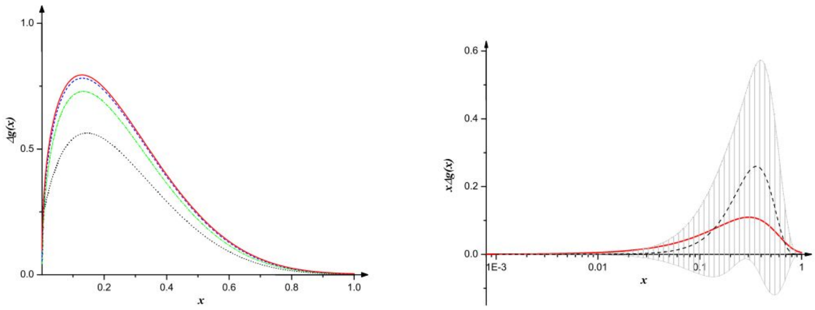

Figure 4.11: $\Delta g(x)$ and $x\Delta g(x)$ calculated in the MIT bag model. On the left , the results show successive additions of s, p, d, f wave contributions. On the right the result (red solid line) is compared with that from phenomenological fit (dashed line surrounded by an uncertainty band).

densities is described by the spin-dependent DGLAP evolution equations [169]:

$$\frac{d}{d\ln Q^2}\begin{pmatrix}\Delta q\\ \Delta g\end{pmatrix}(x,Q^2)=\int_x^1\frac{dz}{z}\begin{pmatrix}\Delta P_{qq}(\alpha_s(Q^2),z) & \Delta P_{qg}(\alpha_s(Q^2),z)\\ \Delta P_{gq}(\alpha_s(Q^2),z) & \Delta P_{gg}(\alpha_s(Q^2),z)\end{pmatrix}\begin{pmatrix}\Delta q\\ \Delta g\end{pmatrix}\left(\frac{x}{z},Q^2\right)\,, \tag{4.208}$$

The ΔP_{ij} are the spin-dependent “splitting functions”, which are evaluated in QCD perturbation theory. Δg contributes to the scaling violations of g_1. Figure 4.12 shows the current theoretical “uncertainty bands” for Δg from DIS scaling violations. A tendency toward a positive Δg is seen. The COMPASS collaboration [157] using their deuteron DIS data [158] have found two “allowed” regions for Δg, one with positive, one with negative gluon polarization. Much better estimation of $\Delta g(x,Q^2)$ over a wide range of x and Q^2 from scaling violations of g_1 would be possible at a polarized electron-ion collider, EIC [159], due to its larger kinematic region.

Global analysis

A complete determination of the gluon polarization will require the consideration of all existing data through a “global analysis”. The are several advantages of such a global analysis:

- The information from the various reaction channels is all combined into a single result for $\Delta g(x)$.

- The global analysis fixes the gluon distribution at definite values of x. Figure 4.13 highlights the importance of this. The figure [167] shows the contributions of the various x regions to the spin-dependent cross section for $pp \to \pi^0 X$ at RHIC, for six different sets of polarized

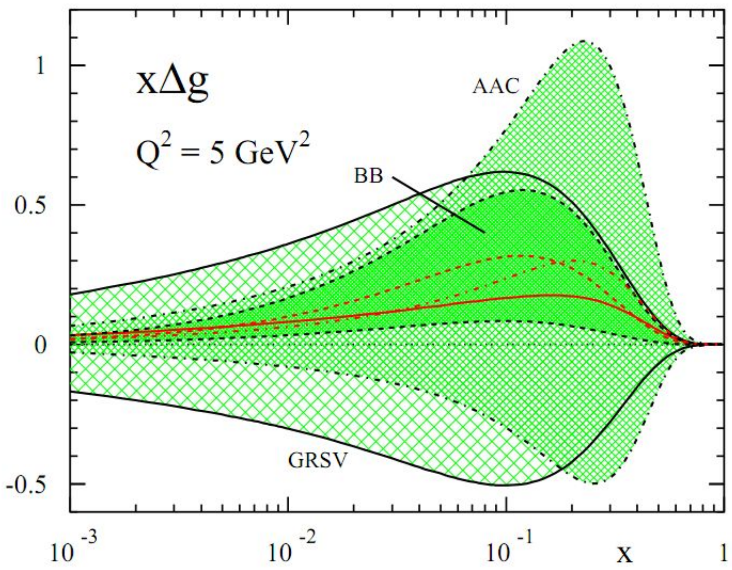

Figure 4.12: $x\Delta g(x, Q^2 = 5\ \mathrm{GeV}^2)$ from several analyses [160, 161, 162] of polarized DIS.

parton distributions [161] mostly differing in the gluon distribution. The distributions are very broad. The x-region that is probed depends on the size and form of the polarized gluon distribution. This makes it difficult to assign an estimate of the gluon momentum fraction to a data point at a given pion transverse momentum. The global analysis solves this problem.

- NLO theoretical calculations can be used without approximations.
- It becomes possible to determine an error on the gluon polarization.

Global analyses have been developed successfully over many years for the unpolarized parton densities. Global analyses of RHIC-Spin and polarized DIS data in terms of polarized parton distributions can be found in [164, 165, 166].

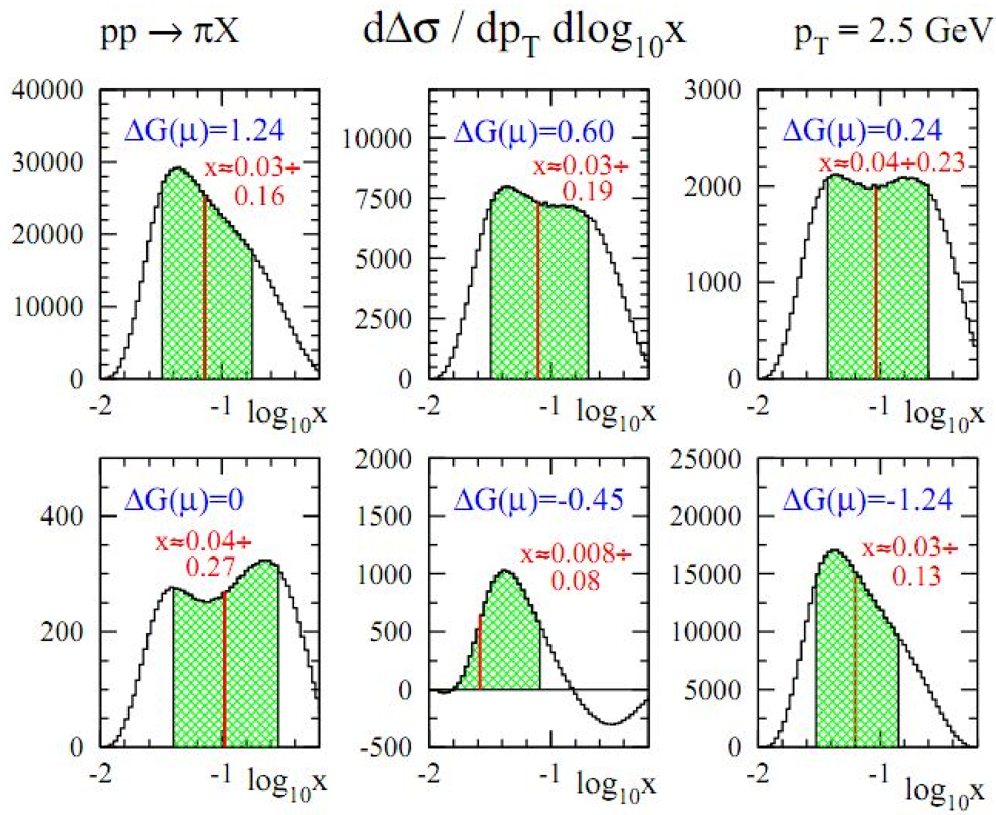

Figure 4.13: NLO $d\Delta\sigma/dp_T d\log_{10}(x)$ for the reaction $pp \to \pi^0 X$ at RHIC, for $p_T = 2.5\,\mathrm{GeV}$ and six different values for $\Delta G(\mu^2)$ at $\mu \approx 0.4$ GeV [161]. The shaded areas denote in each case the x-range dominantly contributing to $d\Delta\sigma$. From [167].

Summary and Conclusion

In this thesis we tried to investigate how the spin of the proton originates from the spin of the quarks and gluons. The surprising result of the EMC experiment suggested that the quarks carry almost zero fraction of the nucleon spin. We conjecture that most of the missing proton spin originates from the spin of the gluons and their orbital motion. We presented a possible spin decomposition in the framework of the constituent quarks embedded in the polarized sea of quarks, antiquarks and gluons. For a nucleon we have a relation:

$$\frac{1}{2} = \frac{1}{2}(0.45 + 0.30 + 0.25)$$

The gluons contribute 45% of the proton spin, another 30% comes from the spin of the quarks, and 25% percent is coming from the orbital motion of the quarks.

A gluon contribution to the proton mass is a well established experimental fact. We expect a connection between the origin of the proton mass and the spin crisis. To understand this connection we have to provide a clear picture of the proton composition. Detailed theoretical investigation of the strongly bounded systems is impossible at the moment. Our approach is based on the phenomenologically accessible parameters such as distribution functions for quarks and gluons. The dynamics of the nucleon can be studied on the lattice.

The exploration of the dynamical structure of the nucleon, both in experiment and theory, continues. In recent years transverse spin structure of the nucleon received a considerable interest. New methods of General Parton Distribution functions are used to understanding the three dimensional structure of the proton.

Acknowledgments

I would like to thank Prof. Dr. Harald Fritzsch for constant support, understanding and patience during all stages of my work. This project would have been not possible without his help.

This work has been funded by DFG-Graduiertenkolleg at the University of Munich. I am thankful to the speaker of Graduiertenkolleg Prof. Dr. Otmar Biebel for his help with legal issues and organization of many research seminars and conferences.

In discussions with Prof. Dr. Gerhard Buchalla I learned a lot about physics and science. I am thankful to him for his support and encouragement.

During this research i had many interesting discussions with my colleagues at the university of Munich: Volker Pillip, Matthäus Bartsch, Sebastian Jäger, Gamal Eldahoumi, Abdul Aziz Bhatti, Michael Spannowsky - i would like to thank them.

Finishing this project would be much harder without my friends Sophio Pataraia, Michael Spannowsky, Michael Brunnhuber, Jan Homann, Enrico Pajer, Adrian Mertens to whom i am thankful for their support and friendship.

I am thankful to my parents for constant support and motivation to accomplish this project.

Bibliography

[1] Particle Data Group: C. Amsler *et al.*, Phys. Lett. B **667** (2008) 1.

[2] F. E. Close and R. G. Roberts, Phys. Lett. B **316** (1993) 165.

[3] H.Fritzsch, M.Gell-Mann and H.Leutwyler, Phys. Lett. 47B, 365 (1973)

[4] S. D. Bass, Rev. Mod. Phys. **77** (2005) 1257.

[5] G. Altarelli and G. G. Ross, Phys. Lett. B **212** (1988) 391.

[6] R. D. Carlitz, J. C. Collins and A. Mueller, Phys. Lett. B **214** (1988) 229.

[7] S. D. Bass, B. L. Ioffe, N. N. Nikolaev and A. W. Thomas, J. Moscow Phys. Soc. **1** (1991) 317.

[8] W. K. H. Panofsky, *Proc.14th Intl. Conf. on High Energy Physics, Vienna*, p23: Geneva: CERN Information Service, 1968

[9] J. Ashman *et al.* [European Muon Collaboration], *Phys. Lett.* B 206 (1988) 364

[10] J. R. Ellis and R. L. Jaffe, *Phys. Rev.* D 9 (1974) 1444 [Erratum- *Phys. Rev.* D 10 (1974) 1669]

[11] E. Leader and M. Anselmino, *Z. Phys.* C 41 (1988) 239

[12] J. D. Bjorken, *Phys. Rev.* 179 (1969) 1547

[13] E. S. Ageev *et al.* [COMPASS Collaboration], *Phys. Lett.* B 633 (2006) 25 , preprint hep-ex/0511028.

[14] E. Leader, A. V. Sidorov and D. B. Stamenov, *Phys. Rev.* D 73 (2006) 034023 , preprint hep-ph/0512114.

[15] X. Ji, *Int. J. Mod. Phys.* A 18 (2003) 1303

[16] S. Wandzura and F. Wilczek, *Phys. Lett.* B 72 (1977) 195

[17] H. Burkhardt and W. N. Cottingham, *Ann. Phys. (N.Y.)* 56 (1970) 453

[18] A. V. Efremov, O. V. Teryaev and E. Leader, *Phys. Rev.* D 55 (1997) 4307 , preprint hep-ph/9607217.

[19] M. Anselmino, A. Efremov and E. Leader, *Phys. Rep.* 261 (1995) 1 ; Erratum-ibid. 281 (1997) 399, preprint hep-ph/9501369.

[20] S. D. Bass, *Rev. Mod. Phys.* 77 (2005) 1257 , preprint hep-ph/0411005.

[21] M. J. Alguard *et al.*, *Phys. Rev. Lett.* 37 (1976) 1261

[22] M. J. Alguard *et al.*, *Phys. Rev. Lett.* 41 (1978) 70

[23] G. Baum *et al.*, *Phys. Rev. Lett.* 45 (1980) 2000

[24] G. Baum *et al.*, *Phys. Rev. Lett.* 51 (1983) 1135

[25] J. Ashman *et al.* [European Muon Collaboration], *Nucl. Phys.* B 328 (1989) 1

[26] J. Alcorn *et al.*, *Nucl. Instrum. Meth.* A 522 (2004) 294

[27] Hall A Status Report - 2007

[28] B. Adeva *et al.* [Spin Muon Collaboration], *Phys. Lett.* B 302 (1993) 533

[29] D. Adams *et al.* [Spin Muon Collaboration (SMC)], *Phys. Lett.* B 329 (1994) 399

[30] B. Adeva *et al.* [Spin Muon Collaboration (SMC)], *Phys. Lett.* B 369 (1996) 93

[31] B. Adeva *et al.* [Spin Muon Collaboration], *Phys. Rev.* D 58 (1998) 112001

[32] B. Adeva *et al.* [Spin Muon Collaboration], *Phys. Rev.* D 60 (1999) 072004 [Erratum- *Phys. Rev.* D 62 (2000) 079902]

[33] P. L. Anthony *et al.* [E142 Collaboration], *Phys. Rev. Lett.* 71 (1993) 959

[34] P. L. Anthony *et al.* [E142 Collaboration], *Phys. Rev.* D 54 (1996) 6620

[35] K. Abe *et al.* [E143 Collaboration], *Phys. Rev. Lett.* 74 (1995) 346

[36] K. Abe *et al.* [E143 Collaboration], *Phys. Rev. Lett.* 75 (1995) 25

[37] K. Abe *et al.* [E143 collaboration], *Phys. Rev.* D 58 (1998) 112003

[38] P. L. Anthony *et al.* [E155 Collaboration], *Phys. Lett.* B 463 (1999) 339

[39] P. L. Anthony *et al.* [E155 Collaboration], *Phys. Lett.* B 493 (2000) 19

[40] K. Abe *et al.* [E154 Collaboration], *Phys. Rev. Lett.* 79 (1997) 26

[41] K. Abe *et al.* [E154 Collaboration], *Phys. Lett.* B 405 (1997) 180

[42] K. Abe *et al.* [E143 Collaboration], *Phys. Rev. Lett.* 78 (1997) 815

[43] K. Abe *et al.* [E154 Collaboration], *Phys. Lett.* B 404 (1997) 377

[44] P. L. Anthony *et al.* [E155 Collaboration], *Phys. Lett.* B 553 (2003) 18

[45] K. Ackerstaff *et al.* [HERMES Collaboration], *Phys. Lett.* B 404 (1997) 383

[46] A. Airapetian *et al.* [HERMES Collaboration], *Phys. Lett.* B 442 (1998) 484

[47] A. Airapetian *et al.* [HERMES Collaboration], *Phys. Rev.* D 75 (2007) 012007

[48] A. Airapetian *et al.* [HERMES Collaboration], *Phys. Rev.* D 71 (2005) 012003

[49] A. Airapetian *et al.* [HERMES Collaboration], *Phys. Rev.* D 75 (2007) 011103 , preprint hep-ex/0605108.

[50] A. Airapetian *et al.* [HERMES Collaboration], *Phys. Lett.* B 648 (2007) 164 , preprint hep-ex/0612059.

[51] A. Airapetian *et al.* [HERMES Collaboration], *Phys. Rev. Lett.* 84 (2000) 2584

[52] V. Y. Alexakhin *et al.* [COMPASS Collaboration], *Phys. Lett.* B 647 (2007) 8

[53] E. S. Ageev *et al.* [Compass Collaboration], *Phys. Lett.* B 647 (2007) 330

[54] M. Alekseev *et al.* [COMPASS Collaboration], *Phys. Lett.* B 660 (2008) 458 , preprint hep-ex/0707.4077.

[55] S. S. Adler *et al.* [PHENIX Collaboration], *Phys. Rev.* D 73 (2006) 091102

[56] B. I. Abelev *et al.* [STAR Collaboration], *Phys. Rev. Lett.* 97 (2006) 252001

[57] A. Adare *et al.* [PHENIX Collaboration], *Phys. Rev.* D 76 (2007) 051106 , preprint hep-ex/0704.3599.

[58] B. I. Abelev *et al.* [STAR Collaboration], *Phys. Rev. Lett.* 100 (2008) 232003 , preprint hep-ex/0710.2048.

[59] M. Amarian *et al.* [Jefferson Lab E94-010 Collaboration], *Phys. Rev. Lett.* 89 (2002) 242301 , preprint nucl-ex/0205020.

[60] M. Amarian *et al.* [Jefferson Lab E94-010 Collaboration], *Phys. Rev. Lett.* 92 (2004) 022301

[61] M. Amarian *et al.* [Jefferson Lab E94-010 Collaboration], *Phys. Rev. Lett.* 93 (2004) 152301

[62] Z. E. Meziani *et al.*, *Phys. Lett.* B 613 (2005) 148 , preprint hep-ph/0404066.

[63] J. P. Chen, A. Deur and Z. E. Meziani, *Mod. Phys. Lett.* A 20 (2005) 2745

[64] X. Zheng *et al.* [Jefferson Lab Hall A Collaboration], *Phys. Rev. Lett.* 92 (2004) 012004

[65] X. Zheng *et al.* [Jefferson Lab Hall A Collaboration], *Phys. Rev.* C 70 (2004) 065207

[66] K. Kramer *et al.* [Jefferson Lab E97-103 Collaboration], *Phys. Rev. Lett.* 95 (2005) 142002

[67] P. Solvignon *et al.* [Jefferson Lab E01-012 Collaboration], preprint nucl-ex/0803.3845.

[68] JLab E97-110 Collaboration, "The GDH Rule and the Spin Structure of ^{3}He and the Neutron Using Nearly Real Photons", J. P. Chen, A. Deur and F. Garibaldi, spokespersons.

[69] J. L. Friar, B. F. Gibson, G. L. Payne, A. M. Bernstein and T. E. Chupp, *Phys. Rev.* C 42 (1990) 2310

[70] C. Ciofi degli Atti and S. Scopetta, *Phys. Lett.* B 404 (1997) 223 , preprint ucl-th/9606034.

[71] F. R. P. Bissey, V. A. Guzey, M. Strikman and A. W. Thomas, *Phys. Rev.* C 65 (2002) 064317 , [preprint hep-ph/0109069.

[72] B. A. Mecking *et al.* [CLAS Collaboration], *Nucl. Instrum. Meth.* A 503 (2003) 513

[73] J. Yun *et al.* [CLAS Collaboration], *Phys. Rev.* C 67 (2003) 055204

[74] R. Fatemi *et al.* [CLAS Collaboration], *Phys. Rev. Lett.* 91 (2003) 222002

[75] K. V. Dharmawardane *et al.* [CLAS Collaboration], *Phys. Lett.* B 641 (2006) 11

[76] P. E. Bosted *et al.* [CLAS Collaboration], *Phys. Rev.* C 75 (2007) 035203

[77] P. E. Bosted and M. E. Christy, preprint hep-ph/0711.0159.

[78] M. E. Christy and P. B. Bosted, preprint hep-ph/0712.3731.

[79] R. De Vita *et al.* [CLAS Collaboration], *Phys. Rev. Lett.* 88 (2002) 082001 [Erratum-ibid. 88 (2002) 189903], preprint hep-ex/0111074.

[80] A. S. Biselli *et al.* [CLAS Collaboration], *Phys. Rev.* C 78 (2008) 045204 , preprint nucl-ex/0804.3079.

[81] S. Chen *et al.* [CLAS Collaboration], *Phys. Rev. Lett.* 97 (2006) 072002 , preprint hep-ex/0605012.

[82] P. E. Bosted and H. Avakian, in preparation.

[83] F. R. Wesselmann *et al.* [RSS Collaboration], *Phys. Rev. Lett.* 98 (2007) 132003

[84] S.I. Adler, Phys. Rev. **177** (1969) 2426; J.S. Bell and R. Jackiw, N.C. **51A** (1969) 47.

[85] R. Jackiw, 'Current algebra and anomalies', World Scientific, Singapore (1985).

[86] C. Cronström and J. Mickelsson, J. Math. Phys. **24** (1983) 2528.

[87] X. D. Ji, *Phys. Lett.* B 309 (1993) 187 , preprint hep-ph/9307303.

[88] X. D. Ji and P. Unrau, *Phys. Lett.* B 333 (1994) 228 , preprint hep-ph/9308263.

[89] E. Leader and E. Predazzi, *Camb. Monogr. Part. Phys. Nucl. Phys. Cosmol.* 4 (1996) 1

[90] J. Blumlein and N. Kochelev, *Nucl. Phys.* B 498 (1997) 285 , preprint hep-ph/9612318.

[91] B. Ehrnsperger, A. Schafer and L. Mankiewicz, *Phys. Lett.* B 323 (1994) 439 , preprint hep-ph/9311285].

[92] J. P. Chen, A. Deur and Z. E. Meziani, *Mod. Phys. Lett.* A 20 (2005) 2745 , preprint nucl-ex/0509007.

[93] S. B. Gerasimov, *Sov. J. Nucl. Phys.* 2 (1966) 430 ; [*Yad. Fiz.* 2 (1966) 598].

[94] S. D. Drell and A. C. Hearn, *Phys. Rev. Lett.* 16 (1966) 908

[95] M. Anselmino, B. L. Ioffe and E. Leader, *Sov. J. Nucl. Phys.* 49 (1989) 136 ; [*Yad. Fiz.* 49 (1989) 214].

[96] B. L. Ioffe, V. A. Khoze and L. N. Lipatov, "Hard Processes. Vol. 1: Phenomenology, Quark Parton Model," *Amsterdam, Netherlands: North-Holland* (1984) 340p

[97] D. Drechsel, B. Pasquini and M. Vanderhaeghen, *Phys. Rep.* 378 (2003) 99 ; preprint hep-ph/0212124.

[98] N. Bianchi and E. Thomas, *Phys. Lett.* B 450 (1999) 439 , preprint hep-ph/9902266.

[99] S. Simula, M. Osipenko, G. Ricco and M. Taiuti, *Phys. Rev.* D 65 (2002) 034017 , preprint hep-ph/0107036.

[100] K. Slifer *et al.* [E94010 Collaboration], *Phys. Rev. Lett.* 101 (2008) 022303 , preprint nucl-ex/0803.2267.

[101] D. Drechsel, O. Hanstein, S. S. Kamalov and L. Tiator, *Nucl. Phys.* A 645 (1999) 145

[102] X. D. Ji and W. Melnitchouk, *Phys. Rev.* D 56 (1997) 1 , preprint hep-ph/9703363.

[103] M. Gockeler *et al.*, *Phys. Rev.* D 63 (2001) 074506 , preprint hep-lat/0011091.

[104] X. D. Ji, C. W. Kao and J. Osborne, *Phys. Lett.* B 472 (2000) 1 , preprint hep-ph/9910256.

[105] D. Drechsel, S. S. Kamalov and L. Tiator, *Phys. Rev.* D 63 (2001) 114010 , preprint hep-ph/0008306.

[106] JLab E06-014, "Precision Measurements of the Neutron d_2: Towards the Electric χ_E and Magnetic χ_B Color Polarizabilities", S. Choi, X. Jiang, Z. E. Meziani and B. Sawatzky, spokespersons.

[107] JLab E12-06-121, "A Path to 'Color Polarizabilities' in the Neutron: A Precision Measurement of the Neutron g_2 and d_2 at High Q^2 in Hall C", T. Averett, Z. E. Meziani, W. Korsch and B. Sawatzky, spokespersons.

[108] JLab E07-003, "Spin Asymmetries on the Nucleon Experiment-SANE", S. Choi, Z. E. Meziani and O. Randon, spokespersons.

[109] A. Deur, preprint nucl-ex/0508022.

[110] M. Osipenko *et al.*, *Phys. Lett.* B 609 (2005) 259 , preprint hep-ph/0404195.

[111] M. Osipenko *et al.*, *Phys. Rev.* D 71 (2005) 054007 , preprint hep-ph/0503018.

[112] A. Deur *et al.*, *Phys. Rev. Lett.* 93 (2004) 212001 , preprint hep-ex/0407007.

[113] A. Deur *et al.*, *Phys. Rev.* D 78 (2008) 032001 , preprint nucl-ex/0802.3198.

[114] P. Mergell, U. G. Meissner and D. Drechsel, *Nucl. Phys.* A 596 (1996) 367 , preprint hep-ph/9506375.

[115] A. Piccione and G. Ridolfi, *Nucl. Phys.* B 513 (1998) 301 , preprint hep-ph/9707478.

[116] J. Blumlein and A. Tkabladze, *Nucl. Phys.* B 553 (1999) 427 , preprint hep-ph/9812478.

[117] D. Drechsel and L. Tiator, *Ann. Rev. Nucl. Part. Sci.* 54 (2004) 69 , preprint nucl-th/0406059.

[118] J. Ahrens *et al.* [GDH Collaboration], *Phys. Rev. Lett.* 87 (2001) 022003

[119] H. Dutz *et al.* [GDH Collaboration], *Phys. Rev. Lett.* 91 (2003) 192001

[120] H. Dutz *et al.* [GDH Collaboration], *Phys. Rev. Lett.* 94 (2005) 162001 .

[121] S. Hoblit *et al.* [LSC Collaboration],

[122] K. Helbing, *Prog. Part. Nucl. Phys.* 57 (2006) 405 , preprint nucl-ex/0603021.

[123] X. D. Ji and J. Osborne, *J. Phys.* G 27 (2001) 127 preprint hep-ph/9905410.

[124] V. Bernard, T. R. Hemmert and U. G. Meissner, *Phys. Rev.* D 67 (2003) 076008 , preprint hep-ph/0212033.

[125] A. Airapetian *et al.* [HERMES Collaboration], *Eur. Phys. J.* C 26 (2003) 527 , preprint hep-ex/0210047.

[126] C. Ciofi degli Atti, E. Pace and G. Salme, *Phys. Rev.* C 51 (1995) 1108 preprint nucl-th/9411006.

[127] Y. Prok *et al.* [CLAS Collaboration], preprint nucl-ex/0802.2232.

[128] J. Soffer and O. Teryaev, *Phys. Rev.* D 70 (2004) 116004 , preprint hep-ph/0410228.

[129] V. D. Burkert and B. L. Ioffe, *Phys. Lett.* B 296 (1992) 223

[130] V. D. Burkert, preprint nucl-th/0004001.

[131] A. Deur, V. Burkert, J. P. Chen and W. Korsch, *Phys. Lett.* B 665 (2008) 349 , preprint hep-ph/0803.4119.

[132] A. Deur, V. Burkert, J. P. Chen and W. Korsch, *Phys. Lett.* B 650 (2007) 244 , preprint hep-ph/0509113.

[133] S. J. Brodsky and G. F. de Teramond, *Phys. Rev. Lett.* 96 (2006) 201601 , preprint hep-ph/0602252.

[134] C. W. Kao, T. Spitzenberg and M. Vanderhaeghen, *Phys. Rev.* D 67 (2003) 016001 , preprint hep-ph/0209241.

[135] JLab E03-006, "The GDH Sum Rule with nearly real photons and the proton g_1 structure function at low momentum transfer", M. Battaglieri, A. Deur, R. De Vita and M. Ripani, spokespersons.

[136] JLab E08-027, "A Measurement of g_2^p and the Longitudinal-Transverse Spin Polarizability", J. P. Chen, A. Camsonne and K. Slifer, spokespersons.

[137] S.D. Drell and J.D. Walecka, Ann. Phys. **28** (1964) 18.

[138] C.E. Carlson and Wu-ki Tung, Phys. Rev. **D5** (1972) 721; J.S. Bell and R. Jackiw, N.C. **51A** (1969) 47.

[139] A.J.G. Hey and J.E. Mandula, Phys. Rev. **D5** (1972) 2610.

[140] M. Anselmino, Phys. Rev. **D19** (1979) 2803.

[141] M.J. Alguard *et al.*, Phys. Rev. Lett. **41** (1978) 70.

[142] G. Baum *et al.*, Phys. Rev. Lett. **51** (1983) 1135; V.W. Hughes *et al.*, Phys. Lett. **212** (1988) 511.

[143] G. Baum *et al.*, Phys. Rev. Lett. **51** (1983) 1135; V.W. Hughes *et al.*, Phys. Lett. **212** (1988) 511.

[144] J. Ashman *et al.*, Phys. Lett. **B206** (1988) 364.

[145] J. Ashman *et al.*, Nucl. Phys. **B328** (1989) 1.

[146] B. Adeva *et al.*, Phys. Lett. **B302** (1993) 533.

[147] B. Adeva *et al.*, Phys. Lett. **B320** (1994) 400.

[148] D.L. Anthony *et al.*, Phys. Rev. Lett. **71** (1993) 759.

[149] E. Leader and M. Anselmino, Z. Phys. **C41** (1988) 239.

[150] A.V. Efremov, 'A model for the estimation of jet handedness

[151] G. Altarelli and G. Parisi, Nucl. Phys. **B126** (1977) 298.

[152] L.N. Epele, H. Fanchiotti, C.A. Garcia Canal, E. Leader and R. Sassot, Birkbeck College Preprint, October 1993.

[153] L.N. Epele, H. Fanchiotti, C.A. Garcia Canal and R. Sassot, Phys. Lett. **287** (1992) 247.

[154] C. Bourrely, E. Leader and J. Soffer, Phys. Rep. **59** (1980) 95.

[155] C. Ciofi degli Atti, S. Scarpetta, E. Pace and G. Salmè, Phys. Rev. **C48** (1993) R968.

[156] R.M. Woloshyn, Nucl. Phys. **A496** (1989) 749.

[157] Mallot GK 2006 arXiv:hep-ex/0612055

[158] Ageev ES [COMPASS Collaboration] 2007 arXiv:hep-ex/0701014

[159] Deshpande A, Milner R, Venugopalan R, Vogelsang W 2005 *Ann. Rev. Nucl. Part. Sci.* **55** 165; Bruell A *et al.* http://www.physics.rutgers.edu/np/EIC-science-1.7.pdf

[160] Blümlein J and Böttcher H 2002 *Nucl. Phys.* **B636** 225

[161] Glück M, Reya E, Stratmann M, Vogelsang W 2001 *Phys. Rev.* **D63** 094005

[162] Asymmetry Analysis Collaboration, Hirai M, Kumano S, Saito N 2004 *Phys. Rev.* **D69** 054021

[163] Aidala C *et al.* http://spin.riken.bnl.gov/rsc/report/masterspin.pdf *(Research Plan for Spin Physics at RHIC)*; *update:* Bunce G *et al.* http://www.physics.rutgers.edu/np/RHIC_spin_LRP07.pdf

[164] Asymmetry Analysis Collaboration, Hirai M, Kumano S, Saito N 2006 *Phys. Rev.* **D74** 014015

[165] de Florian D, Navarro GA, Sassot R 2005 *Phys. Rev.* **D71** 094018; Navarro GA, Sassot R 2006 *Phys. Rev.* **D74** 011502

[166] Stratmann M and Vogelsang W 2001 *Phys. Rev.* **D64** 114007

[167] Stratmann M, talk presented at the "14th International Workshop on Deep Inelastic Scattering (DIS 2006)", Tsukuba, Japan, April 20-24, 2006

[168] Chen P. and Ji X. arxiv:hep-ph/0612174

[169] Sasaki K 1975 *Prog. Theor. Phys.* **54** 1816; Ahmed MA and Ross GG 1976 *Nucl. Phys.* **B111** 441; Altarelli G and Parisi G 1977 *Nucl. Phys.* **B126** 298

[170] A. V. Manohar, Phys. Rev. Lett. **66**, 289 (1991).